TAL TECH

DOCTORAL THESIS

Ice-Binding Proteins in Pseudomonas Fluorescens AQP671: Isolation, Characterization and Applications in Food

Õnnela Luhila

TALLINNA TEHNIKAÜLIKOOL
TALLINN UNIVERSITY OF TECHNOLOGY
TALLINN 2026

TALLINN UNIVERSITY OF TECHNOLOGY
DOCTORAL THESIS
53/2026

Ice-binding proteins in *Pseudomonas fluorescens* AQP671: isolation, characterization and applications in food

ÕNNELA LUHILA

TAL TECH PRESS

TALLINN UNIVERSITY OF TECHNOLOGY
School of Science
Department of Chemistry and Biotechnology
This dissertation was accepted for the defence of the degree Doctor of Philosophy in Food Science on the 14th of June 2026.

Supervisor:
Dr Allan Olspert
School of Science
Tallinn University of Technology
Tallinn, Estonia

Co-supervisor:
Dr Katrin Laos
School of Science
Tallinn University of Technology
Tallinn, Estonia

Opponents:
Prof Aneta Białkowska
Faculty of Biotechnology and Food Sciences
Institute of Molecular and Industrial Biotechnology
Lodz University of Technology
Lodz, Poland

Prof Triinu Visnapuu
Institute of Molecular and Cell Biology
Chair of Genetics
Tartu University
Tartu, Estonia

Defence of the thesis: 07/09/2026, Tallinn

Declaration:
Hereby I declare that this doctoral thesis, my original investigation and achievement, submitted for the doctoral degree at Tallinn University of Technology has not been submitted for doctoral or equivalent academic degree.

Õnnela Luhila

---
signature

European Union
European Regional
Development Fund

Investing
in your future

ISSN 2585-6898 (paperback)
ISBN 978-9916-80-548-0 (paperback)
ISSN 2585-6901 (PDF)
ISBN 978-9916-80-544-2 (PDF)
https://doi.org/10.23658/taltech.53/2026

Luhila, Õ. (2026). *Ice-binding proteins in Pseudomonas fluorescens AQP671: isolation, characterization and applications in food* [TalTech Press]. https://doi.org/10.23658/taltech.53/2026

TALLINNA TEHNIKAÜLIKOOL
DOKTORITÖÖ
53/2026

Pseudomonas fluorescens AQP671 jääga seonduvad valgud: puhastamine, iseloomustamine ja kasutamine toidus

ÕNNELA LUHILA

TAL TECH KIRJASTUS

Contents

List of Publications

The list of the author's publications, on the basis of which the thesis has been prepared:

I **Luhila, Õ**., Paalme, T., Tanilas, K., & Sarand, I. (2022). Omega-3 fatty acid and B12 vitamin content in Baltic algae. *Algal Research*, *67*.

II **Luhila, Õ**., Karro, K., Zakrevskaja, K., Nisamedtinov, I., & Paalme, T. (2024). Cryo-protective effect of ice-binding proteins produced by *Pseudomonas fluorescens* AQP671 on wholegrain wheat bread dough during freezing and frozen storage. LWT, 214.

III **Luhila, Õ.,** Nisamedtinov, I., Paalme, T., Laos, K., & Olspert, A. (2025). The effect of temperature and nitrogen source modulation on Pseudomonas fluorescens AQP671 ice recrystallization inhibition activity. *Plos*, *20*(9), 1–12.

IV **Luhila, Õ.**, Sarand, I., Calcines-Cruz, C., Laos, K., Nisamedtinov, I., Paalme, T., Olspert, A. Isolation and characterization of ice-binding proteins in *Pseudomonas fluorescens* AQP671" (manuscript).

Author's Contribution to the Publications

Contribution to the papers in this thesis is:

I I conducted all experiments, performed the statistical analyses, and wrote and reviewed the manuscript.

II I led the experimental planning and execution, performed all statistical analyses, and wrote the manuscript in its entirety.

III I was responsible for all experimental work, statistical analysis, and manuscript preparation, and contributed substantially to the experimental design and study planning.

IV I was responsible for experimental conception, execution, statistical analysis, and manuscript drafting.

Introduction

Psychrophilic and psychrotolerant microorganisms inhabiting polar, alpine, and marine environments have evolved a wide range of adaptive mechanisms that enable survival under conditions of prolonged cold exposure, freeze–thaw stress, and limited nutrient availability. Among these adaptations, the production of ice-binding proteins (IBPs) has attracted considerable scientific and industrial interest due to their unique ability to interact with ice crystals and modify ice growth behavior.

IBPs have been identified in a wide range of organisms, including fish, insects, plants, fungi, algae, and bacteria, where they contribute to freeze tolerance and cellular protection in cold environments. Their physicochemical properties have led to increasing attention toward their potential application in biotechnology, medicine, agriculture, and the food industry.

Ice-binding proteins function by adsorbing to specific planes of ice crystals, thereby inhibiting further crystal growth. One of the functional properties of IBPs is ice recrystallization inhibition (IRI), which prevents the growth of large ice crystals at the expense of smaller ones at temperatures close to their melting point. Ice recrystallization is a major cause of structural damage in frozen biological systems and food matrices, negatively affecting texture, moisture retention, and overall product quality. Consequently, IBPs have emerged as promising natural additives capable of improving the stability and quality of frozen foods such as ice cream, frozen meat, frozen vegetables, and bakery products.

The present thesis focuses on the isolation and characterization of ice-binding proteins from *Pseudomonas fluorescens* AQP671, a bacterial strain isolated from brown algae collected along the coast of Scotland. The thesis investigates the production and purification of IBPs from this bacterium and evaluates their functional properties with emphasis on IRI activity. In addition to purification and recombinant expression, this thesis investigates the effects of environmental factors such as pH and temperature on IBP expression and activity, as well as the thermal stability of these proteins.

To assess their practical potential, the purified proteins were incorporated into frozen dough systems to examine their cryoprotective effects during frozen storage, as ice recrystallization and freeze–thaw stress can negatively affect dough quality, and IBPs may help preserve dough structure and functionality by limiting ice crystal growth.

This thesis also explores the presence of potential IBP-producing bacteria associated with Baltic Sea seaweeds. By comparing bacterial isolates and reviewing relevant literature, the study aimed to evaluate whether Baltic marine environments may represent additional sources of IBP-producing microorganisms.

Abbreviations

AFP	Antifreeze protein
AFPG	Antifreeze glycoprotein
CTAB	Cetyltrimethylammonium bromide
DUF	Domain of unknown function
IAP	Ice affinity purification
IBP	Ice-binding protein
IBS	Ice-binding site
INA	Ice nucleating activity
INP	Ice nucleating protein
IPTG	Isopropyl β-D-1-thiogalactopyranoside
IRI	Ice recrystallization inhibition
PfAdh	*Pseudomonas fluorescens* AQP671 adhesin type protein
PfMp	*Pseudomonas fluorescens* AQP671 metallopeptidase type protein
RIP	Recrystallization inhibition protein
RTX	Repeats-in-toxin
SP	Sulfopropyl-Sephadex-binding
TH	Thermal hysteresis
QAE	Quaternary aminoethyl-Sephadex-binding

1 Literature review

1.1 Ice-binding proteins and their importance

Water accounts for about 60-90% of most organisms in terms of weight, playing an essential role in most biological functions. The freezing of water is a natural phenomenon that usually starts with ice crystal formation. This process consists of two phases: nucleus formation and grain growth. During nucleation, water molecules combine to form ordered ice particles. During the ice crystal growth stage, the sizes of nucleation particles increase by adding more water molecules in an orderly manner (Chen et al., 2020).

Depending on the purity of water, ice nucleation can be divided into two forms. First is homogeneous nucleation, which takes place in the absence of impurities in the water (Sanz et al., 2013). Second is heterogeneous nucleation, which takes place in non-pure water systems. During the heterogeneous nucleation process, water molecules are aggregated into crystals on nucleating agents, such as biological compounds or crystalline surfaces (X. Chen et al., 2020; Fitzner et al., 2015)

The freezing of water can be detrimental to organisms inhabiting areas where temperatures regularly drop below zero. Therefore, these organisms have evolved to produce many cryoprotective agents, such as ice-binding proteins (IBPs). IBPs are a heterogeneous group of proteins that adhere to ice and can inhibit ice recrystallization or growth (Bar Dolev et al., 2016; Białkowska et al., 2020; Chasnitsky & Braslavsky, 2019; Davies, 2014).

The evolutionary history of IBPs goes back 10-30 million years, when the sea levels began to freeze in Antarctica (Gharib et al., 2022). However, the first IBPs were identified only ~55 years ago, when it was discovered that the serum freezing points of some Antarctic fishes were below the freezing point of seawater. The concentrations of urea, salts, and free amino acids in the serum accounted for only a portion of the freezing point depression; the rest was attributed to a carbohydrate-containing protein (DeVries & Wohlschlag, 1969). These glycoproteins circulate in the bloodstream of Antarctic Notothenioid fishes and serve the purpose of stopping ice crystal growth. (Chen et al., 2020; Davies, 2014; Mahatabuddin et al., 2017).

To date, IBPs have been discovered in fish, insects, plants, nematodes, algae, fungi and microorganisms. Despite their common ability to bind to ice, they exhibit large variability in size and structure (Bar Dolev et al., 2016; Białkowska et al., 2020; Davies, 2014; Ramløv & Friis, 2020).

Many modelling studies have suggested that the mechanisms by which IBPs adhere to ice involve the organization of water molecules into a constrained ice-like pattern by the ice-binding site (IBS). This ice-like pattern resembles the quasi-liquid layer of water next to the ice surface. When these two layers combine, the IBPs are frozen to the ice surface at temperatures below the melting point (Davies, 2014; Voets, 2017).

In general, IBPs have one to two IBSs that can be described as extensive, consisting of many hydrophobic residues creating a relatively flat surface in which several polar residues are inserted at regular intervals or dispersedly. It is also devoid of charged residues when compared to the rest of the IBP, and it has been concluded that good alignment formation of threonine (Thr) residues with their intervals matching the ice lattice may be the key for ice inhibition (Davies, 2014; Ramløv & Friis, 2020; Xue et al., 2019; Yamauchi et al., 2020). Other contributors that may play a part in IBP adhesion to

ice are van der Waals interactions, hydrogen bonding and hydrophobic forces (Davies, 2014; Voets, 2017).

The binding of IBPs to the ice surface causes a microcurvature (Figure 1A). According to the Kelvin effect, it is thermodynamically more difficult for water to add to a curved ice surface than to a flat one; therefore, the freezing temperature is depressed below the freezing point (Figure 1B). Due to the surface adsorption of IBPs, the melting temperature is also slightly elevated. The sum of the large freezing hysteresis and small melting hysteresis is called thermal hysteresis (TH) (Chen et al., 2020).

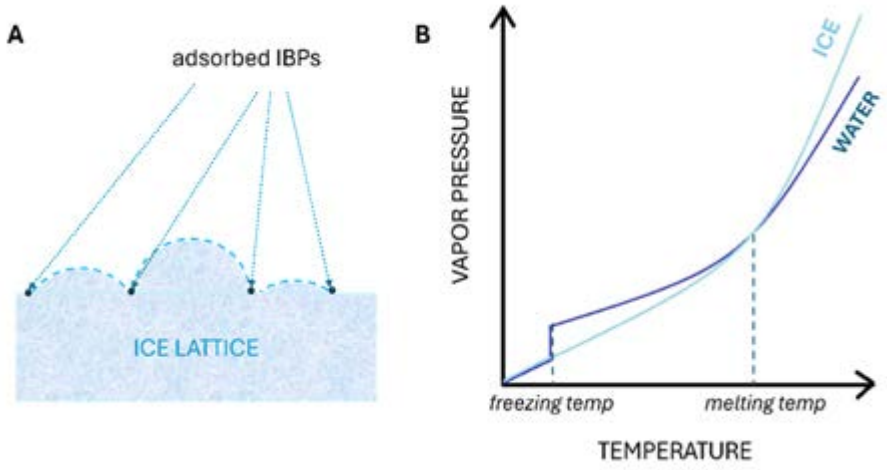

Figure 1: The changes in the surface curvature of the ice lattice when IBPs are adsorbed to it (A) and the corresponding changes in the vapor pressure and freezing and melting temperatures (B). Adapted from Ramløv & Friis (2020).

In addition to the TH activity, IBPs can also exhibit ice recrystallization inhibition (IRI), dynamic ice shaping and ice nucleation activity (INA) (Bar Dolev et al., 2016; Mahatabuddin et al., 2017; Voets, 2017).

Ice recrystallisation is a process belonging to the Ostwald ripening class. It occurs when larger ice crystals grow at the expense of smaller ones at a constant temperature. This process leads to an increase in mean crystal size, a decrease in the number of crystals and total crystal surface area (Rahman et al., 2019). Ice recrystallisation takes place due to small size differences between ice crystals. Larger ice crystals have a slightly lower curvature and therefore a higher melting temperature. This leads to a net flux of water molecules from smaller ice crystals to larger ones. In the presence of IBPs, the difference in melting temperatures between larger and smaller ice crystals is decreased due to the change in ice surface curvature (Ramløv & Friis, 2020).

In pure water, ice crystals grow and melt continuously in the shape of a flat disk (Figure 2). IBPs change the photomicroscopic structure of an ice crystal to a hexagonal bipyramid or a lemon-like shape, depending on the type and number of ice planes that the IBPs are bound to (Bar Dolev et al., 2016; Mahatabuddin et al., 2017; Voets, 2017).

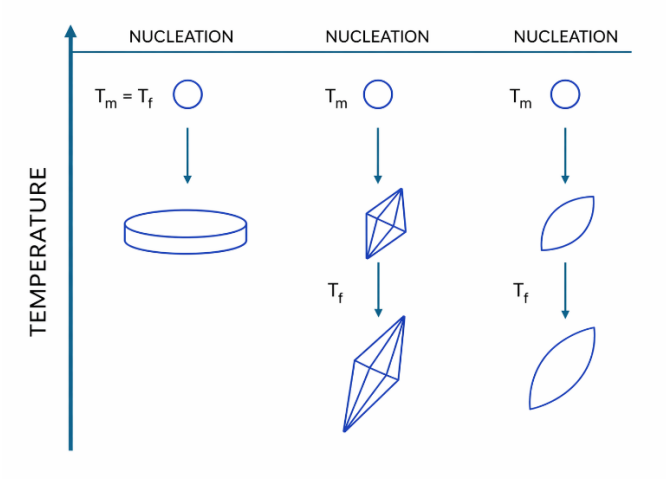

Figure 2: Ice crystal shapes in pure water ($T_m = T_f$) and in the presence of ice-binding proteins ($T_m \neq T_f$), T_m - melting temperature, T_f - freezing temperature (adapted from Bar Dolev et al., 2016; Mahatabuddin et al., 2017; Voets, 2017)

In addition to the named properties of IBPs, some secondary, possibly protective functions have been identified. One such property could be the stabilization of membranes when the organisms are exposed to cold; another could be the stabilization of the organism's ion balance during cold exposure, and some antifreeze proteins have anti-virulence effects, which may be adaptive to cold-tolerant organisms (Ramløv & Friis, 2020).

1.2 Categorization of ice-binding proteins

Ice-binding proteins exhibit considerable diversity, reflecting their widespread occurrence across a variety of organisms. This variation is evident in their structural features, modes of action, and ice-binding activity. Accordingly, IBPs can be categorized based on differences in their function, levels of activity, and structure (Ramløv & Friis, 2020).

1.2.1 Categorization according to function and activity

Ice-binding proteins can largely be grouped into three categories based on their primary activity: ice nucleating proteins (INPs), which exhibit ice nucleating activity, antifreeze (glyco)proteins (AF(G)Ps), which exhibit thermal hysteresis activity and recrystallization inhibition proteins (RIPs), which exhibit ice recrystallization inhibition activity, as shown in Figure 3 (Gharib et al., 2022).

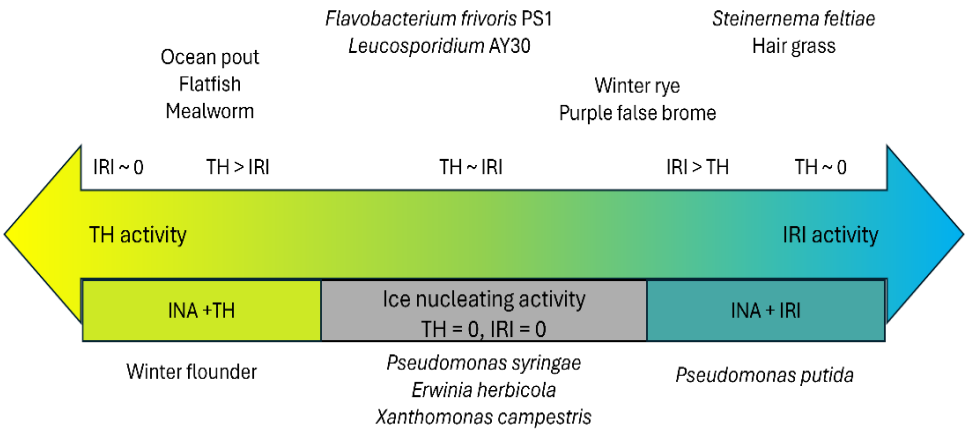

Figure 3: Range of activities characteristic of ice-binding proteins with examples of organisms producing proteins with the respective activities. INA - ice nucleating activity, IRI – ice recrystallization inhibition activity, TH – thermal hysteresis activity. Adapted from Gharib et al. (2022), Ramløv and Friis (2020) and Chang et al. (2024).

The primary function of INPs is to control the formation of ice crystals (Gharib et al., 2022). This function is important for organisms that need to regulate the location where ice crystals are created. For example, in plants, ice nucleating proteins (INPs) are secreted to keep the ice extracellular and therefore avoid ice crystals in the cytosol (Bar Dolev et al., 2016). The formation of ice in the extracellular space increases the solute concentration outside the cell, creating an osmotic gradient that drives water efflux from the cytosol. This dehydration reduces the likelihood of intracellular ice formation, which is typically more damaging, but also imposes mechanical and osmotic stress on the cell (Bojic et al., 2021; Kato et al., 2023). Alternatively, plant pathogenic bacteria, for example, *Pseudomonas syringae,* use INPs to cause frost damage to plants to obtain nutrients (Roeters et al., 2021). Other organisms known to produce INPs include *Pseudomonas borealis, Pseudomonas fluorescens, Pseudomonas viridiflava, Pseudomonas putida, Pseudomonas antarctica, Erwinia herbicola, Erwinia ananas, Erwinia uredovora and Xanthomonas campestris.* These bacteria can catalyze ice formation at temperatures as high as -2 °C to -3 °C (Garnham et al., 2011; Kawahara, 2002; Qiu et al., 2019; Sun et al., 1995; Xu et al., 1998)

Antifreeze proteins (AFPs) and antifreeze glycoproteins (AFGPs) decrease the freezing point of body fluids of freeze-tolerant organisms. These proteins exhibit high TH values, indicating their ability to depress the freezing temperature and inhibit ice crystal growth. AFPs and AFGPs have mainly been found in fish and insects, but also in certain microorganisms (Gauthier et al., 1998, 2005, 2008; Gharib et al., 2022; Leiter et al., 2016). AFPs and AFGPs can be categorized based on their TH values. Hyperactive proteins have a TH value of 2-13 °C, whereas moderately active AFPs and AFGPs have a TH value of up to 2 °C at equimolar concentrations (Vance et al., 2019). The hyperactivity of proteins with a high TH value has been associated with their ability to bind to multiple ice planes (Ekpo et al., 2022).

RIPs inhibit the recrystallization of ice and mitigate the damage done by growing ice crystals (Gharib et al., 2022). RIPs are mainly found in plants, nematodes, fungi, algae and microorganisms, but they have also been identified in animals, for example, in the

Wood frog (*Rana sylvatica*), which can survive in temperatures as low as -16 °C (Gharib et al., 2022; Le Tri et al., 2019).

The IRI activity of different proteins can be compared by calculating the inhibitory concentration, which is the concentration causing 50% inhibition of recrystallisation and is calculated by plotting the rate constant as a function of IBP concentrations, as shown in Figure 4. Based on these values, IBPs can be classified as very effective ($C_i < 10^{-1}$ µmol/L), effective (10^{-1} µmol/L < $C_i < 10^3$ µmol/L) and ineffective ($C_i > 10^3$ µmol/L) (Vance et al., 2019).

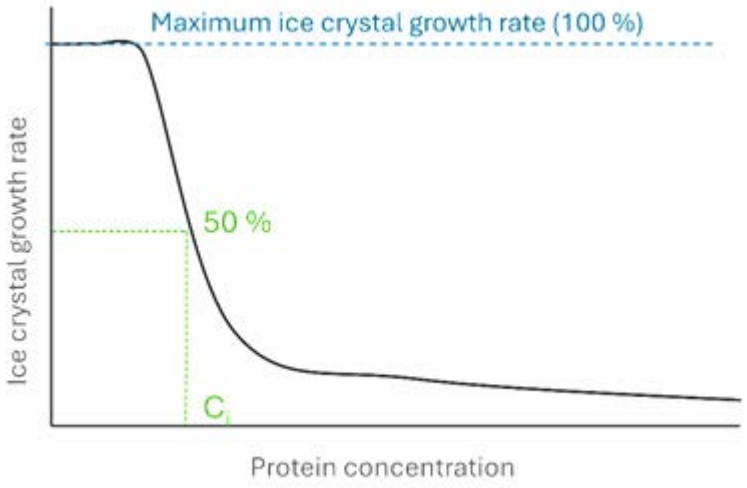

Figure 4: Graphical evaluation of the 50% inhibitory concentration (C_i) of ice recrystallization.

There is also proof that IRI activity is dependent on the manner in which the IBP binds to the ice planes. For example, proteins that adhere to multiple ice planes have a higher IRI activity than those that adhere to a singular plane (Rahman et al., 2019).

In some organisms, AFPs or RIPs also have a weak INP activity and vice versa, which possibly acts as a means to increase freeze tolerance (Bar Dolev et al., 2016; Chang et al., 2024). Additionally, since IRI and TH activity are often associated with the same protein, the exact characterization of the protein may differ across the literature. Because of that, the broader term, ice-binding proteins, is commonly used for those proteins (Gharib et al., 2022).

1.2.2 Categorization according to structure

IBPs have a large structural diversity. In general, they rely more on hydrogen and disulfide bonds and less on a hydrophobic core. Some of the known structures to date include α-helices, single β-solenoids, globular proteins, four-helix bundles and polyproline type II helix bundles (Bar Dolev et al., 2016; Davies, 2014). Examples of these structures are shown in Figure 5.

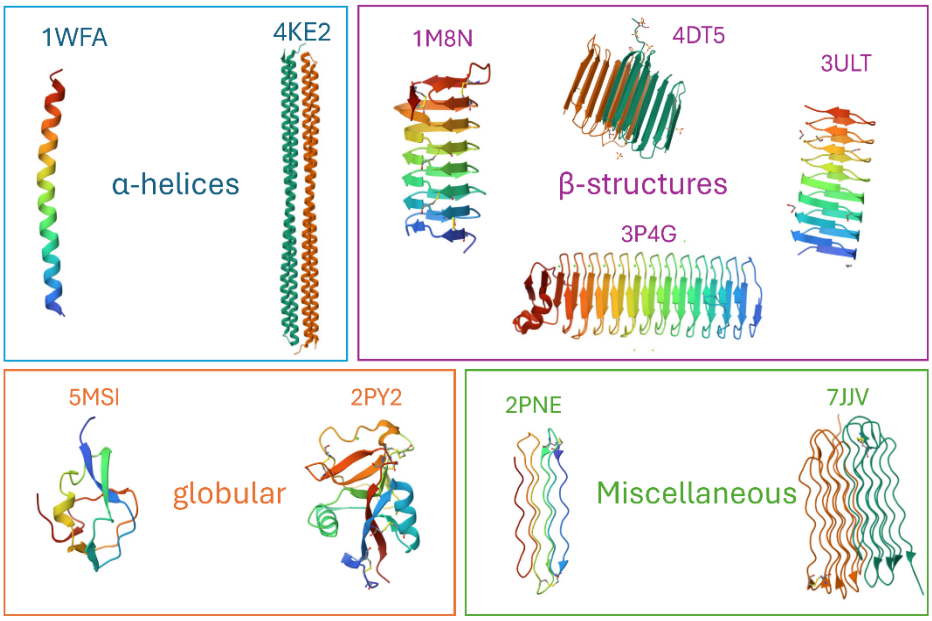

Figure 5: Structures of various ice-binding proteins, including α-helices (1WFA, 4KE2 from winter flounder), β-structures (1M8N from spruce budworm, 4DT5 from ribbed pine porer, 3ULT from perennial ryegrass, 3P4G from Marinomonas primoryensis), globular (5MSI from ocean pout, 2PY2 from herring) and miscellaneous helix bundles (2PNE from the snow flea and 7JJV from springtail). Adapted from Bar Dolev et al. (2016), Davies (2014), and Ramløv and Friis (2020). *Structures are taken from the RCSB Protein Data Bank (2025)*

AFGPs contain 4 to 50 tripeptide repeats (Ala–Ala–Thr, in some cases substituted by Pro–Ala–Thr in AFGPs 6–8) with galactose-N-acetylgalactosamine attached to each Thr. In the described unit, the carbohydrate moiety makes up about 60% of the mass. AFGPs can be categorized into 8 classes according to size. AFGP type 1 is the largest (Mw = 33.7 kDa), and the rest go in decreasing order, with the smallest being AFGP type 8 (Mw = 2.6 kDa) (Bouvet & Ben, 2003; Devries, 1982).

Each of the 8 classes also contains several isoforms. The general secondary structure has been described as a type II polyproline helix, but only at low temperatures. In this configuration, each triplet (Ala-Ala-Thr) makes one turn in the coil and the carbohydrate units result in a regular arrangement on one side of the molecule. This gives the molecule an overall amphipathic character, where the protein backbone with the methyl group of Ala is more hydrophobic, and the carbohydrate side is more hydrophilic (Ramløv & Friis, 2020; Voets, 2017). An exceptionally large (150 kDa) AFGP in *Pleuragramma antarcticum* has also been reported. This is also the only AFGP known to be hyperactive (Yang, D. S. C., Sax, M., Chakrabartty, A., & Hew, 1988).

AFPs are also categorized into four classes according to their genetics, size, and structure. Their structure can be described as amphipathic, while the ice-binding site is somewhat hydrophobic (Ramløv & Friis, 2020; Voets, 2017).

Type I AFPs are alanine-rich α-helixes with a molecular weight of 3,3–4,5 kDa (Voets, 2017; Yang, D. S. C., Sax, M., Chakrabartty, A., & Hew, 1988). There are also subsets of type I AFPs. Firstly, liver-type AFPs, which have signal peptides and are secreted into the bloodstream. Secondly, skin-type AFPs, which lack signal peptides and are mainly present

in the skin and other peripheral tissues (Ramløv & Friis, 2020). Some *Pleuronectiformes* also have a third, larger isoform, which has also been referred to as "hyperactive type I AFP" due to its superior activity compared to other type I AFPs (Gauthier et al., 2005; Graham et al., 2008).

Type II AFPs are 11–24 kDa globular proteins, consisting of two α-helixes and nine β-strands in two β-sheets. These proteins are cysteine-rich C-lectin-like proteins. They all share a great identity in amino acid sequence and conserved gene sequences, and have a unique disulfide bond pattern. C-lectin proteins traditionally have 2-4 disulfide bonds; type II AFPs, however, have five of the aforementioned bonds (Ramløv & Friis, 2020; Voets, 2017). Type II AFPs can also be divided into two distinct groups. Some require Ca^{2+} as a cofactor for activity, for example, AFPs from herring and smelt. These AFPs have ice-binding sites corresponding to the carbohydrate-binding site of C-lectins (Ramløv & Friis, 2020; Vanya Ewart et al., 1996). Ca^{2+}-independent AFPs of the same type have the IBS at a different location and therefore don't require Ca^{2+} for activity. For example, AFPs from sea raven and poacher (Loewen et al., 1998).

Type III AFPs are small, globular proteins without cysteines that do not bind to the basal plane of ice (Chasnitsky & Braslavsky, 2019). These proteins have been found in a variety of fish, but mainly eelpouts and wolf fish. Their folding pattern is complex, consisting of several short strands paired in two antiparallel β-sheets, in addition to several helices. The primary sequence of these AFPs also shows no obvious repeats (Ramløv & Friis, 2020; Voets, 2017). Type III AFPs are found in two structural variants that can be differentiated based on their isoelectric point. Quaternary aminoethyl-Sephadex-binding (QAE) forms have a pI value below 7, and sulfopropyl-Sephadex-binding (SP) forms have a pI value above 7 (Choi et al., 2021). It has been shown that the QAE forms have a higher activity. It is most likely that these two forms cooperate in the organisms in which they are present (Ramløv & Friis, 2020; Voets, 2017).

Type IV AFPs are lipoprotein-like proteins with a molecular weight of about 12 kDa. Their structure consists of four amphipathic α-helixes of similar length that are folded into a four-helix bundle (Ramløv & Friis, 2020; Voets, 2017). They are present in several fish. However, they show low thermal hysteresis activities. Therefore, it has been speculated that these AFPs have other functions in the organisms (Gauthier et al., 2008). For example, they may be involved in embryogenesis (Xiao et al., 2014).

The structures of AFPs present in insects have been described for five orders of insects: *Coleoptera, Hymenoptera, Lepidoptera, Diptera* and *Hemiptera*. The structures are very diverse, but often rich in β-solenoids and silk-like solenoids (Ramløv & Friis, 2020; Voets, 2017). These AFPs also have a significantly higher antifreeze activity (10-100 times higher than fish AFPs), most likely an adaptation to the significantly lower terrestrial temperatures they inhabit (Kuiper et al., 2015). This higher activity can also be linked to the disulfide bonds present in insect IBPs, which enhance conformational stability and reduce the likelihood of cold-induced structural destabilization (Bar et al., 2006; Liou et al., 2000).

IBPs from bacteria, diatoms, plants, and fungi have been shown to have a similar secondary structure, which may be the result of horizontal gene transfer across the species. One example is the PFAM11999 (previously DUF3494) domain. The 3D structure of proteins containing this domain is generally a discontinuous beta-solenoid with a triangular cross-section and an adjacent alpha-helix. An α-helix runs along the A-face, parallel to the longitudinal axis of the β-helix. This fold, typical for PFAM11999 IBPs, has been called the IBP-1 fold (Raymond & Remias, 2019; Vance et al., 2019). Despite similar

structures across all of the proteins in this group, these proteins present a diverse magnitude of activity, both in terms of thermal hysteresis as well as ice recrystallisation. The proteins are usually secreted into the environment of the host cell or are anchored onto their cell membranes (Arai et al., 2019; Raymond & Remias, 2019; Vance et al., 2019).

Additionally, some ice-binding proteins, for example, adhesins from Antarctic bacteria, *Marinomonas primoryensis* and *Marinomonas arctica* (BSI20414), have the repeats-in-toxin (RTX) motif (GGXGXDX(L/I/F)X) associated with the ice-binding site of these IBPs. It is believed that these bacteria use IBPs to adhere to floating ice crystals and use them as a means of transport to nutrients and oxygen in the phototrophic zone (Garnham et al., 2008; Guo et al., 2017; Liao et al., 2021).

1.3 Ice-binding proteins in *Pseudomonas* species

Pseudomonas species have been studied for their ability to produce ice-binding proteins, including both ice-nucleating proteins and antifreeze proteins, which play distinct but sometimes complementary roles in cold adaptation.

Pseudomonas syringae is one of the most well-characterized microorganisms used to demonstrate the function of INPs. The INP responsible for this activity in *P. syringae* has been extensively analyzed and is characterized by a highly repetitive central domain flanked by non-repetitive N- and C-terminal domains (Roeters et al., 2021; Saki et al., 2023).

The central region consists of repeating units, with the largest repeat element being 48 residues in length, composed of three 16-residue repeats. Disruption of this 48-residue periodicity results in a loss of ice-nucleating activity, highlighting its structural importance. The N- and C-terminal domains are thought to function as anchors, facilitating attachment of the protein to the outer membrane. Structurally, the INP adopts a β-helix conformation (Graether & Jia, 2001).

Another species, *Pseudomonas putida*, has also been shown to produce IBPs. The strain *P. putida* GR12-2, isolated from the rhizosphere of Arctic plants, is capable of surviving harsh winter conditions and proliferating at low temperatures (~5°C). When concentrated growth medium from cultures grown at 5°C for six days was analyzed, the average freezing and melting temperatures were 0.15°C and 0.13°C, respectively, corresponding to a thermal hysteresis (TH) value of 0.02°C (Sun et al., 1995).

Notably, antifreeze activity was predominantly detected in the extracellular fraction, despite its lower total protein content compared to cytoplasmic and periplasmic fractions, indicating that IBPs are primarily secreted (Sun et al., 1995).

Initial SDS-PAGE analysis estimated the protein mass at ~32 kDa; however, further purification revealed a much larger molecular mass of approximately 164 kDa. The smaller observed protein is thought to be a degradation product. This IBP exhibits both antifreeze and ice-nucleating activities, which may explain its relatively large size compared to other bacterial IBPs. A significant portion of the molecular mass consists of carbohydrate, consistent with antifreeze glycoproteins, and lipid moieties are also present (Singh et al., 2014; Sun et al., 1995; Xu et al., 1998).

Further biochemical analyses suggest structural features important for activity. Partial loss of function following treatment with β-mercaptoethanol indicates the presence of cysteine residues, likely involved in disulfide bond formation. Sensitivity to α-chymotrypsin suggests the presence of exposed aromatic residues such as tyrosine, phenylalanine, or tryptophan. In contrast, the protein remains stable in 1% SDS,

indicating considerable structural robustness. The presence of cysteine residues likely contributes to resistance against denaturation by detergents or elevated temperatures (Sun et al., 1995).

Additionally, the functional behavior of the protein appears to depend on its aggregation state. Large aggregates exhibit high ice-nucleating activity, whereas monomeric forms display antifreeze activity. Ice nucleation is likely facilitated by lipid-carbohydrate moieties involved in aggregation, whereas antifreeze activity does not require such structures. This suggests that the two opposing functions are complementary and context-dependent (Xu et al., 1998).

Pseudomonas ficuserectae, isolated from cryoconite holes, produces IBPs with high antifreeze activity. The molecular weight of the protein is approximately 23 kDa, and its TH value can reach up to 2°C, which is among the highest reported for bacterial IBPs. Different strains of *P. ficuserectae* exhibit significant variation in ice IRI activity. Two IBPs from Arctic *P. ficuserectae* strains both displayed strong TH activity (~2°C at 2 mg/mL), yet differed markedly in IRI performance. One protein exhibited only moderate IRI activity at 0.1 mg/mL, whereas the other showed strong IRI activity at concentrations as low as 0.05 mg/mL (Ramløv & Friis, 2020; Singh et al., 2014).

In *Pseudomonas fluorescens* KUAF-68, both ice-nucleating and antifreeze activities have been observed. These functions are associated with separate proteins. The antifreeze protein exhibits a relatively low TH value of 0.03°C. SDS-PAGE analysis revealed molecular weights of approximately 80 kDa for the antifreeze protein and 600 kDa for the ice-nucleating protein. These proteins are thought to have stabilizing effects on the membranes of the bacteria (Kawahara et al., 2004).

1.4 Frozen food systems

Freezing has become a widespread method of food preservation (S. Xiao et al., 2024). It consists of three stages: pre-cooling, phase transition and tempering. In the pre-cooling stage, the product is cooled to its freezing point. During phase transition, the latent heat of fusion is removed, and in the tempering stage, the product is cooled to its final storage temperature (Kiani & Sun, 2011).

During freezing, the amount of free water in the product decreases, which lowers water activity (S. Xiao et al., 2024). Therefore, the rate of chemical reactions and the activity of enzymes and microorganisms are slowed down, and the shelf-life of food products is extended (Tirado-Kulieva et al., 2022).

1.4.1 Problems related to freezing

Although freezing of food products helps reduce chemical reactions and microbiological activity in food, it can also cause structural disruptions in food. This is caused by the mechanical stress of growing ice crystals, which damages the cells and tissues. Another major challenge related to frozen food products is the maintenance of the cold chain, aimed at keeping optimal storage temperature during production, storage and distribution. Inappropriate refrigeration during distribution is estimated to be one of the main causes of food waste (X. Chen et al., 2020; Mangiagalli et al., 2020).

The physical changes of frozen food during storage can be described as cracking, recrystallisation, moisture loss and migration of unfrozen water. During freezing, the formation of ice excludes solutes from the crystal lattice, leading to a progressive reduction in free water and a corresponding increase in solute concentration in the remaining unfrozen phase. Chemical changes of frozen foods include deterioration of

flavor, vitamins, minerals and pigments, denaturation of proteins, inactivation of enzymes and oxidation of lipids. The freeze-thaw process caused by temperature fluctuations can lead to additional structural and textural changes that negatively impact the quality of the end product (X. Chen et al., 2020; Hu & Xie, 2021; Tirado-Kulieva et al., 2022).

For example, frozen storage can cause physical damage to muscle tissues and cell structures, influencing the water-holding capacity and texture of meat and meat products (Leygonie et al., 2012; Wang et al., 2021). The lipid and protein degradation caused by the freeze-thaw process can lead to the release of factors that intensify oxidative reactions and promote the formation of carbonyl compounds, malondialdehyde or other oxidative products, which change the flavor and color of meat products (Huang et al., 2013; Leygonie et al., 2012; Utrera et al., 2014).

Similarly, freeze-thaw cycles decrease the quality of various seafood products. It has been shown that they cause cooking and centrifugal losses, structural deterioration and a reduction in amino acid content in frozen Chilean jack mackerel (*Trachurus murphyi*) and destabilize the muscle structure of catfish (*Silurus glanis Linne*) (Benjakul & Bauer, 2001; Hu & Xie, 2021). Comparable results have been observed for shrimp; repeated freeze-thaw cycles cause an increase in free water and a decline in the texture of the frozen product (Lan et al., 2020). The damage was found to be proportional to the size of the ice crystals (Hu & Xie, 2021).

Freezing is particularly harmful to fruits and vegetables due to their high free water content. Growing ice crystals harm the cell walls of plants, causing dehydration and deterioration of product quality. Another main reason for such deterioration is ice recrystallisation during storage linked to temperature fluctuations, as repeated freeze-thaw cycles have a negative effect on product firmness and cause an increase in drip loss (X. Chen et al., 2020, 2021; Provesi et al., 2019).

The formation of ice crystals during freezing and the freeze-thaw process can cause starch retrogradation and disrupt the dough matrix, gluten network and yeast viability, resulting in reduced dough strength and compromised baking performance. This leads to loss of gas retention, poor loaf volume and significant deterioration in the textural properties of the final product. (Ding et al., 2020; Sharadanant & Khan, 2003a, 2003b; Yang et al., 2019; Zhao et al., 2022). Literature has indicated that whole wheat dough may have better resistance to freezing compared to white wheat dough when it comes to maintaining loaf volume and softness. However, the decrease in quality is still significant, with an 8.8% and 17.9% decrease in loaf volume and 28.8% and 39.9% decrease in softness, respectively (Bae et al., 2014).

The formation and recrystallisation of ice crystals in frozen dairy products have a significant effect on their sensory quality and textural and structural stability. Ice recrystallization causes the mean size of ice crystals to increase, which in turn results in a coarse mouthfeel (X. Chen et al., 2020; Kaleda et al., 2018; Liu, Liang, Wang, et al., 2018; Mangiagalli et al., 2020; Zhang et al., 2016).

1.4.2 Improving the quality of frozen food products with IBPs

Since IBPs have good control over ice crystals, they can be used in food processing to improve the nutritional value and quality of frozen foods. Some possible applications of IBPs in food include use in frozen meat, fish, fruits, vegetables, dough and dairy products (X. Chen et al., 2020; Mangiagalli et al., 2020).

IBPs can be introduced into food matrices through mechanical methods like mixing, soaking, injecting or vacuum infiltration or through genetic approaches, for example, to create more cold-resistant crops (Chen et al., 2021). When IBPs are added to food products through mechanical methods, they are referred to as ice-structuring proteins (Chen et al., 2020; Mangiagalli et al., 2020).

In frozen meat products, IBPs could be added to the surface to create smaller ice crystals and prevent their growth, leading to a product with less nutrient loss and also with a better protein fiber microstructure. It has also been shown that injecting live animals with IBPs up to 24 hours before slaughter has a positive effect on the meat once it's frozen and thawed. There is less water dripping and nutrient loss detected (X. Chen et al., 2020; Mangiagalli et al., 2020).

Recrystallisation in frozen fruits and vegetables can be prevented with the use of IBPs. For example, a patent has been created for the use of fish antifreeze proteins in frozen vegetables. In this patent, the vegetables are first blanched, then the antifreeze protein is infiltrated through the use of vacuum infiltration and then the products are frozen. This type of IBP use has been shown to improve the quality of frozen carrots (X. Chen et al., 2020; Patent-WO2003055320A1, 2003). Other proteins exhibiting IRI or TH activity have been used to improve the quality of various fruits and vegetables, such as cherries, bananas, green beans, onions, cucumbers and zucchinis (X. Chen et al., 2021; Kashyap et al., 2020; Kong et al., 2017; Song et al., 2019).

Additionally, IBPs from cold-acclimated carrots have been expressed in transgenic tomatoes, increasing their tolerance to cold temperatures, potentially through the stabilization of cell membranes (Rajeev Kumar et al., 2014).

The addition of IBPs to frozen dough can improve its texture and help maintain bread volume due to increased gas production. In addition to that, the use of IBPs or freeze-tolerant yeasts has been shown to improve dough softness after freezing. IBPs extracted from *Pichia pastoris* GS115, for example, could effectively inhibit gluten deterioration upon temperature fluctuations during frozen storage, and AFPs from pig collagen could improve the texture and baking characteristics of frozen bread dough. (X. Chen et al., 2020; Liu, Liang, Wang, et al., 2018; Mangiagalli et al., 2020; Nguyen et al., 2018).

IBPs from many different sources have been assessed for their ability to improve the shelf-life and quality of ice cream. Positive effects have been noted with fish AFPs, IBPs from wheatgrass, cold-acclimated oat and pig collagen. It has been shown that IBPs from these organisms improve ice cream's melting stability and inhibit recrystallisation (X. Chen et al., 2020; Kaleda et al., 2018; Liu, Liang, Wang, et al., 2018; Mangiagalli et al., 2020; Regand & Goff, 2006; Zhang et al., 2016). However, recent research has shown that IBPs may aggregate higher-order structures, which induce hardness or roughness, which is not favorable in ice cream. Therefore, the addition of any IBP alone may not be enough to guarantee an improved frozen dairy product (Kaleda et al., 2018).

1.4.3 Stability of IBPs in food systems

The effectiveness of IBPs is closely linked to their structural and physicochemical stability under food-relevant conditions. IBP stability can be considered at multiple levels, including molecular stability (protein folding), functional stability (ice-binding activity), and system-level stability (performance within complex food matrices), all of which are influenced by environmental and processing conditions (Baskaran et al., 2021; Ramløv & Friis, 2020; S. Xiao et al., 2024).

Although IBPs are well-suited to low-temperature environments, their sensitivity to elevated temperatures can limit their stability during thermal processing such as pasteurization. The thermal stability of IBPs varies widely depending on their structure and origin. Reported melting temperatures range from below 20 °C to above 80 °C, reflecting significant diversity among AFPs (Chao et al., 1996; Friis et al., 2009; Lin et al., 2011). Insect AFPs, often rich in disulfide bonds, tend to exhibit higher thermal stability, whereas fish AFPs generally show intermediate stability. Some AFPs can refold and regain activity after heat exposure, while others lose function irreversibly (Ramløv & Friis, 2020).

In contrast, IBPs typically exhibit broad pH stability, remaining active across a wide range (approximately pH 2–12) (Chao et al., 1994; Delesky et al., 2021; Gauthier et al., 1998; Kristiansen et al., 2005; Leiter et al., 2016). This is largely due to the ice-binding mechanism, which does not rely heavily on charged amino acids and is therefore less sensitive to pH changes. However, extreme pH conditions can reduce activity, particularly at high pH, where key residues involved in ice binding may be chemically modified. This wide pH tolerance is advantageous for application across diverse food systems (Delesky et al., 2021; Gauthier et al., 1998; Peramo, 2018; Ramløv & Friis, 2020).

The stability and functionality of IBPs in food systems are also strongly influenced by matrix interactions and environmental factors. In frozen foods, IBPs primarily act by inhibiting ice recrystallisation, thereby reducing structural damage during storage and freeze–thaw cycles (Eskandari et al., 2020; S. Xiao et al., 2024). However, their effectiveness depends on maintaining the integrity of the ice-binding surface, as conformational changes can reduce activity. Interactions with other food components, including proteins, lipids, and polysaccharides, can affect IBP solubility, distribution, and accessibility to ice interfaces, leading to variability in performance (Ramløv & Friis, 2020). Additionally, solution properties such as solute concentration influence IBP behavior and activity at the ice interface (Chasnitsky & Braslavsky, 2019).

Despite their potential, several limitations restrict the use of IBPs in food systems. Proteins with only ice-binding functionality may not fully prevent freeze-induced damage, and effective cryoprotection often requires combined ice-binding and stabilizing functions (Zhu et al., 2021). Furthermore, variability in thermal stability, sensitivity to processing conditions, and challenges related to large-scale production and cost limit their industrial application (Fu et al., 2025). Protein denaturation during processing or storage can also reduce long-term effectiveness (Baskaran et al., 2021).

Future developments are likely to focus on improving IBP stability and functionality through protein engineering and formulation strategies. Engineering approaches have shown potential to enhance thermal stability, broaden pH tolerance, and improve resistance to freeze–thaw cycles (Fu et al., 2025). Additionally, combining IBPs with other stabilizing agents offers a promising route to improve performance in complex food systems (Zhu et al., 2021).

1.4.4 Safety of using IBPs in food systems

The introduction of IBPs into food poses a potential risk as proteins can elicit an allergic reaction in individuals sensitive to that protein. Research into IBP consumption from natural sources shows that their intake may be substantial in northern and temperate regions, mainly through edible plants and fish. It is estimated that short-term exposure to IBPs is approximately a few hundred milligrams. In addition to that, based on the known history of IBP consumption, it does not impart a toxicologically significant effect in the short or long term. However, to introduce these proteins into food products, an

analysis of possible allergic reactions is a prerequisite for marketing the food (Bindslev-Jensen et al., 2003; Venketesh & Dayananda, 2008).

The sequence of the AFP type III from ocean pout has been compared with known allergens as well as assessed for pepsin resistance. It was found that the type III protein, or any heptamer peptides produced from it, showed no sequence similarity with known allergens. Also, the type III antifreeze protein and type III glycoconjugates were rapidly hydrolyzed by pepsin, resulting in fragments with a molecular weight less than 4 kDa. Hence, it can be concluded that type III, its glycoconjugates, and pepsin hydrolysis products are unlikely to provoke allergic responses in individuals sensitized to known allergens or to induce an IgE-mediated response from unsensitized individuals (Baderschneider et al., 2002; Venketesh & Dayananda, 2008).

Similarly, serum screening with IgE and histamine release from basophils from twenty fish-allergic individuals concluded that none of the patients exhibited IgE binding or histamine release from basophils concerning the type III AFP from cod. From these results, it could be concluded that AFPs do not pose an allergic risk to humans. Also, through the analysis of fish allergens, which are a health risk, it was established that AFP is not among the allergen proteins (Bindslev-Jensen et al., 2003).

In terms of toxicity, in vivo and in vitro genotoxicity assays have been conducted, which included bacterial mutation, chromosome aberration, mammalian cell gene mutation and rat bone marrow micronucleus, and a repeat-dose gavage study in rats for 3 months to evaluate the toxicological properties of an AFP type III. The protein did not exhibit genotoxic potential or subchronic toxicity during oral administration in rats (Hall-Manning et al., 2004). The evaluation of the effect on general health and immunogenicity of AFP type III on healthy volunteers who consumed the protein for 8 weeks showed that AFPs do not have any effect on general health, nor are they immunogenic (Crevel et al., 2002; Venketesh & Dayananda, 2008). Therefore, IBPs appear to be non-toxic and unlikely to elicit an allergic reaction in most individuals.

2 Aims of this dissertation

The aim of this dissertation is to characterize ice-binding proteins produced by *Pseudomonas fluorescens* AQP671 and evaluate their production under different growth conditions, as well as assess their applicability in frozen foods. The specific aims to achieve those objectives are:

I. Evaluate the expression and activity of ice-binding proteins produced by *Pseudomonas fluorescens* AQP671 under various temperature conditions.
II. Assess the effect of nitrogen source modulation on the expression and activity of *P. fluorescens* AQP671 IBPs.
III. Purify the proteins from the culture media and identify their DNA and amino acid sequences.
IV. Evaluate their applicability in frozen wheat dough to improve its quality and shelf life.
V. Identify potential IBP-producing bacteria on algae from the Baltic Sea.

3 Materials and Methods

3.1 Cultivation of *Pseudomonas fluorescens* AQP671

3.1.1 Culture and cultivation conditions

Pseudomonas fluorescens strain AQP671 was provided by Lallemand Inc. The strain was isolated from a *Laminaria* (brown algae) sample collected at Ganavan Bay, Oban, Scotland. The bacteria were maintained at 30 °C on Lysogeny Broth Agar (LB, Lab M) and cultivated at 30 °C in mineral medium (pH 7) containing $MgSO_4$ (1.5 g/L) and KH_2PO_4 (1.5 g/L), adding glycerol (20 g/L) as the carbon source and NH_4Cl (3 g/L) as the nitrogen source.

Cultivation was carried out on a shaker (Innova 43 Incubator Shaker Series) at 180 rpm, followed by growth in a 7 L bioreactor (Biobench, Applikon, The Netherlands). In the bioreactor, the pH was controlled at 7.0 using titration with 5 M NaOH and dissolved oxygen concentration pO2 > 10% of air saturation by adjusting the aeration rate and stirrer speed. The bioreactor was inoculated (1:9, v/v) with the 48-h shake flask-grown pre-culture and grown until glycerol was almost depleted. Then, for initiation of IBP production, the temperature was decreased to 5 °C, and glycerol (20 g/L) and NH_4Cl (3 g/L) or yeast extract (Lab M, 10 g/L) were added.

3.1.2 Nitrogen source modulation assessment

To study the impact of individual amino acids, a portion of the culture was withdrawn prior to the temperature shift-down and used to inoculate shake flasks (1:9, v/v) containing 20 mL of mineral medium with glycerol (20 g/L) and a single amino acid added as the sole nitrogen source. Each flask contained only one of the following amino acids: L-alanine, L-arginine, L-asparagine, L-glutamine, L-isoleucine, L-methionine, L-proline, L-serine, L-threonine, or L-valine, added in a concentration that corresponded to 1 g N/L.

These results were compared to those obtained using mineral medium supplemented with either yeast extract or ammonium chloride as the nitrogen source. The nitrogen content of the yeast extract was estimated based on the total amino acid content provided by the manufacturer.

3.1.3 Temperature modulation assessment

The effect of temperature was assessed in the presence of L-asparagine as the nitrogen source. The temperature values of 5, 10, 15, and 20 °C were selected to represent a biologically relevant range spanning from cold stress conditions, which are known to induce ice-binding protein production, up to moderate temperatures favorable for bacterial growth. Samples were collected at 24-hour intervals.

3.1.4 pH stability assessment

To evaluate the effect of pH on ice recrystallization inhibition activity, the pH of the culture supernatant obtained after 24 h of incubation at 5 °C was adjusted to 2, 4, 6, 8, 10, and 12, covering the physiological pH range relevant to *Pseudomonas fluorescens'* natural environment, as well as extreme pH values to assess protein stability and activity under stress conditions.

3.2 Ice recrystallization inhibition assessment

IRI activity was measured using the modified "sucrose sandwich" assay with some modifications, as previously described (Kaleda et al., 2018). 25 µl of supernatant of *P. fluorescens* AQP671 culture medium was mixed with a 70% sucrose solution (1:1, v/v ratio), and 3 µl of the solution was placed on a glass microscope slide, covered with a cover slip, and the edges were sealed with silicone oil. The microscope slide was then flash-frozen in liquid nitrogen and placed on a cooling stage (Linkam PE 120, UK) of a microscope (Nikon Eclipse E 200, Japan). The temperature for the cooling stage was set close to the ice crystal melting point of 35% sucrose solution (T = - 6.8 °C) and set to change according to the preset profile (Figure 6).

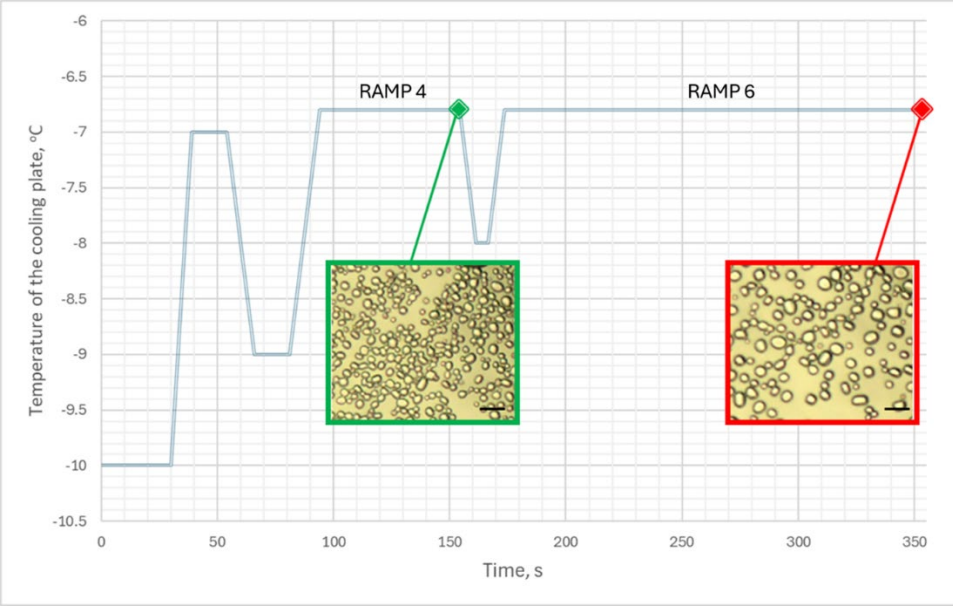

Figure 6: Temperature profile set points of the cooling plate for ice recrystallization inhibition (IRI) activity assessment. Images are taken at time points 154 and 354 s, highlighted in green and red accordingly. The microscope images shown are for the 35% sucrose solution at -6.8 °C.

The images of ice crystals were obtained using the Motic Images 3.0 program at the end of temperature ramps 4 and 6 (highlighted in green and red, respectively). Images were analyzed using the ImageJ image analysis tool, and the ice crystal growth rates were calculated using the Ostwald law equation (C. Budke et al., 2009) (eq. 1).

$$k = (r^3 - r_0^3)/t, \text{ where} \qquad \text{(eq. 1)}$$

k – ice crystal growth rate, µm^3/min
r – average ice crystal radius at the end of temperature ramp 6, µm
r_0 – average ice crystal radius at the end of temperature ramp 4, µm
t – time, min.

The dilution $D_{k50\%}$ of the sample, resulting in a 2-fold decrease of the maximum crystal growth speed k, was utilized to express the ice recrystallization inhibition activity (IRI).

The dilution $Dk_{50\%}$ was determined by preparing a series of 2-fold dilutions of the sample. The first dilution, 1:1 (v/v) of the sample, was made with a 70% sucrose solution, and the following 1:1 (v/v) with a 35% sucrose solution to maintain the 35% (m/v) sucrose concentration. Dilutions were made until the original sample was diluted up to 128 times (Figure 7).

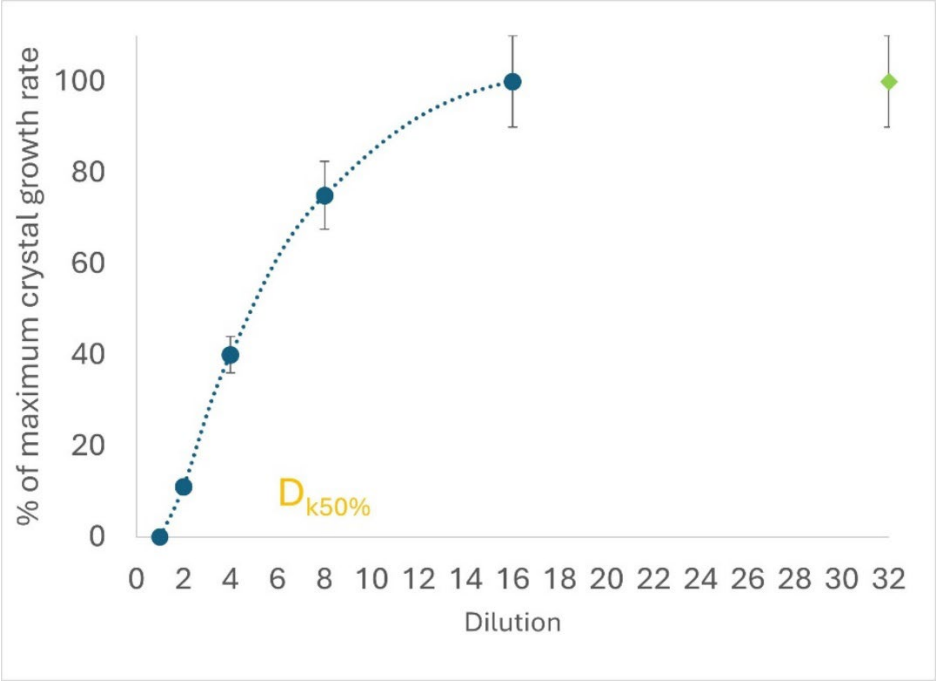

Figure 7: Graphical assessment of ice recrystallization inhibition (IRI) activity. Data represents mean values with standard deviation error bars (n = 3). The IRI activity is expressed as $D_{k50\%}$, calculated from the quadratic polynomial trend line (blue dotted line). The green marker at 32× dilution indicates a plateau in ice crystal growth rates across the dilution series.

The dilution D at which the ice crystal growth rate *k* reached half of the maximum speed ($D_{k50\%}$) was calculated by solving the quadratic equation (eq. 2) corresponding to the second-order polynomial trendline of the dilution graph as follows:

$$y = aD_{k50\%}^2 + bD_{k50\%} + c$$
$$y = 50$$
$$D_{k50\%} = \frac{-b \pm \sqrt{b^2 - 4a(c-50)}}{2a} \text{ , where} \qquad \text{(eq. 2)}$$

a, b, c – quadratic, linear and constant term
y – ice crystal growth rate relative to the maximum growth rate, %
$Dk_{50\%}$ - dilution at the growth rate corresponding to 50% of the maximum growth rate

This point was defined as the $D_{k50\%}$ inhibition point, corresponding to IRI activity. All samples were measured in triplicate.

3.3 Purification and identification of *P.fluorescens* AQP671 ice-binding proteins

3.3.1 Ice affinity purification

Ice affinity purification was carried out using the ice-shell method as previously described (Marshall et al., 2016). A 500 mL round-bottom flask was filled with 100 mL of distilled water and placed into a cooling bath containing 95% ethanol and dry ice (T = -80 °C). The flask was manually rotated for 1 minute until 20-25 mL of water was incorporated into the ice shell. The excess water was then removed, and the volume was measured. The ice shell was placed back into the cooling bath to fully freeze and form cracks in the shell.

The flask was attached to a rotary device and submerged in a cooling bath containing water, crushed ice and NaCl (T = -1.5 °C to -2.0 °C). The cooled IBP sample (250 mL) was slowly added to the flask, and the cooling bath was covered with an insulating material. The sample was rotated in the cooling bath for 1–2 h until about half of it was incorporated into the ice shell. The liquid fraction was removed, the shell rinsed with cooled phosphate buffer (0.5 M), and the ice shell melted and its volume measured.

The ice affinity purification was repeated for the ice shell two additional times, resulting in three ice fractions (IAP1, IAP2 and IAP3) and three liquid fractions (L1, L2, and L3). All fractions were analyzed for their ice recrystallization inhibition activity as described above and total protein content using Pierce™ Modified Lowry Protein Assay Kit (Thermo Fisher Scientific).

3.3.2 Ultrafiltration according to size

The ice affinity purification fraction with the highest specific activity according to protein concentration (IAP3) was further sequentially fractionated using ultrafiltration (Millipore, MWCO 100 kDa, 50 kDa, 30 kDa and 10 kDa). To improve protein filtration efficiency, samples were pretreated with detergents (Triton X-100 or Chaps) to reduce aggregation.

The samples were first passed through a 100 kDa cut-off filter, and the filtrate was collected and subsequently filtered through a 50 kDa unit. This stepwise filtration process was repeated with 30 kDa and finally 10 kDa filters, ensuring that each filtrate was sequentially processed through the next lower molecular weight cut-off filter. Retentates from each filtration step and the filtrate from the final filtration step were collected separately for ice-recrystallization inhibition assessment. Protein content at each filtration step was measured spectrophotometrically at 280 nm and using the Pierce™ Modified Lowry Protein Assay Kit (Thermo Fisher Scientific).

3.3.3 Protein identification via Mass-Spectrometry

Samples containing the highest IRI activity were sent to The Proteomics Core Facility of the University of Tartu for protein identification via LC-MS/MS. The sample was trypsin-digested, and the data were analyzed with MaxQuant (Cox et al., 2014), both de novo peptides and those matched against the protein database of AQP671 were used in downstream analysis. The resulting protein list was screened using BLAST non-redundant and Conserved Domain databases to determine their similarities to known ice-binding proteins.

3.3.4 Cloning and expression in *E. coli*

Genes encoding selected proteins were amplified by PCR using gene-specific primers with restriction sites (NdeI, BamHI) for cloning into the pET-15b vector, incorporating an N-terminal His6-tag for purification and ampicillin resistance for selection. The PCR products were ligated into the vector, and the recombinant plasmids were then transformed into chemically competent E. coli (DH5-alpha) cells by heat shock. Plasmids were purified and verified by sequencing. For protein expression, BL21RP+ cells were transformed and cultured in LB medium supplemented with 100 µg/mL ampicillin and 1% glucose at 37 °C until OD reached ≈ 0.6. For protein expression, IPTG (1 mM) was added, and cultures were incubated at 20 °C overnight.

3.3.5 Purification of recombinant proteins

After protein expression, *E. coli* cells were harvested by centrifugation at 4500 x g for 10 min. A total of 2-3 g of cell pellet was resuspended in 10 mL of the lysis buffer (50 mM NaH_2PO_4, 300 mM NaCl and 10 mM imidazole, pH 8) and flash frozen. The cells were then thawed and sonicated on ice in 10-second intervals with 10-15-second breaks, for a total of 9 cycles. The lysate was divided into 2 mL aliquots and centrifuged (14,000 rpm, 25 min) to remove cell debris.

The supernatant was loaded onto a Ni-NTA affinity column pre-equilibrated with the lysis buffer. The column was washed with the buffer (50 mM NaH_2PO_4, 300 mM NaCl) containing 20 mM imidazole to remove non-specifically bound proteins, and the His-tag protein was eluted using the buffer containing 250 mM imidazole. Eluted fractions were analyzed by SDS-PAGE to confirm purity and assessed for IRI activity and total protein content using the Pierce™ Modified Lowry Protein Assay Kit (Thermo Fisher Scientific). Results were compared to a negative control, which was the recombinant turnip mosaic virus (TuMV) NIb protein.

3.4 Thermal stability evaluation

To evaluate the thermal stability of the ice-binding proteins, samples were incubated at temperatures between 20 and 95 °C in 15 °C intervals for 15 min. After heat exposure, the samples were rapidly cooled on ice and then assessed for IRI activity by measuring ice crystal growth rates as previously described. Protein concentrations were selected to approximate the concentration associated with 50% IRI activity for each protein, enabling sensitive detection of temperature-dependent changes in activity. The results were compared with those obtained for recombinant type II fish antifreeze protein from sea raven (SRAFP), supplied by Lallemand Inc.

3.5 Assessment of the cryo-protective effect of *P. fluorescens* AQP 671 IBPs on frozen dough

3.5.1 Bread dough recipe

Wholegrain wheat flour (Tartu Mill, lot 137060), sugar (Extra Line), dry yeast (Kitchen Mood), salt (Santa Maria), canola oil (Olivia) and milk (Alma, 2.5% fat) were purchased from local grocery stores in Tallinn, Estonia. All reagents used were of analytical grade.

Pseudomonas fluorescens strain AQP671 was cultivated at 30 °C in shaker flasks on media containing 20 g/L glycerol and 10 g/L yeast extract for 48 h. The cells were removed, and the supernatant was collected by centrifugation at 1968 g for 20 min at 10

°C. Cells were resuspended in fresh original media for an additional 72 h at 10 °C to promote IBP production. The culture was centrifuged as above, and the supernatant was stored at -20 °C. Negative control and IBP solution were both assessed for ice recrystallization inhibition activity, and the total protein concentration was measured using Pierce™ Modified Lowry Protein Assay Kit (Thermo Fisher Scientific) according to the manufacturer's instructions.

3.5.2 Dough and bread preparation

The recipe for the dough, according to 1 kg of wholegrain wheat flour, contained 400 g of milk, 400 g of IBP solution or negative control, 130 g of sugar, 50 g of oil, 17 g of salt and 17 g of dry yeast. The ingredients were incorporated using a KitchenAid Heavy Duty 5KPM5 (Whirlpool Corporation, USA) mixer at speed 1 (60 rpm) for 2 minutes and at speed 2 (90 rpm) for 3 minutes. The dough was divided into 80 g portions, wrapped in low-density polyethene film and flash frozen at -18 °C for 4 h using a Foster Surf Navigation freezer. The dough was thawed immediately after freezing and further thawed at 2-week intervals at 4 °C overnight (15 h). During storage, the dough was kept at -18 °C.

The negative control contained the uninduced supernatant of *P. fluorescens* AQP671, and the samples enhanced with ice-binding proteins contained the cold-induced supernatant of *P. fluorescens* AQP671. The final concentrations of the cold-induced *P. fluorescens* supernatant in the dough were 1.25%, 2.5%, 5%, 10% and 20% (indicated as IBP-1.25%, IBP-2.5%, IBP-5%, IBP-10% and IBP-20%). The equivalent total added protein concentration in the doughs was 0.02 mg/mL, 0.04 mg/mL, 0.09 mg/mL, 0.18 mg/mL and 0.36 mg/mL as measured using the Pierce™ Modified Lowry Protein Assay Kit (Thermo Fisher Scientific) according to the manufacturer's instructions.

Once thawed, the dough was held at 32 °C, 80% RH using the Metos System Rational HCPC oven for 45 min to rise and then baked at 200 °C, 50% RH for 15 min.

3.5.3 Dough analysis

3.5.3.1 Yeast survival

The yeast survival rates were determined as previously reported (Zhao et al., 2022). Thawed dough (20 g) was suspended in distilled water (180 mL) and mixed for 30 min using a magnetic stirrer and then allowed to settle for 15 min. The solution was mixed with methylene blue dye (1:9, v/v) and incubated at room temperature for 10 min. The yeast cells were counted under a microscope (Nikon Eclipse E 200), using the Brüker chamber. All samples were measured in three replications.

3.5.3.2 Rising properties

The dough portions were placed in pre-greased baking moulds, flattened, and the height of the dough was measured (0.1 cm accuracy). The same measurement was recorded after rising to assess the rising properties of the dough. All measurements were done in 8 replications, and results were calculated as a percentage of the initial height.

3.5.3.3 Dough texture profile analysis

The dough and bread texture profile was determined using the TA-XT2i Stable Micro Systems texture profile analyzer, and results were analyzed with the Texture Expert Exceed program. The parameters for the analysis were chosen according to the literature (Rodríguez-Sandoval et al., 2008; Sharadanant & Khan, 2003a).

For the dough analysis, a cylindrical P25 probe (d = 25 mm) was used. The thawed dough was shaped into a 10 x 10 mm cylinder, placed onto the platform, compressed to 30% of its initial height, held for 10 seconds and compressed again. The speed was set to 1 mm/s.

Seven textural parameters were determined (hardness, elasticity, springiness, adhesiveness, cohesiveness, chewiness and gumminess) in 5 replications.

3.5.3.4 Starch microscopy

The size of the starch granules in the dough was analyzed as previously described (Yang et al., 2019) with slight modification. The starch slurry was dried as a thin layer on a microscope slide at 35 °C until the weight of the sample was constant. The sample was observed under a microscope (Nikon Eclipse E 200, Japan) at 100x and 400x magnification and the size of the starch granules was measured using the ImageJ image analysis tool. Approximately 300-500 starch granules were measured for each sample.

3.5.3.5 IRI activity in the dough

To assess the residual IRI activity in the dough, the dough was repeatedly washed with 50 mM phosphate buffer. The final ratio of dough to buffer was 1:2, w/w. The samples were then analyzed as previously described.

3.5.4 Bread analysis

3.5.4.1 Specific volume

The specific volume was assessed as described in the literature (Sharadanant & Khan, 2003b). After baking, the bread was allowed to cool down (1.5 h) and then weighed. The volume of the loaves was measured using silica gel granules (d = 0.5 cm). A 1 L beaker was filled to the line with the granules. Approximately ¾ of the granules were removed, the bread was placed into the beaker and filled again to the line with the granules. The unused granules representing the volume of the bread were measured using a graduated cylinder (2.5 cm^3 accuracy). Specific volume was calculated as cm^3/g, and measurements were done in 5 replications.

3.5.4.2 Bread texture profile analysis

The bread texture profile was determined using the TA-XT2i Stable Micro Systems texture profile analyzer, and results were analyzed with the Texture Expert Exceed program. The parameters for the analysis were chosen according to the literature (Sharadanant & Khan, 2003b). For the bread analysis, a cylindrical P36R probe (d = 36 mm) was used. A 25 mm slice of bread was cut from the cooled loaf, deformed to 40% of its initial height, held for 5 s and deformed again. The test speed was 1 mm/s.

Seven textural parameters were determined (hardness, elasticity, springiness, adhesiveness, cohesiveness, chewiness and gumminess) in 5 replications.

3.5.4.3 Sensory evaluation

Sensory evaluation of the bread samples was performed on the day of baking by a panel of 5–7 trained assessors. The breads were sliced into 1.5 cm pieces and evaluated against a commercially available wholegrain wheat bread (Täisterasepik, Eesti Pagar) used as the reference sample. Attributes related to appearance (color, porosity), texture (elasticity, crumbliness, moisture, softness, adhesiveness), aroma (intensity, sourness, yeast notes), and taste (intensity, sourness, saltiness, bitterness) were scored on a 0–10 scale relative to the predefined characteristics of the reference bread.

3.6 Statistical analysis

The statistical analysis of IRI activity and starch microscopy images was carried out using the ImageJ image analysis tool as well as Microsoft Excel. The data from the cultivation experiments were analyzed using Microsoft Excel (ANOVA, two-tailed paired t-test and Pearson's Correlation Coefficient). Results are presented with 95% confidence intervals. A p-value < 0.05 was considered statistically significant.

The data from the dough and bread experiments were analyzed using analysis of variance (ANOVA) with Tukey's Honest Significant Difference (HSD) test. The analysis was performed using Microsoft Excel's Data Analysis Toolpak, and a significance level of $p < 0.05$ was adopted, with calculations conducted using the ASTATSA program.

3.7 Identification of potential IBPs in Baltic Seaweed samples

DNA was extracted from approximately 5 g of frozen seaweed using a modified CTAB (cetyltrimethylammonium bromide) protocol. Seaweed samples were homogenized in saline solution with glass beads, and bacterial cells were concentrated through multiple centrifugation steps. The bacterial pellet was then lysed using pre-warmed CTAB buffer and mechanical disruption with glass beads, followed by incubation at 65°C.

DNA was purified by extraction with chloroform:isoamyl alcohol (24:1), and the aqueous phase containing DNA was recovered. DNA was precipitated using sodium acetate and cold isopropanol, incubated overnight at −20°C, and collected by centrifugation. The pellet was washed with 70% ethanol, air-dried, and resuspended in 30 µL of sterile water.

DNA concentration was quantified using a Qubit BR kit. The bacterial 16S rRNA gene V4 region was amplified using primers 515F and 806R and sequenced on an Illumina iSeq 100 platform using paired-end 2 × 150 bp reads according to the manufacturer's instructions. The BION-meta program was used for the microbiome data analysis.

4 Results and discussion

This dissertation is being defended on the basis of three publications and a manuscript, the results of which are summarized below.

4.1 Expression of IRI activity in *Pseudomonas fluorescens* AQP671 culture

IBPs are generally produced as a protective mechanism against freezing temperatures. Therefore, ice recrystallization inhibition (IRI) activity of *P. fluorescens* AQP671 was evaluated during cultivation on mineral media at 25 °C and after a temperature shift to 5 °C. Additionally, either yeast extract or NH_4Cl was used as a nitrogen source to assess the activity of potential IBPs in the presence of organic and inorganic nitrogen and at different temperature points (Publication III).

As shown in Figure 8, no IRI activity was detected during growth at 25 °C or following the shift to 5 °C when glycerol and NH_4Cl were used. In contrast, replacing NH_4Cl with yeast extract in the culture medium led to a rapid increase in IRI activity. Notably, this activity continued to rise throughout the 140-hour incubation period, reaching a dilution ($D_{k50\%}$) of 40 even after the culture had entered the stationary phase. Although this behavior has not previously been reported for ice-binding proteins (IBPs), similar patterns have been observed for other cold-inducible proteins. For example, cold-shock proteins in *Bacillus subtilis* and *Caulobacter crescentus* are known to be upregulated during the stationary phase (Graumann & Marahiel, 1999; Santos et al., 2015). The results of these cultivation experiments also highlight that a temperature shift-down is required for detectable IRI activity, indicating that it is an adaptation to cold.

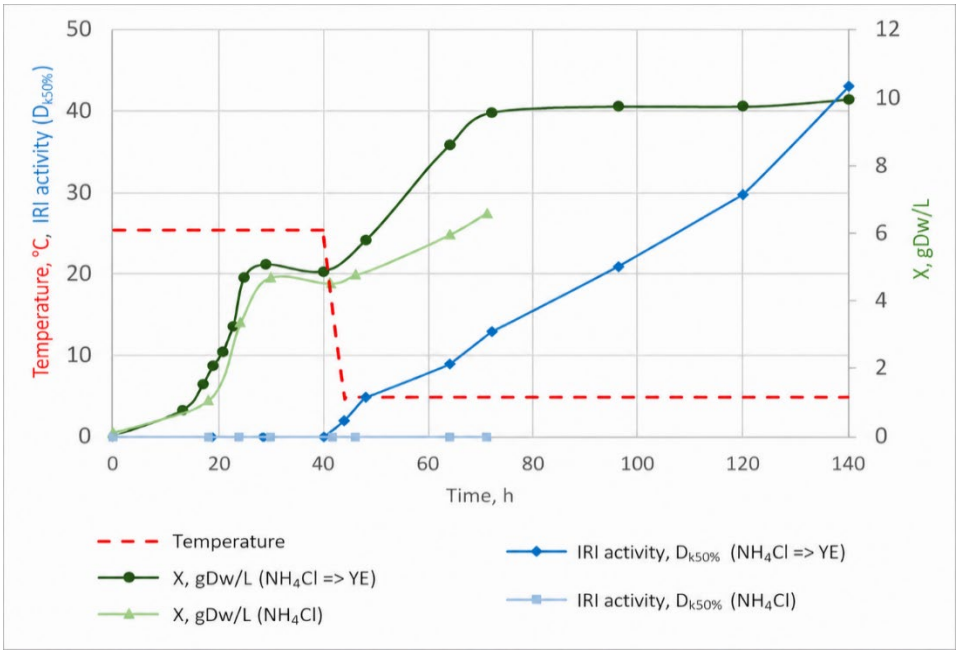

Figure 8: Comparison of two experiments assessing the growth and ice recrystallization inhibition (IRI) activity of Pseudomonas fluorescens AQP671 cultivated with different nitrogen sources following a temperature shift-down to 5 °C. In Experiment 1, ammonium chloride (NH_4Cl) was used

as the nitrogen source throughout cultivation (biomass (X): green line; IRI activity: blue line). In Experiment 2, yeast extract was added as the nitrogen source after the temperature shift-down (biomass (X): green line; IRI activity: blue line). The bioreactor temperature set point is shown by the red line.

Once the culture reached a biomass concentration of 10 gDW/L in the bioreactor, an aliquot of *P. fluorescens* AQP671 was transferred into flasks containing pre-cooled (5 °C) base medium supplemented with individual organic nitrogen sources: L-alanine (A), L-arginine (R), L-asparagine (N), L-glutamine (Q), L-isoleucine (I), L-methionine (M), L-proline (P), L-serine (S), L-threonine (T), or L-valine (V) to understand the effects of individual amino acids on IRI activity. Yeast extract (YE) served as a positive control, and NH_4Cl as a negative control. The cultures were then incubated at 5 °C with shaking (180 rpm) for 168 h.

Although each amino acid supplied an equivalent nitrogen concentration (1 g N/L), the highest biomass (5 gDW/L) was observed in the yeast extract medium, likely due to its more balanced nutrient profile (Tao et al., 2023). In comparison, cultures grown on single amino acids produced significantly lower biomass, ranging from 0.7 gDW/L with L-threonine to 1.5 gDW/L with L-alanine.

The effects of different nitrogen sources on IRI activity and total extracellular protein production after 168 h at 5 °C are shown in Figure 9.

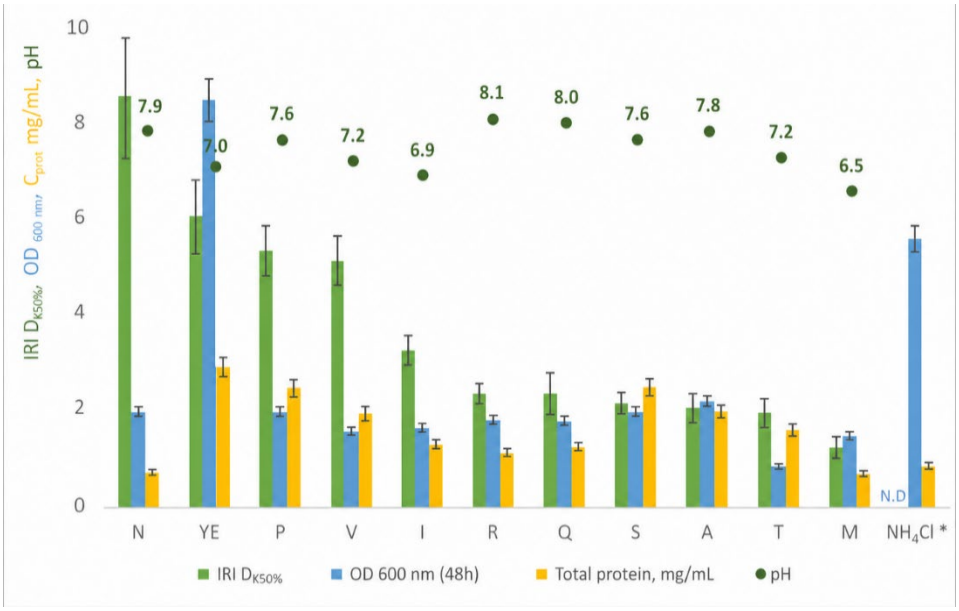

*Figure 9: The effect of nitrogen source (L-asparagine (N), yeast extract (YE), L-proline (P), L-valine (V), L-isoleucine (I), L-arginine (R), L-glutamine (Q), L-serine (S), L-alanine (A), L-threonine (T), L-methionine (M) on P. fluorescens AQP671 IRI activity (green bars) after 48 h incubation at 5 °C. Blue bars - the biomass concentration (OD 600 nm) at 48 h, orange bars - total protein concentration in the culture media at 168 h of incubation, yellow boxes - pH of the culture media after 168 h of incubation. Data represent mean values with standard deviation error bars (n = 3). The full data for each time point can be found in the supporting materials, Table S1. * As a comparison, NH_4Cl results correspond to the results from the experiment in the bioreactor at 71 h, shown in Figure 3. N.D – no activity detected.*

L-asparagine resulted in the highest IRI activity ($D_{k50\%}$) in the culture supernatant, followed by yeast extract, L-proline, and L-valine, whereas the other amino acids produced comparatively lower activity. When expressed relative to total protein concentration, L-asparagine showed substantially greater specific IRI activity than all other nitrogen sources evaluated.

The time course of IRI activity is presented in Figure 10. Across all nitrogen sources, IRI activity increased rapidly during the first 24 h after the temperature shift.

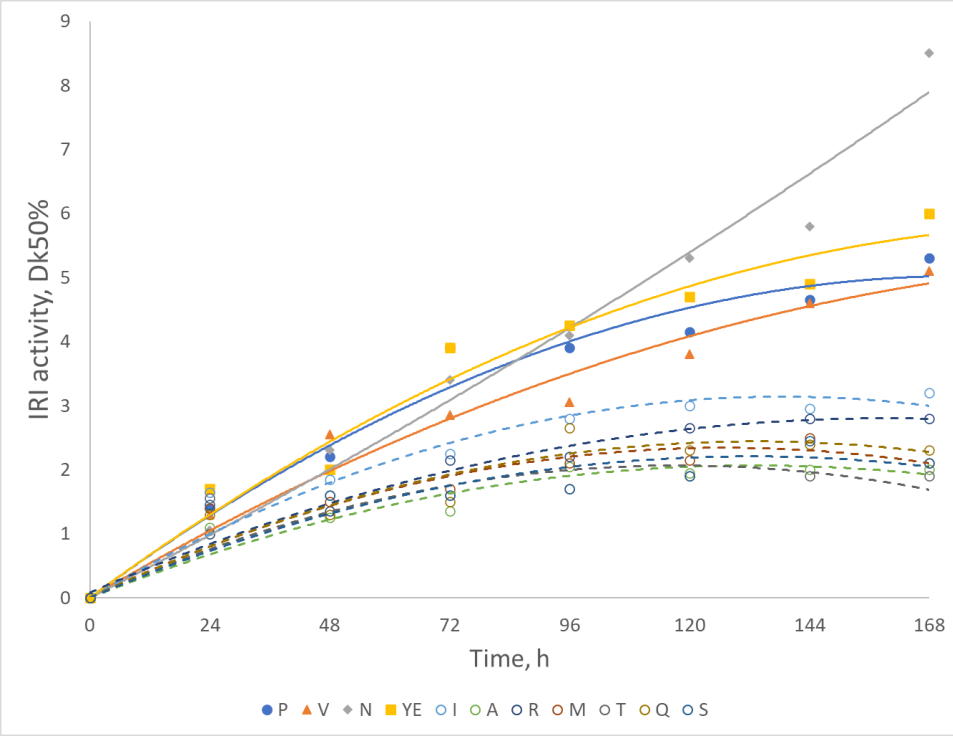

Figure 10: The change in ice recrystallization inhibition activity in Pseudomonas fluorescens AQP671 culture supplemented with different nitrogen sources during incubation at 5 °C on a shaker, 180 rpm. Solid lines – high activity group: L-proline (P), L-valine (V), L-asparagine (N) and yeast extract (YE), dashed lines – low activity group: L-isoleucine (I), L-alanine (A), L-arginine (R) and L-methionine (M), L-threonine (T), L-glutamine (Q), L-serine (S). Data represent mean values (n = 3).

Based on the observed IRI activity, the tested nitrogen sources could be classified into two groups. The high-activity group, comprising L-asparagine, yeast extract, L-proline, and L-valine, displayed a continuous linear increase in IRI activity throughout the experiment ($R^2 > 0.9$), even after biomass formation had stopped. In contrast, the moderate- to low-activity group, including L-isoleucine, L-alanine, L-arginine, L-methionine, L-threonine, L-glutamine, and L-serine, showed a slower rise in IRI activity that plateaued with growth, reaching $Dk_{50}\%$ values between 2 and 3.

For most nitrogen sources, IRI activity exhibited a strong positive correlation with cell density (Pearson correlation coefficient, PCC > 0.9). However, weaker correlations were observed for L-asparagine (PCC = 0.87), L-glutamine (PCC = 0.83), and L-threonine (PCC = 0.64). No detectable IRI activity was found when NH_4Cl served as the sole nitrogen

source, indicating that organic nitrogen is necessary for IBP induction. Nevertheless, due to the unknown specific activity of IBPs, it was not possible to directly relate protein concentration to IRI activity.

Similar enhancement of antifreeze activity has been reported in *P. fluorescens* KUAF-68, where supplementing L-asparagine (0.025%w/v N) nearly doubled thermal hysteresis activity (Kawahara et al., 2004). While the mechanisms underlying amino-acid-specific IRI enhancement remain unclear, *Pseudomonas* species possess enzymes such as L-asparaginase that facilitate nitrogen assimilation specifically from L-asparagine (De Groot & Lichtenstein, 1960; Sindhu & Manonmani, 2018). Furthermore, amino acid assimilation engages distinct metabolic pathways compared to inorganic nitrogen, potentially triggering specific gene regulation required for IBP production (Brown et al., 1973; Hervás et al., 2009).

To evaluate the effect of temperature on IRI activity, bioreactor-derived precultures were incubated for 96 h at 5, 10, 15, and 20 °C in medium supplemented with L-asparagine as the nitrogen source. IRI activity in the culture supernatant was detected at temperatures of 15 °C and below (Figure 11).

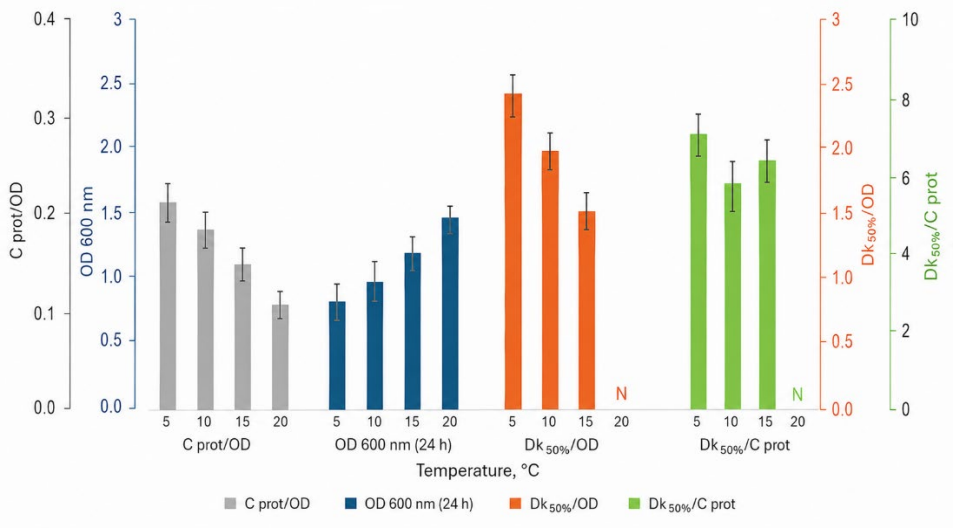

Figure 11: Total protein concentration normalized to cell density (gray), biomass concentration at 24 h (blue), IRI activity normalized to biomass concentration (orange), and IRI activity normalized to total protein concentration in the culture media of P. fluorescens AQP671 after incubation for 24 h at 5, 10, 15 and 20 °C. Data represent mean values with standard deviation error bars (n = 3). N – not detected.

The results indicate that both total protein content and IRI activity, when normalized to cell density, increased with decreasing cultivation temperature. However, in agreement with previous observations using other amino acids, no clear correlation was found between total extracellular protein concentration and IRI activity, suggesting that the proteins responsible for IRI constitute only a minor fraction of the secreted proteins. This is consistent with earlier reports demonstrating that IRI activity can be detected at nano- to micromolar concentrations of IBPs (Ramløv & Friis, 2020; Vance et al., 2019).

Although biomass concentrations declined at lower temperatures, both total protein production and IRI activity per unit biomass increased. In contrast, IRI activity normalized to protein concentration remained relatively stable.

At 5–10 °C, IRI activity increased linearly over the course of the incubation. No significant differences in activity were observed among 5, 10, and 15 °C during the first 72 h ($p > 0.05$); however, after 96 h, activity was significantly higher at 10 °C and lowest at 15 °C.

Overall, the temperature range for IBP induction in *P. fluorescens* AQP671 was comparable to previously reported values for bacterial IBPs, including *P. fluorescens* KUAF-68 (5 °C), *Pseudomonas putida* GR12-2 (10 °C), and *Moraxella* sp. (10 °C) (Kawahara et al., 2004).

4.2 The effect of pH on ice recrystallization inhibition activity of *P. fluorescens* AQP671 supernatant

The influence of pH on IRI activity was assessed by cultivating bioreactor-derived precultures at 5 °C in flasks supplemented with 1 g N/L L-asparagine until a biomass concentration of 1 gDW/L was attained. The culture supernatant was subsequently adjusted to pH values of 2, 4, 6, 8, 10, and 12 and immediately analyzed for ice-binding protein activity. As illustrated in Figure 12, the highest IRI activity was observed at pH 6, whereas it decreased sharply under acidic conditions (pH 2 and 4) and more moderately under alkaline conditions (pH 10 and 12).

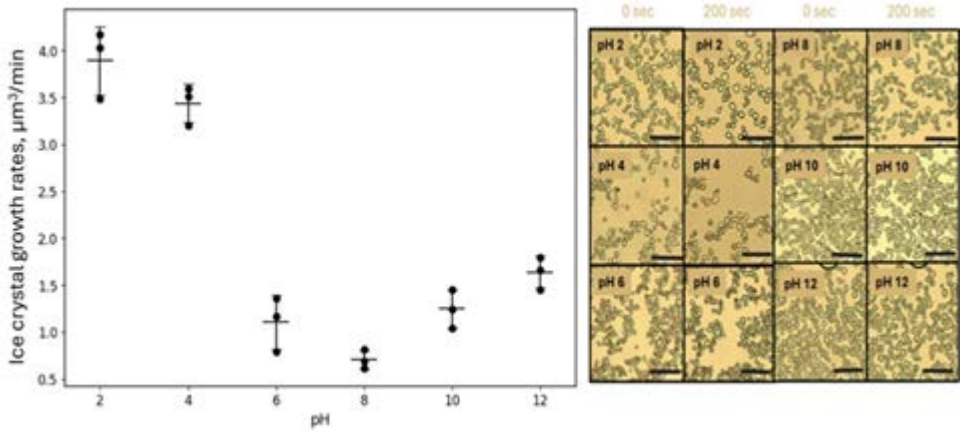

Figure 12: Ice recrystallization inhibition activity in P. fluorescens AQP671 culture supernatant. Data represent mean values with standard deviation error bars (n = 3) (left). Microscopic images of the ice crystals in the culture supernatant (2x diluted) at different pH values. The scale vars are 50 µm (right).

These findings partially contrast with earlier studies reporting that antifreeze proteins (AFPs) from fish and insects, which exhibit both thermal hysteresis and IRI activity, show minimal or no dependence on pH (Chao et al., 1994; Kristiansen et al., 2005; Leiter et al., 2016; Li et al., 1998). However, type III AFPs and ice-binding proteins (IBPs) from spruce budworm have been shown to display a slight reduction in activity under acidic conditions, consistent with the behavior observed in the present study (Gauthier et al., 1998). This reduction has been linked to alterations in the secondary structure tendencies of protonated residues, potentially decreasing the number of nearby water

molecules and disturbing the solvation structure at the ice-binding and basal surfaces (Gauthier et al., 1998; Peramo, 2018).

Among characterized IBPs, those derived from *Marinomonas primoryensis* (MpIBPs) exhibit a pH stability profile most comparable to that of *P. fluorescens* AQP671. MpIBPs lose ice-binding capability at pH ≤ 4 and ≥ 13, whereas within the pH range of 6–12, they reduce ice crystal grain size, and between pH 6 and 10, they additionally demonstrate dynamic ice shaping (Delesky et al., 2021). Together, these observations suggest that pH sensitivity in IBPs is not a universal feature but is instead dependent on species and protein structure.

4.3 Purification of IBPs

The purification, identification and verification of IBPs is shown in manuscript IV. Ice-affinity purification was used to isolate ice-binding proteins from *Pseudomonas fluorescens* AQP671. The efficiency of the purification process was assessed by determining IRI activity normalized to protein concentration. As illustrated in Figure 13, specific activity increased with each successive purification step, and 50% inhibition of ice recrystallization was achieved at progressively lower protein concentrations, indicating effective enrichment of IBPs.

Nevertheless, measurable IRI activity persisted in the liquid fractions, suggesting incomplete recovery of IBPs, potentially due to weak ice-binding interactions or the presence of non-protein components in the aqueous phase that also contribute to ice recrystallization inhibition.

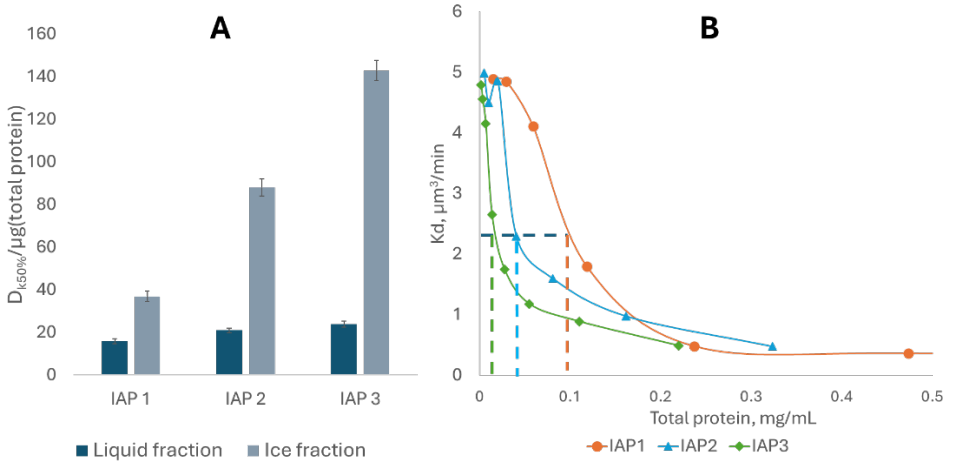

Figure 13: Specific activity of ice recrystallization inhibition in ice and liquid fractions of three consecutive purifications (left) of Pseudomonas fluorescens AQP671 culture media. Dilution curves relating the total protein content and ice recrystallization inhibition activity in each corresponding purified ice fraction (right).

The total protein yield of the final ice-affinity purification fraction (IAP3) was ≈ 1.5% of the initial sample, indicating effective removal of most non-IBP active contaminants, as confirmed by SDS-PAGE analysis. Most protein bands remained in the liquid fractions,

while the ice fraction primarily contained protein bands with the molecular weights of approximately 30 kDa and 150 kDa.

These findings do not align with the results observed in the study by Kawahara et. al (2004), describing two IBPs with molecular masses approximately 80 kDa and over 600 kDa. The discrepancies in SDS-PAGE profiles could be attributed to strain variability, differences in protein purification methods, variations in protein oligomerization, or degradation. It is also possible that the protein bands observed on SDS-PAGE represent contaminants, while the ice-binding proteins in the solution exist at concentrations too low to be detected. To further identify the proteins responsible for ice recrystallization inhibition activity, additional purification steps were performed.

The final ice fraction obtained from ice-affinity purification (IAP3) was subjected to sequential filtration using membranes with defined molecular weight cut-offs to estimate the size range of the ice-binding proteins and reduce contaminants. Filtration was first carried out without pretreatment, followed by additional steps in the presence of detergents such as Triton X and CHAPS. The resulting fractions, along with their corresponding ice crystal growth rates and total protein concentrations, are summarized in Table 1.

Table 1: Ice crystal growth rates and total protein concentration after filtration of sample IAP3 with and without pretreatment with detergents. Fractions exhibiting ice recrystallization inhibition are highlighted. N.D – not detected.

	IAP 3		IAP 3 + Triton X		IAP 3 + CHAPS	
Molecular weight (Mw)	K_d, $\mu m^3/min$	C_{prot}, µg/ml	K_d, $\mu m^3/min$	C_{prot}, µg/ml	K_d, $\mu m^3/min$	C_{prot}, µg/ml
> 100 kDa	0.49	0.277	1.05	0.073	1.20	0.038
50 – 100 kDa	3.99	0.005	0.51	0.010	0.97	0.030
30 – 50 kDa	4.55	0.003	3.45	0.015	0.45	0.043
10 – 30 kDa	5.21	N.D	3.79	N.D	0.66	0.031
< 10 kDa	5.07	N.D	5.60	N.D	4.79	N.D

In the untreated IAP3 sample, IRI activity was detected exclusively in the fraction containing proteins larger than 100 kDa, suggesting possible protein aggregation or association with membrane components. Pretreatment with Triton X enhanced filtration performance, resulting in a shift of peak activity to the 50–100 kDa fraction. In contrast, the addition of CHAPS led to a broader distribution of ice-binding proteins across all size fractions, except for those below 10 kDa.

The differences between Triton X- and CHAPS-treated samples are likely explained by their respective micelle sizes. Triton X forms relatively large micelles (~80 kDa), which restrict passage through smaller molecular weight cut-off filters, whereas CHAPS forms smaller micelles (~10 kDa), facilitating greater protein mobility during filtration (Herrera et al., 2014; Yedgar et al., 1974).

Based on their high IRI activity relative to protein concentration, two fractions were selected for mass spectrometry analysis: the 50–100 kDa fraction from IAP3 treated with Triton X (IAP+T50–100) and the 30–50 kDa fraction from IAP3 treated with CHAPS (IAP+C30–50).

Two samples, the 50 -100 kDa fraction from IAP3 + Triton X (IAP+T50-100) and the 30 – 50 kDa fraction from IAP3 + CHAPS (IAP+C30-50), were selected for mass spectrometry analysis based on their high activity relative to protein content.

4.4 Protein identification via mass spectrometry

Mass spectrometry analysis was performed on the selected fractions (IAP+T50-100 and IAP+C30-50) to identify the proteins potentially responsible for ice recrystallization inhibition activity. The analysis revealed a diverse set of proteins, which were screened using BLAST and Conserved Domain search to identify any proteins that had similarities with proteins or motifs that have been previously described as having IRI activity.

Two proteins of interest were selected from the results. First, a giant adhesin from the LapA family with a molecular weight of 605.83 kDa (PfAdh), which showed similarity to ice-binding adhesins from *Marinomonas primoryensis* and *Marinomonas arctica* (BSI20414). Both adhesins have the repeats-in-toxin (RTX) motif (GGXGXDX(L/I/F)X) associated with the ice-binding site of these IBPs (Garnham et al., 2008; Guo et al., 2017; Liao et al., 2021). The second protein of interest also exhibited the RTX motif but had a smaller molecular weight (49.34 kDa) and was characterized as a metallopeptidase (PfMp).

Interestingly, the domain of unknown function 3494, often found in bacterial IBPs, was not identified in any of the proteins present in IAP+T50-100 and IAP+C30-50.

4.5 Cloning, expression and purification

To validate the identified IBP candidates, both proteins were cloned, expressed, and purified. PfMp was produced as a full-length construct, whereas PfAdh was expressed as a truncated variant (30.33 kDa) containing the domain presumed to confer IBP activity. Successful gene insertion was confirmed by sequencing prior to expression, and protein solubility was verified using SDS-PAGE analysis.

During purification using a Ni-NTA affinity column, eight elution fractions (E1–E8) were collected for each protein. The corresponding ice crystal growth rates and total protein concentrations are summarized in Table 2. For both PfAdh and PfMp, the majority of the protein eluted in the first fraction (E1), which also exhibited the highest ice recrystallization inhibition activity.

Table 2: Ice crystal growth rates and total protein concentrations of elution fractions from the Ni-NTA affinity column of Adhesin (PfAdh) and Metallopeptidase (PfMp), E0 shows the result for the column wash fraction.

	PfAdh		PfMp	
	K_d, µm³/min	C_{prot}, µg/mL	K_d, µm³/min	C_{prot}, µg/mL
E0	5.94 ± 1.44		5.87 ± 1.09	
E1	1.10 ± 0.59	239.7 ± 15.5	0.69 ± 0.22	217.7 ± 11.9
E2	2.37 ± 1.09	99.0 ± 9.6	1.39 ± 0.23	102.7 ± 4.2
E3	2.53 ± 1.06	92.3 ± 5.5	2.01 ± 0.90	79.3 ± 7.1
E4	2.45 ± 0.45	93.0 ± 5.6	4.98 ± 1.03	66.7 ± 1.5
E5	4.32 ± 2.02	91.0 ± 7.0	5.89 ± 1.55	67.0 ± 2.0
E6	5.92 ± 0.64	75.7 ± 11.5	6.00 ± 1.45	65.0 ± 4.0
E7	5.49 ± 1.60	67.7 ± 12.1	5.96 ± 0.60	64.0 ± 4.4
E8	5.99 ± 1.48	63 ± 10.4	5.98 ± 1.57	62.7 ± 2.1

The highest activity fractions, PfAdh E1 and PfMp E1, were further evaluated by creating a row of dilutions and establishing the point at which half of the activity is present ($D_{Kd50\%}$). The resulting dilution curves and their comparison with the original IAP 3 sample, as well as a negative control exhibiting no ice recrystallization inhibition, can be seen in Figure 14.

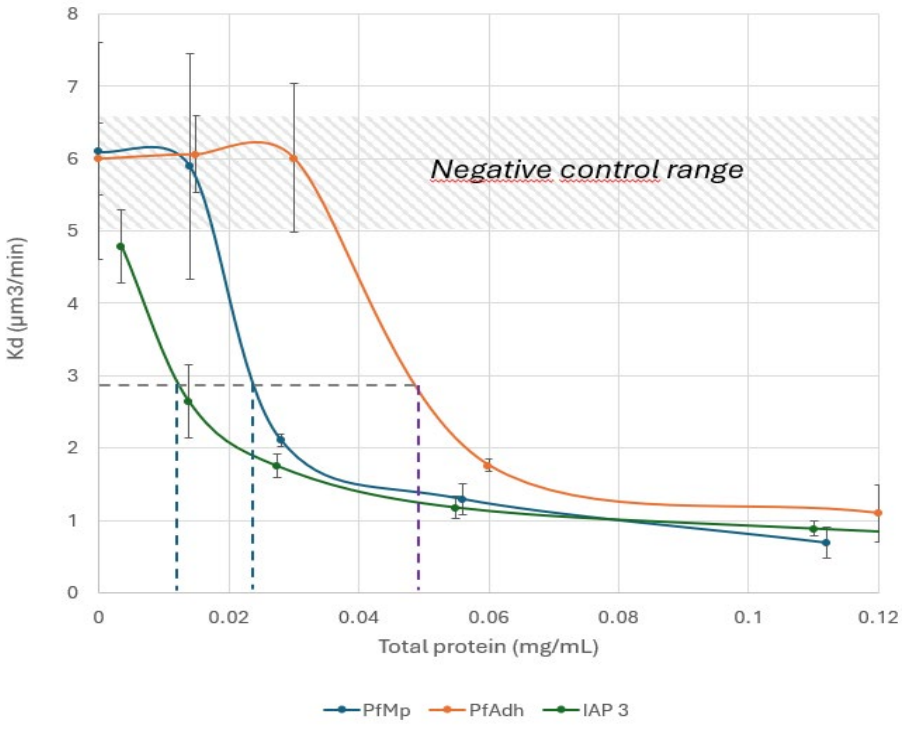

Figure 14: ice recrystallization inhibition assessment of the adhesin (PfAdh) and metallopeptidase (PfMp) proteins compared to the third ice fraction from ice affinity purification (IAP3) and the negative control (TuMV Nib) in relation to protein concentration.

According to the dilution curves, the concentrations correlating to the $C_{Kd50\%}$ values of the proteins of interest were 0.05 mg/mL and 0.02 mg/mL for PfAdh and PfMp, respectively. IBPs exhibiting IRI activity can be classified based on their inhibitory concentrations (C_i, molar concentration causing 50% of ice recrystallization inhibition) as very effective ($C_i < 10^{-1}$ µmol/L), effective ($10^{-1} < C_i < 10^3$ µmol/L) or ineffective ($C_i > 10^3$ µmol/L) (Carsten Budke et al., 2014; Vance et al., 2019). Thus, the IBPs produced by *P. fluorescens* AQP671 can be described as either effective (C_iPfAdh = 2 µmol/L, C_iPfMp = 0.4 µmol/L).

The activities of both individual proteins remained lower than that of the original IAP3 sample, which could indicate reduced ice recrystallization inhibition of recombinant proteins, the presence of an additional ice-binding protein, or other synergistic compounds in the IAP3 sample that increase the activity of the proteins of interest.

4.6 Thermal stability of proteins

The thermal stability of the ice-binding proteins was evaluated to verify whether PfAdh and PfMp were the primary contributors to IRI activity. This was done by measuring IRI activity following incubation at temperatures ranging from 20 to 95 °C (Figure 15).

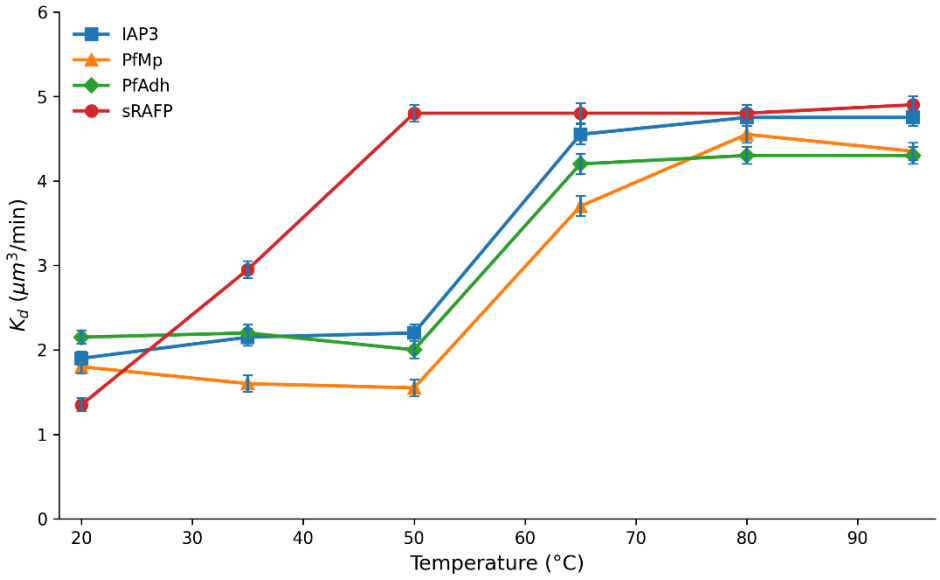

Figure 15: Ice crystal growth rates (Kd) of the Ice-binding proteins at different temperatures in the ice affinity purification fraction (IAP3), the two purified proteins from Pseudomonas fluorescens AQP671 (PfAdh - adhesin, PfMp - metallopeptidase) compared with the antifreeze proteins from Sea Raven (sRAFP)

The ice-affinity purification fraction (IAP3), metallopeptidase (PfMp), and adhesin (PfAdh) samples retained IRI activity after incubation at temperatures up to 50 °C, with no significant changes in ice crystal growth rates observed. At higher temperatures, a reduction in activity became evident, with a pronounced increase in ice crystal growth rates following incubation at ≥ 65 °C, indicating thermal denaturation of the proteins under these conditions. In contrast, the sea raven antifreeze protein exhibited reduced IRI activity at 35 °C and a complete loss of activity at 50 °C.

These results further support the conclusion that PfMp and PfAdh are the primary contributors to the observed IRI activity in *P. fluorescens* AQP671, as proteins with distinct structural characteristics are expected to display different temperature-dependent activity profiles. Similar variability in thermal stability has previously been reported among ice-binding proteins, with denaturation temperatures strongly influenced by protein structure. For example, fish IBPs generally exhibit moderate thermal stability, with melting temperatures ranging from 40–50 °C, whereas insect AFPs often display substantially greater thermostability. Notably, the AFP from *Microdera punctipennis* retained activity even after exposure to 100 °C (Friis et al., 2009). However, not all IBPs are heat-tolerant; rapid loss of activity has been reported for *Campaea perlata* AFPs at 22 °C and for a natural fish type I antifreeze variant at 18 °C (Chao et al., 1996; Lin et al., 2011).

4.7 Cryo-protective effects of *P. fluorescens* AQP671 IBPs on frozen dough

Unbaked dough is particularly susceptible to freezing damage due to its high water content. During freezing, the formation and growth of ice crystals can damage yeast cells, disrupt gluten networks, and alter the morphology of starch granules, ultimately reducing dough quality. Therefore, the use of IBPs as cryoprotective agents shows strong potential for improving the stability and quality of frozen dough. The effect of *P. fluorescens* IBPs on frozen dough is shown in Publication II.

4.7.1 Analysis of the dough

IRI activity was tracked in frozen dough over an 8-week storage period. As shown in Figure 14, the lowest ice crystal growth rates were observed in dough extracts containing the highest IBP concentrations, corresponding to the greatest activity. A decline in activity was most evident at week 4 in the sample supplemented with 20% IBP solution and at week 2 in the remaining samples. Following the initial increase in ice crystal growth rates, the values stabilized.

Despite this reduction, growth rates remained lower than those of the negative control throughout the experiment, indicating that while frozen storage and repeated

freeze–thaw cycles reduce protein stability, they do not completely eliminate IBP activity.

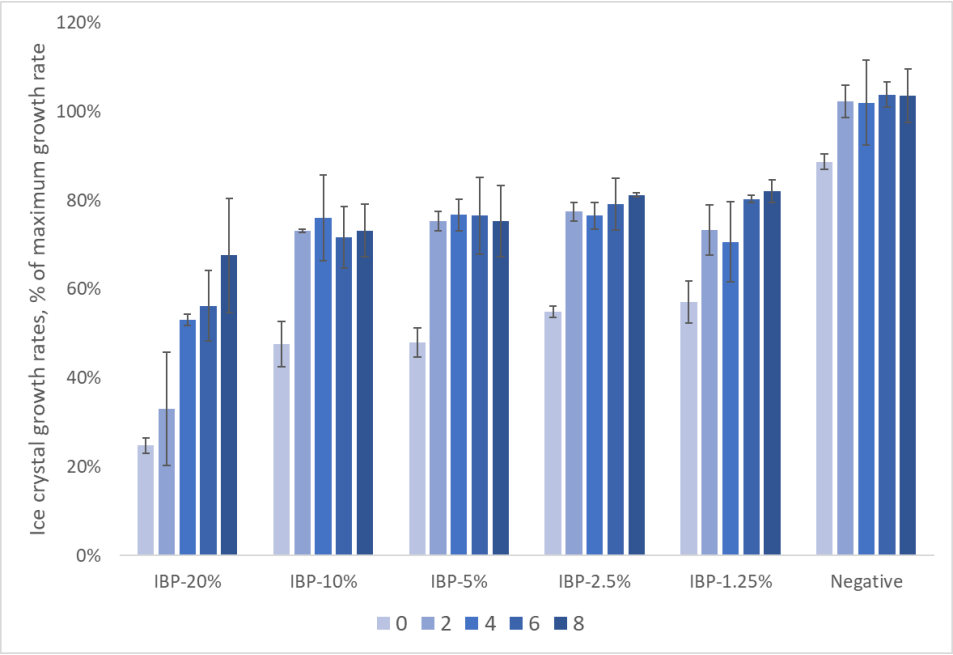

Figure 16: Ice recrystallization inhibition (IRI) activity of 2x diluted frozen dough extracts in 70% sucrose solution. Results are expressed as the percentage of average crystal growth speed relative to the negative control.

Yeast survival during the 8-week frozen storage of whole wheat dough followed a similar trend, as illustrated in Figure 16a. Immediately after freezing (0 h), survival rates decreased by an average of 9.7 ± 2.7% in IBP-treated samples and 17.5 ± 4.0% in the negative control relative to unfrozen dough.

Prolonged frozen storage further reduced yeast viability. In the negative control, survival rates remained relatively stable until week 4, after which they declined. A similar pattern was observed for the two lowest IBP concentrations (IBP-2.5% and IBP-1.25%), with decreases occurring after week 8. In contrast, samples containing higher IBP concentrations (IBP-20%, IBP-10%, and IBP-5%) showed no significant changes in survival throughout the storage period.

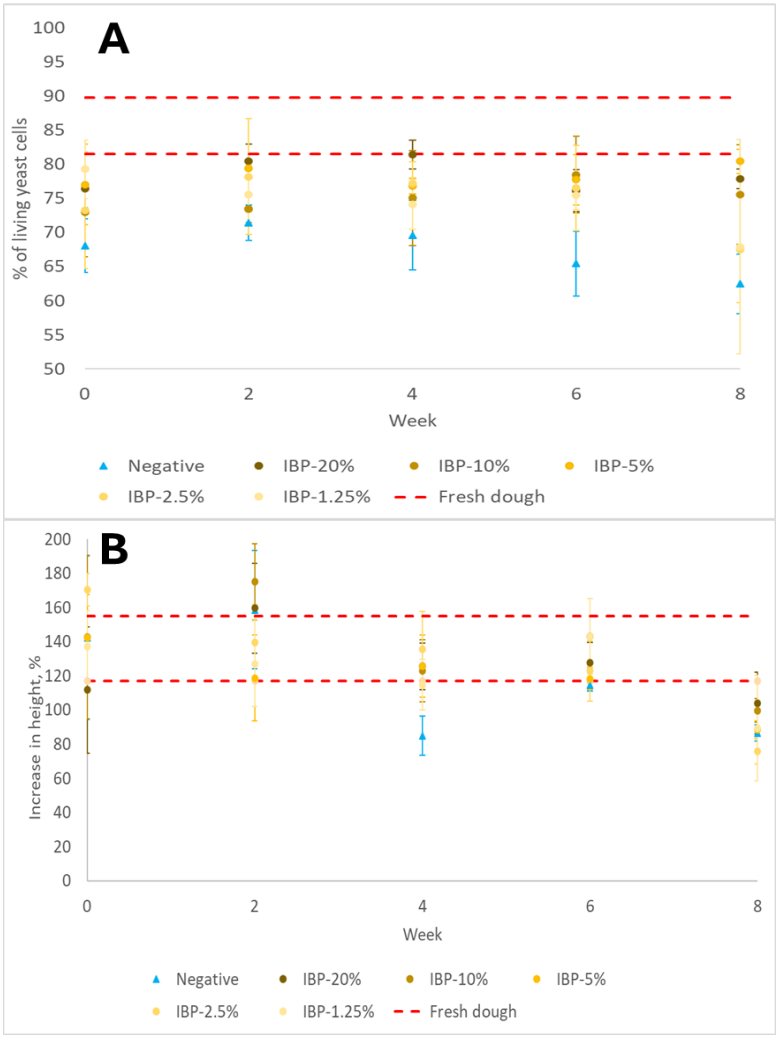

Figure 17: Living yeast cell counts in thawed dough (A) and dough leavening performance (B) in dough containing 0-20% ice-binding proteins (IBPs) during 8 weeks of frozen storage. The red dotted lines indicate the value range for the unfrozen fresh dough (A: 85.5 ± 4.3%, B: 136.0 ± 19.0%).

Ice crystal growth and recrystallization are known to substantially reduce viable yeast cell counts in frozen dough. However, the reductions observed in this study were less severe than those reported in previous literature, where yeast survival has been shown to decline by 53–99% after 45 days of frozen storage (Nguyen et al., 2018; Phimolsiripol, 2009; Tian et al., 2020). The incorporation of ice-binding collagen peptides has been reported to similarly enhance yeast viability, increasing survival by up to 55% and yielding maximum survival rates of approximately 70–80% after 4 weeks of storage (Nguyen et al., 2018; Tian et al., 2020).

Dough leavening performance, expressed as changes in loaf height, reflects yeast vitality and CO_2 production. As shown in Figure 17b, the rising capacity of all samples declined over the 8-week period, with the most pronounced reduction occurring at week 4, coinciding with decreased IBP activity and yeast survival. Among the tested conditions,

samples containing higher IBP concentrations (IBP-20% and IBP-10%) retained the greatest loaf height after 8 weeks, at 88.9% and 85.1%, respectively, relative to freshly prepared dough. In contrast, the negative control and samples with lower IBP concentrations (IBP-5%, IBP-2.5%, and IBP-1.25%) showed reduced retention, ranging from 64.7% to 76.2%.

Freezing can also induce starch retrogradation, leading to various undesirable structural changes in frozen dough. Starch granules are generally classified into two size groups: larger A-type granules (10–35 µm in diameter) and smaller B-type granules (<10 µm). A-type granules have been reported to exhibit greater resistance to freezing stress (Sandeep et al., 2010; Yang et al., 2019).

In all dough samples analyzed, B-type granules were predominant, accounting for 87.9–97.0% of the total granules observed (Figure 18). In unfrozen dough, the mean sizes of A- and B-type granules were 12.69 ± 2.69 µm and 3.87 ± 1.76 µm, respectively. The most pronounced reduction in granule size during storage occurred in the negative control, where the mean B-type granule size decreased from 3.32 ± 1.12 µm at week 0 to 2.54 ± 1.25 µm at week 8. The IBP-1.25% sample maintained a relatively stable granule size for the first 6 weeks, followed by a significant decrease at week 8 to 3.04 ± 1.22 µm.

This reduction in granule size is likely associated with ice crystal growth, which can damage starch granules, leading to the leakage of amylose, proteins, and lipids (Yang et al., 2019). Amylose release, in particular, has been linked to negative effects in baked bread, as it promotes the formation of a network that increases crumb firmness (Bárcenas et al., 2003; Silvas-García et al., 2016). In contrast, the other IBP-treated samples maintained B-type granule sizes comparable to those of fresh dough, ranging from 3.42 to 4.12 µm throughout the 8-week storage period. The larger A-type granules showed no significant changes during freezing, consistent with previous findings (Sandeep et al., 2010).

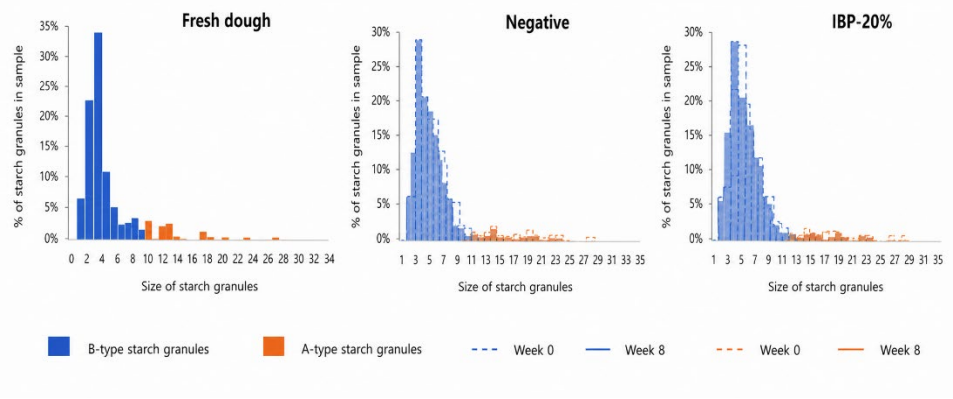

Figure 18: Size distribution of the starch granules in fresh and frozen dough during 8 weeks of frozen storage. A-type granules are in orange and B-type granules in blue. Dotted bars indicate results at week 0, and colored bars indicate results at week 8.

The structural properties of dough are largely determined by the formation of the gluten network during kneading and fermentation (Paraskevopoulou et al., 2010; Totosaus et al., 2013). This network can be disrupted by ice crystal growth during freezing and frozen storage (Cao et al., 2020; Liu, Liang, Wang, et al., 2018; Sharadanant & Khan, 2003b). Additionally, the incorporation of non-gluten-forming proteins may negatively affect

dough structure by diluting the gluten protein content, resulting in a weaker network (Paraskevopoulou et al., 2010; Totosaus et al., 2013).

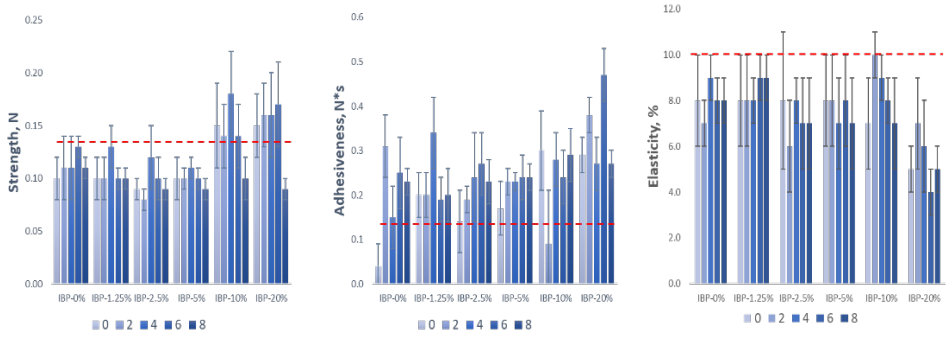

Figure 19: Dough texture parameters during 8 weeks of frozen storage at two-week intervals. The dotted line indicates the average value for fresh dough.

The texture of the whole wheat dough remained similar in terms of cohesiveness and springiness to that of fresh dough throughout frozen storage. As shown in Figure 18, the two highest IBP concentration doughs exhibited an improved dough strength during the first 6 weeks of frozen storage, which could be connected to better preservation of the gluten network. Differences were not significant for lower IBP concentration doughs and the negative control. These results correlate with the gumminess and chewiness of the dough.

The elasticity of the dough decreased after freezing. Additionally, the undiluted IBP sample showed a consistently lower elasticity, whereas the second-highest IBP concentration appeared to help maintain the elasticity of the dough the longest.

The adhesiveness of the dough had the most deviation over the weeks. In general, the adhesiveness of the dough increased after freezing when compared to the fresh dough. Both the decrease in elasticity, as well as the increase in adhesiveness, affected the handling of the dough negatively, which additionally affected the accuracy of the measurements as the variance between individual dough sample measurements increased after freezing and during frozen storage.

4.7.2 Analysis of the bread

The frozen storage of dough can affect both the gluten network and the yeast survivability. These parameters have an important role in the specific volume of the loaf (Bae et al., 2014; X. Chen et al., 2017; Jia et al., 2012; Liu et al., 2018).

In terms of specific volume, the samples analyzed in this work showed good resistance to freezing. The specific volume for freshly prepared wholewheat bread was 1.79 ± 0.15 cm^3/g. The values for the loaves of bread prepared from frozen dough (Figure 20) stayed within the same range throughout the experiment.

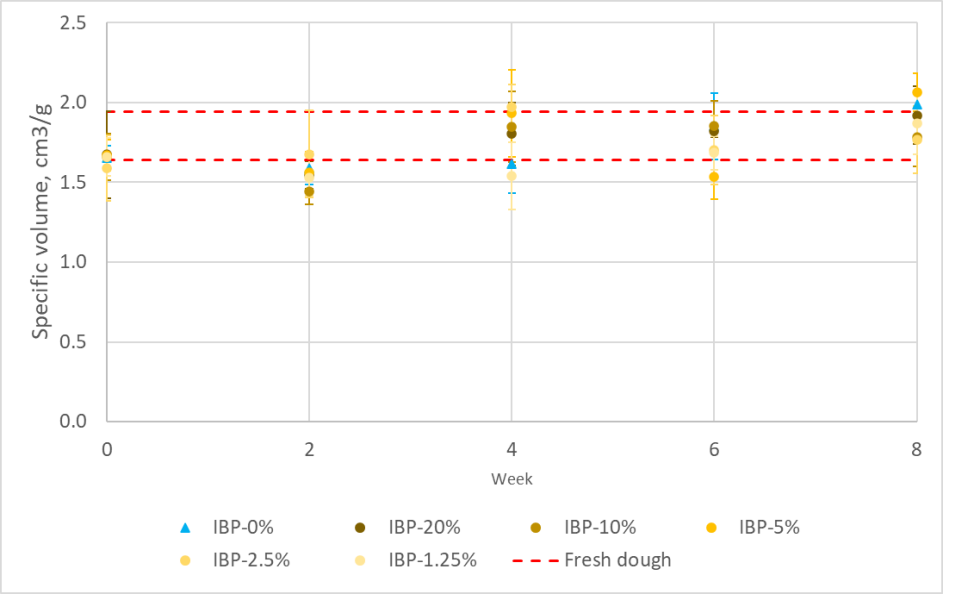

Figure 20: Specific volume values during 8 weeks of frozen storage of loaves prepared from dough containing 0-20% ice-binding proteins (IBPs). The dotted lines indicate the values for the fresh dough (1.79 ± 0.15).

Whole wheat dough has been reported to exhibit greater resistance to freezing in terms of loaf volume retention. For example, bread made from white wheat flour showed a 17.9% reduction in volume after 4 weeks of frozen storage, whereas whole wheat bread decreased by only 8.9% over the same period (Bae et al., 2014). Loaf volume is often associated with yeast viability. However, in the present study, only a moderate correlation was observed between these parameters (correlation coefficients ranging from 0.3 to 0.7). This indicates that factors beyond yeast survival, such as the integrity of the gluten network, likely play a more significant role in maintaining specific loaf volume.

Previous studies have demonstrated that antifreeze peptides derived from pig skin collagen can help preserve loaf volume, with a reduction of 28.06% in the control compared to only 10.57% in treated samples (Chen et al., 2017). Similar effects have been reported for ice-structuring proteins from *Ligustrum vulgare* leaves, where treated dough maintained significantly higher specific volume over 5 weeks of frozen storage (Jia et al., 2012). Additionally, recombinant carrot antifreeze protein expressed in *Pichia pastoris* GS115 has been shown to improve loaf volume during repeated freeze–thaw cycles (Liu et al., 2018). Collectively, these findings suggest that the incorporation of ice-binding proteins can positively influence loaf volume, although the extent of this effect may depend on the dough formulation.

The texture of bread produced from frozen dough is largely influenced by the condition of the gluten network, starch degradation, and yeast survival (Cao et al., 2020; Feng et al., 2020; Liu et al., 2018; Nguyen et al., 2018; Phimolsiripol, 2009). The main changes in bread texture observed over the 8-week storage period are presented in Figure 21.

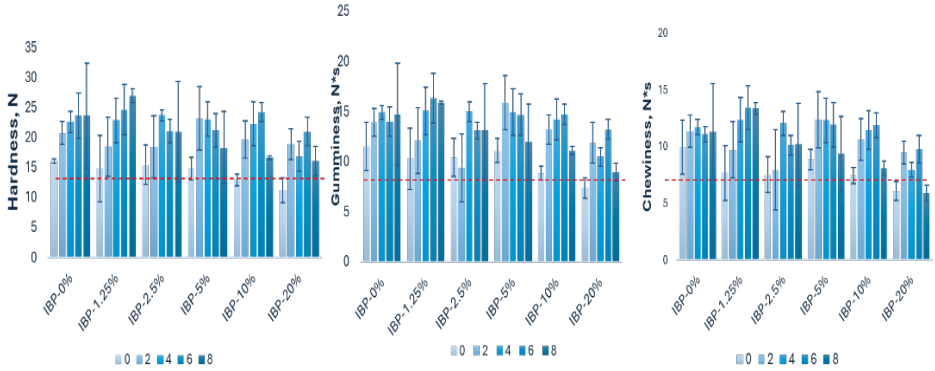

Figure 21: Bread texture parameters during 8 weeks of frozen storage at two-week intervals. The dotted line indicates the average value for fresh dough. Results are given as mean values with standard deviations (n = 5).

Freezing and prolonged frozen storage had a detrimental effect on bread texture, increasing hardness, chewiness, and gumminess. However, the incorporation of ice-binding proteins reduced these parameters by up to 32.2%, 47.9%, and 39.3%, respectively, compared to the control after 8 weeks of storage. Other texture attributes showed minimal variation between samples and remained comparable to those of bread prepared from unfrozen dough.

Comparable effects have been reported for ice-structuring collagen peptides derived from porcine skin hydrolysates, where the hardness and gumminess of steamed bread were reduced by approximately 30% relative to the control after 4 weeks of frozen storage (Nguyen et al., 2018). Similarly, ice-binding proteins isolated from Chinese privet leaves and barley have been shown to enhance bread softness by around 12% and 16%, respectively, in frozen dough applications (Ding et al., 2020; Jia et al., 2012).

The sensory evaluation of the whole wheat bread is shown in Figure 22 for texture and appearance and Figure 23 for taste and aroma.

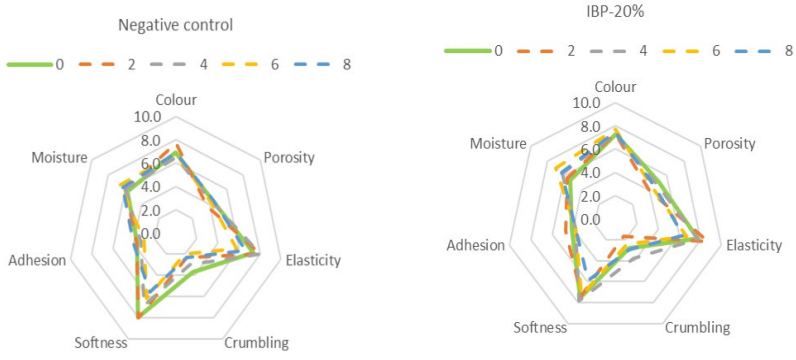

Figure 22: Sensory evaluation of appearance and texture of the whole wheat bread enhanced with ice-binding proteins (IBP-20%) compared to the negative control during 8 weeks of frozen storage.

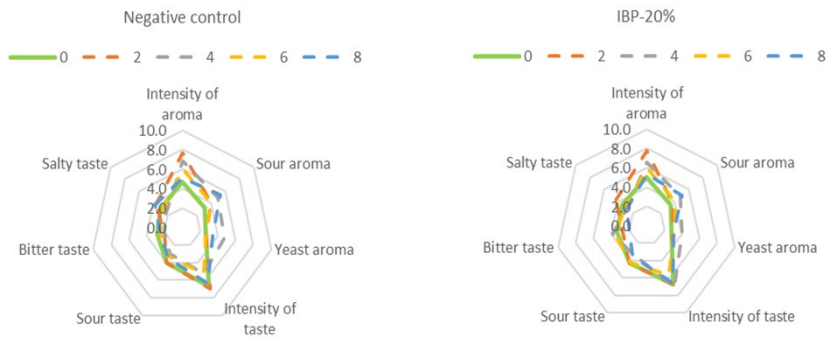

Figure 23: Sensory evaluation of the taste and aroma of the whole wheat bread enhanced with ice-binding proteins (IBP-20%) compared to the negative control during 8 weeks of frozen storage.

The appearance and texture of the bread remained relatively stable over time and across all samples. However, the negative control exhibited a more pronounced decline in softness compared to loaves supplemented with ice-binding proteins, which also showed slightly better retention of porosity and elasticity. Increased crumbliness was observed over time in the negative control and in samples with the lowest IBP concentrations. Overall, these results indicate that the addition of IBPs contributes to improved stability of bread appearance and texture during storage.

Regarding sensory attributes, the intensity of taste decreased in the negative control, while breads containing ice-binding proteins showed little to no change. In contrast, aroma intensity, including yeast and sour notes, increased over the 8-week storage period, with the most notable changes observed in the negative control sample.

In terms of the taste and aroma parameters, the intensity of taste decreased in the negative control sample, whereas the bread enhanced with ice-binding proteins showed little to no difference. Contrarily, the intensity of the aroma, as well as the yeast and sour aroma, appeared to increase during the 8-week experiment, most significantly for the negative control sample.

4.8 Potential ice-binding protein-producing bacteria from the Baltic Sea

Bacteria identified from Baltic seaweed species (Publication I) were compared with bacterial taxa reported in the literature to produce ice-binding proteins. Among the bacterial species detected in the algal samples, members of the Flavobacteriaceae family showed the strongest overall potential for containing IBP-producing taxa. Several experimentally validated IBP-producing bacteria belong to this family, including *Flavobacterium frigoris* PS1 and *Flavobacterium xanthum* (Do et al., 2014; Kawahara et al., 2007; Lorv et al., 2014). Although these exact species were not detected in the Baltic algal samples, multiple closely related *Flavobacterium* species were identified, including *F. degerlachei*, *F. gelidilacus*, *F. glaciei*, *F. jumunjinense*, *F. macrobrachii*, *F. micromati*, *F. resistens*, and *F. xueshanense*. There was also a correlation between higher relative abundances of Flavobacteriaceae and samples collected during the coldest sampling periods (April–May) compared to warmer months (June–September), suggesting that members of this family may possess adaptations that improve survival under low-temperature conditions, potentially including ice-interacting mechanisms.

Additional Flavobacteriaceae genera identified in the samples, such as *Polaribacter*, *Cellulophaga*, *Dokdonia*, *Maribacter*, and *Psychroserpens*, are also commonly associated with marine and psychrophilic environments (Bowman, 2006). While direct experimental evidence for IBP production is currently lacking for most of these species, related taxa have been linked to cold adaptation mechanisms, extracellular polysaccharide production, or putative ice-interacting proteins in previous studies (Lorv et al., 2014).

Species belonging to the genera *Pseudomonas* and *Shewanella* also represent promising candidates for IBP-related activity (Delesky et al., 2019; Kawahara et al., 2004; Singh et al., 2014; Vance et al., 2018; Yin et al., 2005). *Pseudomonas putida* has been experimentally shown to produce an IBP with both ice-nucleation activity and IRI activity (Singh et al., 2014; Sun et al., 1995), and several *Pseudomonas* species are well-known producers of INPs (M. L. Chen et al., 2003; Gharib et al., 2022; Graether & Jia, 2001; Kawahara et al., 2004). In the present samples, multiple *Pseudomonas* taxa were identified, including *P. putida*, *P. fluorescens*, *P. psychrophila*, and *P. anguilliseptica*. Similarly, members of the genus *Shewanella*, including *S. baltica* and *S. oneidensis*, were detected. Although direct evidence for IBP production in these exact species is limited, related *Shewanella* strains have previously been associated with ice-binding activity and cold-environment adaptation (Delesky et al., 2019; Vance et al., 2018).

Overall, the bacterial community associated with Baltic seaweed contained several taxa closely related to known IBP-producing bacteria, particularly within the Flavobacteriaceae and Pseudomonadaceae. While the majority of identified species have not yet been experimentally confirmed to produce IBPs, their phylogenetic relationship to known ice-active bacteria and their occurrence in cold marine environments indicate that Baltic algal microbiomes may represent an unexplored source of novel ice-binding proteins.

5 Conclusions

This thesis investigated the isolation, characterization, and potential food applications of ice-binding proteins produced by *Pseudomonas fluorescens* AQP671 isolated from *Laminaria* collected along the coast of Scotland. The thesis contributes to the growing understanding of marine-derived bacterial IBPs and highlights their relevance as potential cryoprotective agents in frozen food systems.

The effects of environmental conditions on protein expression and activity were evaluated to understand the mechanisms behind the production of IBPs in *P. fluorescens*. IRI activity could only be detected in the culture media when organic nitrogen was available. Additionally, a temperature shift down to 15 °C or below was necessary for detectable activity. Variations in pH also influenced IBP functionality and stability, with a neutral pH supporting the highest activity.

The successful purification and recombinant expression of two IBPs, an adhesin (PfAdh) and a metallopeptidase (PfMp), from *P. fluorescens* AQP671 confirmed its ability to produce proteins with ice-interacting properties. Functional analysis confirmed that the proteins exhibited IRI activity and that PfMp was the primary contributor to the IRI activity in *P. fluorescens,* as it required a lower concentration for similar levels of activity.

Application of the purified proteins in frozen dough systems demonstrated their potential to improve frozen dough stability by limiting ice crystal growth and reducing freeze-related structural damage. These findings support the potential use of IBPs as natural cryoprotective agents in bakery products and other frozen food systems where ice recrystallization negatively affects texture and product quality.

In addition, the comparative investigation of bacterial isolates associated with Baltic Sea seaweeds suggested that these marine environments may also serve as sources of potential IBP-producing microorganisms. This highlights the ecological diversity of cold-adapted marine bacteria and supports the continued exploration of marine microbial communities for novel IBPs with unique functional properties.

Overall, this work demonstrates that *Pseudomonas fluorescens* AQP671 produces functional ice-binding proteins with promising cryoprotective properties and potential applications in frozen food technology.

References

Arai, T., Fukami, D., Hoshino, T., Kondo, H., & Tsuda, S. (2019). Ice-binding proteins from the fungus Antarctomyces psychrotrophicus possibly originate from two different bacteria through horizontal gene transfer. *FEBS Journal*, *286*(5), 946–962. https://doi.org/10.1111/febs.14725

Baderschneider, B., Crevel, R. W. R., Earl, L. K., Lalljie, A., Sanders, D. J., & Sanders, I. J. (2002). Sequence analysis and resistance to pepsin hydrolysis as part of an assessment of the potential allergenicity of ice structuring protein type III HPLC 12. *Food and Chemical Toxicology*, *40*(7), 965–978. https://doi.org/10.1016/S0278-6915(02)00100-X

Bae, W., Lee, B., Hou, G. G., & Lee, S. (2014). Physicochemical characterization of whole-grain wheat flour in a frozen dough system for bake off technology. *Journal of Cereal Science*, *60*(3), 520–525. https://doi.org/10.1016/j.jcs.2014.08.006

Bar Dolev, M., Braslavsky, I., & Davies, P. L. (2016). Ice-Binding Proteins and Their Function. *Annual Review of Biochemistry*, *85*, 515–542. https://doi.org/10.1146/annurev-biochem-060815-014546

Bar, M., Bar-Ziv, R., Scherf, T., & Fass, D. (2006). Efficient production of a folded and functional, highly disulfide-bonded β-helix antifreeze protein in bacteria. *Protein Expression and Purification*, *48*(2), 243–252. https://doi.org/10.1016/j.pep.2006.01.025

Bárcenas, M. E., Haros, M., Benedito, C., & Rosell, C. M. (2003). Effect of freezing and frozen storage on the staling of part-baked bread. *Food Research International*, *36*(8), 863–869. https://doi.org/10.1016/S0963-9969(03)00093-0

Baskaran, A., Kaari, M., Venugopal, G., Manikkam, R., Joseph, J., & Bhaskar, P. V. (2021). International Journal of Biological Macromolecules Anti freeze proteins (Afp): Properties , sources and applications – A review. *International Journal of Biological Macromolecules*, *189*(May), 292–305. https://doi.org/10.1016/j.ijbiomac.2021.08.105

Benjakul, S., & Bauer, F. (2001). Biochemical and physicochemical changes in catfish (Silurus glanis Linne) muscle as influenced by different freeze-thaw cycles. *Food Chemistry*, *72*(2), 207–217. https://doi.org/10.1016/S0308-8146(00)00222-3

Bindslev-Jensen, C., Sten, E., Earl, L. K., Crevel, R. W. R., Bindslev-Jensen, U., Hansen, T. K., Stahl Skov, P., & Poulsen, L. K. (2003). Assessment of the potential allergenicity of ice structuring protein type III HPLC 12 using the FAO/WHO 2001 decision tree for novel foods. *Food and Chemical Toxicology*, *41*(1), 81–87. https://doi.org/10.1016/S0278-6915(02)00212-0

Bojic, S., Murray, A., Bentley, B. L., Spindler, R., Pawlik, P., & Cordeiro, J. L. (2021). *Winter is coming : the future of cryopreservation*. 1–20.

Bouvet, V., & Ben, R. N. (2003). Antifreeze glycoproteins: Structure, conformation, and biological applications. *Cell Biochemistry and Biophysics*, *39*(2), 133–144. https://doi.org/10.1385/CBB:39:2:133

Bowman, J. . (2006). The Marine Clade of the Family Flavobacteriaceae : The Genera Aequorivita , Arenibacter , Cellulophaga , Croceibacter , Formosa , Gelidibacter , Gillisia , Maribacter , Mesonia , Muricauda , Polaribacter , Psychroflexu, Psychroserpens, Robiginitalea, Sale. *Prokaryotes*, *7*, 677–694. https://doi.org/10.1007/0-387-30747-8_26

Brown, C. M., Macdonald-Brown, D. S., & Stanley, S. O. (1973). The mechanisms of nitrogen assimilation in Pseudomonads. *Antonie van Leeuwenhoek*, *39*(1), 89–98. https://doi.org/10.1007/BF02578844

Budke, C., Heggemann, C., Koch, M., Sewald, N., & Koop, T. (2009). Ice recrystallization kinetics in the presence of synthetic antifreeze glycoprotein analogues using the framework of LSW theory. *Journal of Physical Chemistry B*, *113*(9), 2865–2873. https://doi.org/10.1021/jp805726e

Budke, Carsten, Dreyer, A., Jaeger, J., Gimpel, K., Berkemeier, T., Bonin, A. S., Nagel, L., Plattner, C., Devries, A. L., Sewald, N., & Koop, T. (2014). Quantitative efficacy classification of ice recrystallization inhibition agents. *Crystal Growth and Design*, *14*(9), 4285–4294. https://doi.org/10.1021/cg5003308

Cao, H., Zheng, X., Liu, H., Yuan, M., Ye, T., Wu, X., Yin, F., Li, Y., Yu, J., & Xu, F. (2020). Cryo-protective effect of ice-binding peptides derived from collagen hydrolysates on the frozen dough and its ice-binding mechanisms. *Lwt*, *131*(June), 109678. https://doi.org/10.1016/j.lwt.2020.109678

Chang, X. J., Sands, D. C., & Ewart, K. V. (2024). Paradoxical effects on ice nucleation are intrinsic to a small winter flounder antifreeze protein. *Biochimica et Biophysica Acta - Proteins and Proteomics*, *1872*(1), 140973. https://doi.org/10.1016/j.bbapap.2023.140973

Chao, H., DeLuca, C. I., Davies, P. L., Sykes, B. D., & Sönnichsen, F. D. (1994). Structure-function relationship in the globular type III antifreeze protein: Identification of a cluster of surface residues required for binding to ice. *Protein Science*, *3*(10), 1760–1769. https://doi.org/10.1002/pro.5560031016

Chao, H., Hodges, R. S., Kay, C. M., Gauthier, S. Y., & Davies, P. L. (1996). A natural variant of type I antifreeze protein with four ice-binding repeats is a particularly potent antifreeze. *Protein Science*, *5*(6), 1150–1156. https://doi.org/10.1002/pro.5560050617

Chasnitsky, M., & Braslavsky, I. (2019). *Ice-binding proteins and the applicability and limitations of the kinetic pinning model*.

Chen, M. L., Chiou, T. K., Tsao, C. Y., & Jiang, S. T. (2003). Enhancement of the expression of ice-nucleation activity of Pseudomonas fluorescens MACK-4 isolated from mackerel. *Fisheries Science*, *69*(1), 195–203. https://doi.org/10.1046/j.1444-2906.2003.00606.x

Chen, X., Ling, W., & Shao, L. (2017). The cryoprotective effects of antifreeze peptides from pigskin collagen on texture properties and water mobility of frozen dough subjected to freeze – thaw cycles Texture profile analysis. *European Food Research and Technology*, *243*(7), 1149–1156. https://doi.org/10.1007/s00217-016-2830-x

Chen, X., Shi, X., Cai, X., Yang, F., Li, L., Wu, J., & Wang, S. (2020). Ice-binding proteins: a remarkable ice crystal regulator for frozen foods. *Critical Reviews in Food Science and Nutrition*, *0*(0), 1–14. https://doi.org/10.1080/10408398.2020.1798354

Chen, X., Wu, J., Cai, X., & Wang, S. (2021). Production, structure–function relationships, mechanisms, and applications of antifreeze peptides. *Comprehensive Reviews in Food Science and Food Safety*, *20*(1), 542–562. https://doi.org/10.1111/1541-4337.12655

Choi, S. R., Lee, J., Seo, Y. J., Kong, H. S., Kim, M., Jin, E. S., Lee, J. R., & Lee, J. H. (2021). Molecular basis of ice-binding and cryopreservation activities of type III antifreeze proteins. *Computational and Structural Biotechnology Journal*, *19*, 897–909. https://doi.org/10.1016/j.csbj.2021.01.016

Cox, J., Hein, M. Y., Luber, C. A., Paron, I., Nagaraj, N., & Mann, M. (2014). Accurate proteome-wide label-free quantification by delayed normalization and maximal peptide ratio extraction, termed MaxLFQ. *Molecular and Cellular Proteomics*, *13*(9), 2513–2526. https://doi.org/10.1074/mcp.M113.031591

Crevel, R. W. R., Fedyk, J. K., & Spurgeon, M. J. (2002). Antifreeze proteins : characteristics , occurrence and human exposure. *Food and Chemical Toxicology*, *40*, 899–903. https://doi.org/https://doi.org/10.1016/S0278-6915(02)00042-X

Davies, P. L. (2014). Ice-binding proteins: A remarkable diversity of structures for stopping and starting ice growth. *Trends in Biochemical Sciences*, *39*(11), 548–555. https://doi.org/10.1016/j.tibs.2014.09.005

De Groot, N., & Lichtenstein, N. (1960). The action of Pseudomonas fluorescens extracts on asparagine and asparagine derivatives. *BBA - Biochimica et Biophysica Acta*, *40*(C), 99–110. https://doi.org/10.1016/0006-3002(60)91319-6

Delesky, E. A., Frazier, S. D., Wallat, J. D., Bannister, K. L., Heveran, C. M., & Iii, W. V. S. (2019). Ice-Binding Protein from Shewanella frigidimarinas Inhibits Ice Crystal Growth in Highly Alkaline Solutions. *Polymers*, *11*(299), 9–12. https://doi.org/10.3390/polym11020299

Delesky, E. A., Thomas, P. E., Charrier, M., Cameron, J. C., & Srubar, W. V. (2021). Effect of pH on the activity of ice-binding protein from Marinomonas primoryensis. *Extremophiles*, *25*(1), 1–13. https://doi.org/10.1007/s00792-020-01206-9

Devries, A. L. (1982). Biological antifreeze agents in coldwater fishes. *Comparative Biochemistry and Physiology -- Part A: Physiology*, *73*(4), 627–640. https://doi.org/10.1016/0300-9629(82)90270-5

DeVries, A. L., & Wohlschlag, D. E. (1969). Freezing resistance in some antarctic fishes. *Science*, *163*(3871), 1073–1075. https://doi.org/10.1126/science.163.3871.1073

Ding, X., Li, T., Zhang, H., Guan, C., Qian, J., & Zhou, X. (2020). Effect of Barley Antifreeze Protein on Dough and Bread during Freezing and Freeze-Thaw Cycles. *Foods*, *9*(11), 1–14. https://doi.org/10.3390/foods9111698

Do, H., Kim, S., Kim, H. J., & Hyuck, J. (2014). *Structure-based characterization and antifreeze properties of a hyperactive ice-binding protein from the Antarctic bacterium Flavobacterium frigoris PS1 research papers*. *70*, 1061–1073. https://doi.org/10.1107/S1399004714000996

Ekpo, M. D., Tan, S., Xie, J., Hu, Y., Liu, X., Liu, F., Xiang, J., Zhao, R., & Wang, B. (2022). Antifreeze Proteins: Novel Applications and Navigation towards Their Clinical Application in Cryobanking. *International Journal of Molecular Sciences*, *23*(5). https://doi.org/10.3390/ijms23052639

Eskandari, A., Leow, T. C., Rahman, M. B. A., & Oslan, S. N. (2020). Antifreeze proteins and their practical utilization in industry, medicine, and agriculture. *Biomolecules*, *10*(12), 1–18. https://doi.org/10.3390/biom10121649

Feng, W., Ma, S., & Wang, X. (2020). Quality deterioration and improvement of wheat gluten protein in frozen dough. *Grain & Oil Science and Technology*, *3*(1), 29–37. https://doi.org/10.1016/j.gaost.2020.02.001

Fitzner, M., Sosso, G. C., Cox, S. J., & Michaelides, A. (2015). The Many Faces of Heterogeneous Ice Nucleation: Interplay between Surface Morphology and Hydrophobicity. *Journal of the American Chemical Society*, *137*(42), 13658–13669. https://doi.org/10.1021/jacs.5b08748

Friis, D. S., Johnsen, J., Kristiansen, E., Westh, P., & Ramlov, H. (2009). Low thermodynamic- but high kinetic stability of an antifreeze protein from Rhagium mordax. *Protein Science*, *18*(11), 2346–2355. https://doi.org/10.1002/pro.245

Fu, Y., Li, Y., Liu, S., & Chen, J. (2025). Trends in Food Science & Technology The expanding horizons of antifreeze proteins from food science to multidisciplinary technological innovations. *Trends in Food Science & Technology*, *164*(August), 105252. https://doi.org/10.1016/j.tifs.2025.105252

Garnham, C. P., Campbell, R. L., Walker, V. K., & Davies, P. L. (2011). Novel dimeric β-helical model of an ice nucleation protein with bridged active sites. *BMC Structural Biology*, *11*(September). https://doi.org/10.1186/1472-6807-11-36

Garnham, C. P., Gilbert, J. A., Hartman, C. P., Campbell, R. L., Laybourn-Parry, J., & Davies, P. L. (2008). A Ca2+-dependent bacterial antifreeze protein domain has a novel β-helical ice-binding fold. *Biochemical Journal*, *411*(1), 171–180. https://doi.org/10.1042/BJ20071372

Gauthier, S. Y., Kay, C. M., Sykes, B. D., Walker, V. K., & Davies, P. L. (1998). Disulfide bond mapping and structural characterization of spruce budworm antifreeze protein. *European Journal of Biochemistry*, *258*(2), 445–453. https://doi.org/10.1046/j.1432-1327.1998.2580445.x

Gauthier, S. Y., Marshall, C. B., Fletcher, G. L., & Davies, P. L. (2005). Hyperactive antifreeze protein in flounder species: The sole freeze protectant in American plaice. *FEBS Journal*, *272*(17), 4439–4449. https://doi.org/10.1111/j.1742-4658.2005.04859.x

Gauthier, S. Y., Scotter, A. J., Lin, F. H., Baardsnes, J., Fletcher, G. L., & Davies, P. L. (2008). A re-evaluation of the role of type IV antifreeze protein. *Cryobiology*, *57*(3), 292–296. https://doi.org/10.1016/j.cryobiol.2008.10.122

Gharib, G., Saeidiharzand, S., Sadaghiani, A. K., & Koşar, A. (2022). Antifreeze Proteins: A Tale of Evolution From Origin to Energy Applications. *Frontiers in Bioengineering and Biotechnology*, *9*(February), 1–19. https://doi.org/10.3389/fbioe.2021.770588

Graether, S. P., & Jia, Z. (2001). Modeling Pseudomonas syringae ice-nucleation protein as a β-helical protein. *Biophysical Journal*, *80*(3), 1169–1173. https://doi.org/10.1016/S0006-3495(01)76093-6

Graham, L. A., Marshall, C. B., Lin, F. H., Campbell, R. L., & Davies, P. L. (2008). Hyperactive antifreeze protein from fish contains multiple ice-binding sites. *Biochemistry*, *47*(7), 2051–2063. https://doi.org/10.1021/bi7020316

Graumann, P. L., & Marahiel, M. A. (1999). Cold shock proteins CspB and CspC are major stationary-phase-induced proteins in Bacillus subtilis. *Archives of Microbiology*, *171*(2), 135–138. https://doi.org/10.1007/s002030050690

Guo, S., Stevens, C. A., Vance, T. D. R., Olijve, L. L. C., Graham, L. A., Campbell, R. L., Yazdi, S. R., Escobedo, C., Bar-Dolev, M., Yashunsky, V., Braslavsky, I., Langelaan, D. N., Smith, S. P., Allingham, J. S., Voets, I. K., & Davies, P. L. (2017). Structure of a 1.5-MDa adhesin that binds its Antarctic bacterium to diatoms and ice. *Science Advances*, *3*(8), 1–10. https://doi.org/10.1126/sciadv.1701440

Hall-Manning, T., Spurgeon, M., Wolfreys, A. M., & Baldrick, A. P. (2004). Safety evaluation of ice-structuring protein (ISP) type III HPLC 12 preparation. Lack of genotoxicity and subchronic toxicity. *Food and Chemical Toxicology*, *42*(2), 321–333. https://doi.org/10.1016/j.fct.2003.09.007

Herrera, F. E., Garay, A. S., & Rodrigues, D. E. (2014). Structural properties of CHAPS micelles, studied by molecular dynamics simulations. *Journal of Physical Chemistry B*, *118*(14), 3912–3921. https://doi.org/10.1021/jp501729s

Hervás, A. B., Canosa, I., Little, R., Dixon, R., & Santero, E. (2009). NtrC-dependent regulatory network for nitrogen assimilation in Pseudomonas putida. *Journal of Bacteriology*, *191*(19), 6123–6135. https://doi.org/10.1128/JB.00744-09

Hu, C., & Xie, J. (2021). The effect of multiple freeze–thaw cycles on protein oxidation and quality of Trachurus murphyi. *Journal of Food Processing and Preservation*, *45*(12), 1–13. https://doi.org/10.1111/jfpp.15998

Huang, L., Xiong, Y. L., Kong, B., Huang, X., & Li, J. (2013). Influence of storage temperature and duration on lipid and protein oxidation and flavour changes in frozen pork dumpling filler. *Meat Science*, *95*(2), 295–301. https://doi.org/10.1016/j.meatsci.2013.04.034

Jia, C., Huang, W., Wu, C., Zhong, J., Rayas-Duarte, P., & Guo, C. (2012). Frozen bread dough properties modified by thermostable ice structuring proteins extract from Chinese privet (Ligustrum vulgare) leaves. *Cereal Chemistry*, *89*(3), 162–167. https://doi.org/10.1094/CCHEM-11-11-0136

Kaleda, A., Tsanev, R., Klesment, T., Vilu, R., & Laos, K. (2018). Ice cream structure modification by ice-binding proteins. *Food Chemistry*, *246*(April 2017), 164–171. https://doi.org/10.1016/j.foodchem.2017.10.152

Kashyap, P., Kumar, S., & Singh, D. (2020). Performance of antifreeze protein HrCHI4 from Hippophae rhamnoides in improving the structure and freshness of green beans upon cryopreservation. *Food Chemistry*, *320*(August 2019), 126599. https://doi.org/10.1016/j.foodchem.2020.126599

Kato, Y., Matsuda, Y., Uto, T., Tanaka, D., Kobayashi, A., Hazawa, M., Wong, R. W., Hirata, E., Kuroda, K., Ishibashi, K., Ishizaki, T., Ohta, A., Ninomiya, K., & Takahashi, K. (2023). Cell-compatible isotonic freezing media enabled by thermo-responsive osmolyte-adsorption/exclusion polymer matrices. *COMMUNICATIONS CHEMISTRY*, *6*(260), 1–10. https://doi.org/10.1038/s42004-023-01061-7

Kawahara, H. (2002). The Structures and Functions of Ice Crystal-Controlling Proteins from Bacteria. *Journal of Bioscience and Bioengineering*, *94*(6), 492–496. https://doi.org/10.1263/jbb.94.492

Kawahara, H., Iwanaka, Y., Higa, S., Muryoi, N., Sato, M., Honda, M., Omura, H., & Obata, H. (2007). A novel, intracellular antifreeze protein in an antarctic bacterium, Flavobacterium xanthum. *Cryo-Letters*, *28*(1), 39–49.

Kawahara, H., Nakano, Y., Omiya, K., Muryoi, N., Nishikawa, J., & Obata, H. (2004). Production of two types of ice crystal-controlling proteins in antarctic bacterium. *Journal of Bioscience and Bioengineering*, *98*(3), 220–223. https://doi.org/10.1016/S1389-1723(04)00271-3

Kiani, H., & Sun, D. W. (2011). Water crystallization and its importance to freezing of foods: A review. *Trends in Food Science and Technology*, *22*(8), 407–426. https://doi.org/10.1016/j.tifs.2011.04.011

Kong, C. H. Z., Hamid, N., Ma, Q., Lu, J., Wang, B. G., & Sarojini, V. (2017). Antifreeze peptide pretreatment minimizes freeze-thaw damage to cherries: An in-depth investigation. *Lwt*, *84*, 441–448. https://doi.org/10.1016/j.lwt.2017.06.002

Kristiansen, E., Ramløv, H., Hagen, L., Pedersen, S. A., Andersen, R. A., & Zachariassen, K. E. (2005). Isolation and characterization of hemolymph antifreeze proteins from larvae of the longhorn beetle Rhagium inquisitor (L.). *Comparative Biochemistry and Physiology - B Biochemistry and Molecular Biology*, *142*(1), 90–97. https://doi.org/10.1016/j.cbpc.2005.06.004

Kuiper, M. J., Morton, C. J., Abraham, S. E., & Gray-Weale, A. (2015). The biological function of an insect antifreeze protein simulated by molecular dynamics. *ELife*, *4*(MAY), 1–14. https://doi.org/10.7554/eLife.05142

Lan, W., Hu, X., Sun, X., Zhang, X., & Xie, J. (2020). Effect of the number of freeze-thaw cycles number on the quality of Pacific white shrimp (Litopenaeus vannamei): An emphasis on moisture migration and microstructure by LF-NMR and SEM. *Aquaculture and Fisheries*, *5*(4), 193–200. https://doi.org/10.1016/j.aaf.2019.05.007

Le Tri, D., Childers, C. L., Adam, M. K., Ben, R. N., Storey, K. B., & Biggar, K. K. (2019). Characterization of ice recrystallization inhibition activity in the novel freeze-responsive protein Fr10 from freeze-tolerant wood frogs, Rana sylvatica. *Journal of Thermal Biology*, *84*(July), 426–430. https://doi.org/10.1016/j.jtherbio.2019.07.030

Leiter, A., Rau, S., Winger, S., Muhle-Goll, C., Luy, B., & Gaukel, V. (2016). Influence of heating temperature, pressure and pH on recrystallization inhibition activity of antifreeze protein type III. *Journal of Food Engineering*, *187*, 53–61. https://doi.org/10.1016/j.jfoodeng.2016.04.019

Leygonie, C., Britz, T. J., & Hoffman, L. C. (2012). Impact of freezing and thawing on the quality of meat: Review. *Meat Science*, *91*(2), 93–98. https://doi.org/10.1016/j.meatsci.2012.01.013

Li, N., Andorfer, C. A., & Duman, J. G. (1998). Enhancement of insect antifreeze protein activity by solutes of low molecular mass. *Journal of Experimental Biology*, *201*(15), 2243–2251. https://doi.org/10.1242/jeb.201.15.2243

Liao, L., Gao, S., Xu, Y., Su, S., Wen, J., Yu, Y., & Chen, B. (2021). Complete genome sequence of Marinomonas arctica BSI20414, a giant antifreeze protein-producing bacterium isolated from Arctic sea ice. *Marine Genomics*, *57*(October 2020), 2–5. https://doi.org/10.1016/j.margen.2020.100829

Lin, F. H., Davies, P. L., & Graham, L. A. (2011). The Thr- and ala-rich hyperactive antifreeze protein from inchworm folds as a flat silk-like β-Helix. *Biochemistry*, *50*(21), 4467–4478. https://doi.org/10.1021/bi2003108

Liou, Y. C., Daley, M. E., Graham, L. A., Kay, C. M., Walker, V. K., Sykes, B. D., & Davies, P. L. (2000). Folding and structural characterization of highly disulfide-bonded beetle antifreeze protein produced in bacteria. *Protein Expression and Purification*, *19*(1), 148–157. https://doi.org/10.1006/prep.2000.1219

Liu, M., Liang, Y., Wang, Y., Zhang, H., Wu, G., Wang, L., Qian, H., & Qi, X. (2018). Effects of recombinant carrot antifreeze protein from Pichia pastoris GS115 on the physicochemical properties of hydrated gluten during freeze-thawed cycles. *Journal of Cereal Science*, *83*(August), 245–251. https://doi.org/10.1016/j.jcs.2018.08.016

Liu, M., Liang, Y., Zhang, H., Wu, G., Wang, L., Qian, H., & Qi, X. (2018). Production of a recombinant carrot antifreeze protein by Pichia pastoris GS115 and its cryoprotective effects on frozen dough properties and bread quality. *LWT*, *96*(February), 543–550. https://doi.org/10.1016/j.lwt.2018.05.074

Loewen, M. C., Gronwald, W., Sönnichsen, F. D., Sykes, B. D., & Davies, P. L. (1998). The ice-binding site of sea raven antifreeze protein is distinct from the carbohydrate-binding site of the homologous C-type lectin. *Biochemistry*, *37*(51), 17745–17753. https://doi.org/10.1021/bi9820513

Lorv, J. S. H., Rose, D. R., & Glick, B. R. (2014). *Bacterial Ice Crystal Controlling Proteins*. *2014*. https://doi.org/10.1155/2014/976895

Mangiagalli, M., Brocca, S., Orlando, M., & Lotti, M. (2020). The "cold revolution". Present and future applications of cold-active enzymes and ice-binding proteins. *New Biotechnology*, *55*(September 2019), 5–11. https://doi.org/10.1016/j.nbt.2019.09.003

Marshall, C. J., Basu, K., & Davies, P. L. (2016). Ice-shell purification of ice-binding proteins. *Cryobiology*, *72*(3), 258–263. https://doi.org/10.1016/j.cryobiol.2016.03.009

Nguyen, C. T., Yuan, M., Yu, J. S., Ye, T., Cao, H., & Xu, F. (2018). Isolation of ice structuring collagen peptide by ice affinity adsorption, its ice-binding mechanism and breadmaking performance in frozen dough. *Journal of Food Biochemistry*, *42*(3). https://doi.org/10.1111/jfbc.12506

Paraskevopoulou, A., Provatidou, E., Tsotsiou, D., & Kiosseoglou, V. (2010). Dough rheology and baking performance of wheat flour-lupin protein isolate blends. *Food Research International*, *43*(4), 1009–1016. https://doi.org/10.1016/j.foodres.2010.01.010

Patent-WO2003055320A1. (2003). *Antifreeze proteins in vegetables* (pp. 1–17).

Peramo, A. (2018). Molecular dynamics studies show solvation structure of type III antifreeze protein is disrupted at low pH. *Computational Biology and Chemistry*, *73*, 13–24. https://doi.org/10.1016/j.compbiolchem.2018.01.006

Phimolsiripol, Y. (2009). Shelf life determination of frozen bread dough stored under fluctuating temperature conditions. *Kasetsart Journal - Natural Science*, *43*(1), 187–197.

Provesi, J. G., Valentim Neto, P. A., Arisi, A. C. M., & Amante, E. R. (2019). Extraction of antifreeze proteins from cold acclimated leaves of Drimys angustifolia and their application to star fruit (Averrhoa carambola) freezing. *Food Chemistry*, *289*(March), 65–73. https://doi.org/10.1016/j.foodchem.2019.03.055

Qiu, Y., Hudait, A., & Molinero, V. (2019). How Size and Aggregation of Ice-Binding Proteins Control Their Ice Nucleation Efficiency. *Journal of the American Chemical Society*, *141*(18), 7439–7452. https://doi.org/10.1021/jacs.9b01854

Rahman, A. T., Arai, T., Yamauchi, A., Miura, A., Kondo, H., Ohyama, Y., & Tsuda, S. (2019). Ice recrystallization is strongly inhibited when antifreeze proteins bind to multiple ice planes. *Scientific Reports*, *9*(1), 1–9. https://doi.org/10.1038/s41598-018-36546-2

Rajeev Kumar, S., Kiruba, R., Balamurugan, S., Cardoso, H. G., Birgit, A. S., Zakwan, A., & Sathishkumar, R. (2014). Carrot antifreeze protein enhances chilling tolerance in transgenic tomato. *Acta Physiologiae Plantarum*, *36*(1), 21–27. https://doi.org/10.1007/s11738-013-1383-x

Ramløv, H., & Friis, D. S. (2020). Contents of volume 2-antifreeze proteins: Biochemistry, molecular biology, and application. In *Antifreeze Proteins Volume 2: Biochemistry, Molecular Biology and Applications* (Vol. 2). https://doi.org/10.1007/978-3-030-41948-6_1

Raymond, J. A., & Remias, D. (2019). Ice-Binding Proteins in a Chrysophycean Snow Alga: Acquisition of an Essential Gene by Horizontal Gene Transfer. *Frontiers in Microbiology*, *10*(November). https://doi.org/10.3389/fmicb.2019.02697

Regand, A., & Goff, H. D. (2006). Ice recrystallization inhibition in ice cream as affected by ice structuring proteins from winter wheat grass. *Journal of Dairy Science*, *89*(1), 49–57. https://doi.org/10.3168/jds.S0022-0302(06)72068-9

Rodríguez-Sandoval, E., Fernández-Quintero, A., Sandoval-Aldana, A., & Cuvelier, G. (2008). Effect of processing conditions on the texture of reconstituted cassava dough. *Brazilian Journal of Chemical Engineering*, *25*(4), 713–722. https://doi.org/10.1590/S0104-66322008000400008

Roeters, S. J., Golbek, T. W., Bregnhøj, M., Drace, T., Alamdari, S., Roseboom, W., Kramer, G., Šantl-Temkiv, T., Finster, K., Pfaendtner, J., Woutersen, S., Boesen, T., & Weidner, T. (2021). Ice-nucleating proteins are activated by low temperatures to control the structure of interfacial water. *Nature Communications*, *12*(1), 1–9. https://doi.org/10.1038/s41467-021-21349-3

Saki, N., Ghaffari, M., & Nikoo, M. (2023). Effect of active ice nucleation bacteria on freezing and the properties of surimi during frozen storage. *Lwt*, *176*(January), 114548. https://doi.org/10.1016/j.lwt.2023.114548

Sandeep, S., Singh, N., Isono, N., & Noda, T. (2010). Relationship of granule size distribution and amylopectin structure with pasting, thermal, and retrogradation properties in wheat starch. *Journal of Agricultural and Food Chemistry*, *58*(2), 1180–1188. https://doi.org/10.1021/jf902753f

Santos, J. S., da Silva, C. A. P. T., Balhesteros, H., Lourenço, R. F., & Marques, M. V. (2015). CspC regulates the expression of the glyoxylate cycle genes at stationary phase in Caulobacter. *BMC Genomics*, *16*(1), 1–14. https://doi.org/10.1186/s12864-015-1845-1

Sanz, E., Vega, C., Espinosa, J. R., Caballero-Bernal, R., Abascal, J. L. F., & Valeriani, C. (2013). Homogeneous ice nucleation at moderate supercooling from molecular simulation. *Journal of the American Chemical Society*, *135*(40), 15008–15017. https://doi.org/10.1021/ja4028814

Sharadanant, R., & Khan, K. (2003a). *Effect of Hydrophilic Gums on Frozen Dough . I . Dough Quality*. *C*, 764–772. https://doi.org/10.1094/CCHEM.2003.80.6.764

Sharadanant, R., & Khan, K. (2003b). *Effect of Hydrophilic Gums on the Quality of Frozen Dough : II . Bread Characteristics*. *C*. https://doi.org/10.1094/CCHEM.2003.80.6.773

Silvas-García, M. I., Ramírez-Wong, B., Torres-Chávez, P. I., Bello-Pérez, L. A., Carvajal-Millán, E., Barrón-Hoyos, J. M., Rodríguez-García, M. E., Vázquez-Lara, F., & Quintero-Ramos, A. (2016). Effect of freezing rate and storage on the rheological, thermal and structural properties of frozen wheat dough starch. *Starch/Staerke*, *68*(11–12), 1103–1110. https://doi.org/10.1002/star.201500123

Sindhu, R., & Manonmani, H. K. (2018). Protein Expression and Purifi cation Expression and characterization of recombinant L -asparaginase from Pseudomonas fluorescens. *Protein Expression and Purification*, *143*, 83–91. https://doi.org/https://doi.org/10.1016/j.pep.2017.09.009

Singh, P., Hanada, Y., Singh, S. M., & Tsuda, S. (2014). Antifreeze protein activity in Arctic cryoconite bacteria. *FEMS Microbiology Letters*, *351*(1), 14–22. https://doi.org/10.1111/1574-6968.12345

Song, D. H., Kim, M., Jin, E. S., Sim, D. W., Won, H. S., Kim, E. K., Jang, S., Choi, Y. S., Chung, K. H., & An, J. H. (2019). Cryoprotective effect of an antifreeze protein purified from Tenebrio molitor larvae on vegetables. *Food Hydrocolloids*, *94*(April), 585–591. https://doi.org/10.1016/j.foodhyd.2019.04.007

Sun, X., Griffith, M., Pasternak, J. J., & Glick, B. R. (1995). Low temperature growth, freezing survival, and production of antifreeze protein by the plant growth promoting rhizobacterium Pseudomonas putida GR12-2. *Canadian Journal of Microbiology*, *41*(9), 776–784. https://doi.org/10.1139/m95-107

Tao, Z., Yuan, H., Liu, M., Liu, Q., Zhang, S., Liu, H., Jiang, Y., Huang, D., & Wang, T. (2023). Yeast Extract: Characteristics, Production, Applications and Future Perspectives. *Journal of Microbiology and Biotechnology*, *33*(1), 151–166. https://doi.org/10.4014/jmb.2207.07057

Tian, Y., Zhu, Z., & Sun, D. W. (2020). Naturally sourced biosubstances for regulating freezing points in food researches: Fundamentals, current applications and future trends. *Trends in Food Science and Technology*, *95*(May 2019), 131–140. https://doi.org/10.1016/j.tifs.2019.11.009

Tirado-Kulieva, V. A., Miranda-Zamora, W. R., Hernández-Martínez, E., Pantoja-Tirado, L. R., Bazán-Tantaleán, D. L., & Camacho-Orbegoso, E. W. (2022). Effect of antifreeze proteins on the freeze-thaw cycle of foods: fundamentals, mechanisms of action, current challenges and recommendations for future work. *Heliyon*, *8*(10). https://doi.org/10.1016/j.heliyon.2022.e10973

Totosaus, A., López, H., & Güemes-Vera, N. (2013). Effect of Lupinus (Lupinus albus) and Jatropha (Jatropha curcas) Protein Concentrates on Wheat Dough Texture and Bread Quality: Optimization by a D-Optimal Mixture Design. *Journal of Texture Studies*, *44*(6), 424–435. https://doi.org/10.1111/jtxs.12031

Utrera, M., Morcuende, D., & Estévez, M. (2014). Temperature of frozen storage affects the nature and consequences of protein oxidation in beef patties. *Meat Science*, *96*(3), 1250–1257. https://doi.org/10.1016/j.meatsci.2013.10.032

Vance, T. D. R., Bayer-Giraldi, M., Davies, P. L., & Mangiagalli, M. (2019). Ice-binding proteins and the 'domain of unknown function' 3494 family. *FEBS Journal*, *286*(5), 855–873. https://doi.org/10.1111/febs.14764

Vance, T. D. R., Graham, L. A., & Davies, P. L. (2018). An ice-binding and tandem beta-sandwich domain- containing protein in Shewanella frigidimarina is a potential new type of ice adhesin. *The FEBS Journal*, *285*, 1511–1527. https://doi.org/10.1111/febs.14424

Vanya Ewart, K., Yang, D. S. C., Ananthanarayanan, V. S., Fletcher, G. L., & Hew, C. L. (1996). Ca2+-dependent antifreeze proteins: Modulation of conformation and activity by divalent metal ions. *Journal of Biological Chemistry*, *271*(28), 16627–16632. https://doi.org/10.1074/jbc.271.28.16627

Venketesh, S., & Dayananda, C. (2008). Properties, potentials, and prospects of antifreeze proteins. *Critical Reviews in Biotechnology*, *28*(1), 57–82. https://doi.org/10.1080/07388550801891152

Voets, I. K. (2017). From ice-binding proteins to bio-inspired antifreeze materials. *Soft Matter*, *13*(28), 4808–4823. https://doi.org/10.1039/c6sm02867e

Wang, B., Li, F., Pan, N., Kong, B., & Xia, X. (2021). Effect of ice structuring protein on the quality of quick-frozen patties subjected to multiple freeze-thaw cycles. *Meat Science*, *172*(October 2020), 108335. https://doi.org/10.1016/j.meatsci.2020.108335

Xiao, Q., Xia, J. H., Zhang, X. J., Li, Z., Wang, Y., Zhou, L., & Gui, J. F. (2014). Type-IV antifreeze proteins are essential for epiboly and convergence in gastrulation of zebrafish embryos. *International Journal of Biological Sciences*, *10*(7), 715–732. https://doi.org/10.7150/ijbs.9126

Xiao, S., Hu, S., Zhu, K., Bai, T., Wang, W., Cheng, J., & Zhang, J. (2024). Recent advances, challenges and functional applications of antifreeze protein in food industry. *International Journal of Food Science and Technology*, *59*(3), 1169–1186. https://doi.org/10.1111/ijfs.16878

Xu, H., Griffith, M., Patten, C. L., & Glick, B. R. (1998). Isolation and characterization of an antifreeze protein with ice nucleation activity from the plant growth promoting rhizobacterium Pseudomonas putida GR12-2. *Canadian Journal of Microbiology*, *44*(1), 64–73. https://doi.org/10.1139/cjm-44-1-64

Xue, B., Zhao, L., Qin, X., Qin, M., Lai, J., Huang, W., Lei, H., Wang, J., Wang, W., Li, Y., & Cao, Y. (2019). Bioinspired Ice Growth Inhibitors Based on Self-Assembling Peptides [Rapid-communication]. *ACS Macro Letters*, *8*(10), 1383–1390. https://doi.org/10.1021/acsmacrolett.9b00610

Yamauchi, A., Arai, T., Kondo, H., Sasaki, Y. C., & Tsuda, S. (2020). An ice-binding protein from an antarctic ascomycete is fine-tuned to bind to specific water molecules located in the ice prism planes. *Biomolecules*, *10*(5), 1–15. https://doi.org/10.3390/biom10050759

Yang, D. S. C., Sax, M., Chakrabartty, A., & Hew, C. L. (1988). (1988). Crystal structure of an antifreeze polypeptide and its mechanistic implications. *Nature*, *333*(1), 10. https://www.infodesign.org.br/infodesign/article/view/355%0Ahttp://www.abergo.org.br/revista/index.php/ae/article/view/731%0Ahttp://www.abergo.org.br/revista/index.php/ae/article/view/269%0Ahttp://www.abergo.org.br/revista/index.php/ae/article/view/106

Yang, Z., Yu, W., Xu, D., Guo, L., Wu, F., & Xu, X. (2019). Impact of frozen storage on whole wheat starch and its A-Type and B-Type granules isolated from frozen dough. *Carbohydrate Polymers*, *223*(July), 115142. https://doi.org/10.1016/j.carbpol.2019.115142

Yedgar, S., Barenholz, Y., & Cooper, V. G. (1974). Molecular weight, shape and structure of mixed micelles of Triton X-100 and sphingomyelin. *BBA - Biomembranes*, *363*(1), 98–111. https://doi.org/10.1016/0005-2736(74)90009-1

Yin, L. J., Chen, M. L., Tzeng, S. S., Chiou, T. K., & Jiang, S. T. (2005). Properties of extracellular ice-nucleating substances from Pseudomonas fluorescens MACK-4 and its effect on the freezing of some food materials. *Fisheries Science*, *71*(4), 941–947. https://doi.org/10.1111/j.1444-2906.2005.01048.x

Zhang, Y., Zhang, H., Ding, X., Cheng, L., Wang, L., Qian, H., Qi, X., & Song, C. (2016). Purification and Identification of Antifreeze Protein From Cold-Acclimated Oat (Avena sativa L.) and the Cryoprotective Activities in Ice Cream. *Food and Bioprocess Technology*, *9*(10), 1746–1755. https://doi.org/10.1007/s11947-016-1750-x

Zhao, A., Shi, P., Yang, R., Gu, Z., Jiang, D., & Wang, P. (2022). Isolation of novel wheat bran antifreeze polysaccharides and the cryoprotective effect on frozen dough quality. *Food Hydrocolloids*, *125*(August 2021), 107446. https://doi.org/10.1016/j.foodhyd.2021.107446

Zhu, S., Yu, J., Chen, X., Zhang, Q., Cai, X., & Ding, Y. (2021). Trends in Food Science & Technology Dual cryoprotective strategies for ice-binding and stabilizing of frozen seafood : A review. *Trends in Food Science & Technology*, *111*(August 2020), 223–232. https://doi.org/10.1016/j.tifs.2021.02.069

Acknowledgements

I would like to express my sincere gratitude to my supervisors, Allan Olspert and Katrin Laos, for their guidance, support, and valuable feedback throughout the development of this thesis. Their expertise, encouragement, and patience greatly contributed to both this work and my growth as a researcher. I am also thankful to Toomas Paalme, Ildar Nisamedtinov and Inga Sarand for their invaluable help, insights, and support during the process of this thesis.

Special thanks go to my students, Karina Zakrevskaja, Kadi Karro, Kairit Kruusimägi and interns, Cindie Maitre, Quentin Aufranc, Giedre Baltusnikaite and Antoine Candaele, whose curiosity, enthusiasm, and collaboration inspired many meaningful discussions and ideas throughout this work.

I would also like to thank my friends for their encouragement, understanding, and constant support during both the challenging and rewarding moments of this journey. In particular, the friends I've made on this journey, Lachin Huseynli, Anna Angerjas, Atefeh Asadi, Rifaldi Lutfi Fahmi, Roberta Mikk and Lauri Tossavainen, who made even the difficult parts of this journey feel a lot lighter.

Finally, I am especially grateful to my family for their endless belief in me. Their support has been the foundation that made this achievement possible.

I would also like to thank Lallemand for providing the strain used in this research, and I would like to acknowledge that Eesti Teadusagentuur and the European Regional Development Fund (RESTA12 & RESTA13) supported this work.

Abstract

Ice-binding proteins in *Pseudomonas fluorescens* AQP671: isolation, characterization and applications in food

Ice-binding proteins (IBPs) are a diverse group of proteins capable of interacting with ice crystals and modifying their growth and recrystallization. These proteins are produced by a wide range of cold-adapted organisms and play an important role in survival under freezing conditions. Due to their ice recrystallization inhibition (IRI) activity, IBPs have attracted increasing interest for potential applications in biotechnology and the food industry, particularly in frozen food systems where ice crystal growth negatively affects product quality. Despite growing research on IBPs from fish, plants, and fungi, comparatively little is known about bacterial IBPs and their potential industrial applications.

The aim of this thesis was to isolate, characterize, and evaluate the application potential of IBPs produced by *Pseudomonas fluorescens* AQP671 isolated from brown algae collected along the coast of Scotland. The study focused on the purification and characterization of the proteins, recombinant expression in *Escherichia coli*, assessment of IRI activity, and evaluation of their potential use in frozen dough systems. In addition, the effects of environmental conditions such as pH and temperature on protein expression, activity, and thermal stability were investigated. The occurrence of potential IBP-producing bacteria associated with Baltic Sea seaweeds was also explored based on bacterial isolation and literature comparison.

Marine algae-associated bacteria represent a relatively underexplored source of novel cold-adapted microorganisms and IBPs. Therefore, this work contributes to expanding current knowledge regarding marine bacterial IBPs and their possible utilization as natural cryoprotective agents. The novelty of the study lies in the investigation of IBPs derived from *P. fluorescens* associated with Scottish brown algae and the combined evaluation of their biochemical properties and practical food applications.

The cultivation experiments of *P. fluorescens* AQP671 showed that organic nitrogen is necessary for the production of IBPs, and the presence of amino acids, such as L-asparagine, L-valine and L-proline, had a positive effect on IRI activity. Additionally, it was shown that the activity of these proteins was highest at a neutral pH range, whilst acidic conditions decreased the IRI activity dramatically.

IBPs were isolated and purified using ice affinity purification and fractionation according to size. From the mass-spectrometry results of the purified IRI active fractions, two candidate proteins were chosen based on their similarities to other bacterial IBPs. Recombinant expression of the target proteins was carried out in *E. coli* to verify their activity. The two candidate proteins, a giant Lap-A adhesin (PfAdh) and a metallopeptidase (PfMp), both exhibiting the RTX-motif, sometimes present in the ice-binding site of IBPs, were verified to have IRI activity. The metallopeptidase showed a lower inhibitory concentration, indicating that it may be the primary contributor to the activity present in *P. fluorescens* AQP671. The thermal stability analysis of the proteins, as well as an active fraction from the ice affinity purification and a different IBP from sea raven, further confirmed that PfAdh and PfMp were primarily responsible for the inhibition of ice crystal growth.

To investigate practical applications in food systems, the purified IBPs were incorporated into frozen dough formulations. Frozen dough is highly susceptible to

freeze-induced damage because of its high water content, where ice crystal growth may damage yeast cells, disrupt gluten networks, and alter starch granule morphology. The addition of IBPs was therefore evaluated for their potential cryoprotective effects and their ability to improve dough stability during frozen storage.

Application studies in frozen dough systems suggested that the IBPs could contribute to improved frozen dough stability by reducing ice recrystallization-related damage during 8 weeks of frozen storage. The IBPs had a positive effect on yeast viability, dough and bread texture and sensory parameters. These findings support the potential use of bacterial IBPs as natural cryoprotectants in frozen bakery products and other frozen food applications. In addition, the comparison of bacterial isolates associated with Baltic Sea seaweeds indicated that marine environments may represent valuable reservoirs of previously unexplored IBP-producing microorganisms.

In conclusion, this thesis demonstrates that *Pseudomonas fluorescens* AQP671 is a promising source of functional ice-binding proteins with potential applications in frozen food technology. The thesis contributes to the understanding of bacterial IBPs from marine environments and highlights their relevance as natural cryoprotective agents.

Lühikokkuvõte

Jääga seonduvad valgud *Pseudomonas fluorescens AQP671*: puhastamine, iseloomustamine ja kasutamine toidus

Jääga seonduvad valgud (*ice-binding proteins*, IBP-d) on mitmekesine valkude rühm, millel on võime seonduda jääkristallidega ning mõjutada nende kasvu ja rekristallisatsiooni. Neid valke toodavad erinevad külmaga kohastunud organismid ning neil on oluline roll ellujäämisel madalatel temperatuuridel ja külmumistingimustes. Tänu oma jää rekristallisatsiooni inhibeerivale (IRI) aktiivsusele on IBP-d pälvinud järjest suuremat tähelepanu nii biotehnoloogias kui ka toiduainetööstuses, eriti külmutatud toodete puhul, kus jääkristallide kasv mõjutab otseselt toote kvaliteeti. Kuigi kaladest, taimedest ja seentest pärinevaid IBP-sid on põhjalikult uuritud, on bakteriaalsete IBP-de ning nende võimalike tööstuslike rakenduste kohta teadmisi endiselt suhteliselt vähe.

Käesoleva doktoriitöö eesmärk oli Šotimaa rannikult kogutud pruunvetikatelt isoleeritud *Pseudomonas fluorescens* AQP671 toodetud jääsiduvate valkude puhastamine ja funktsionaalse aktiivsuse uurimine, rekombinantne ekspressioon *Escherichia coli*-s ning nende võimaliku kasutamise hindamine külmutatud nisutaignas. Lisaks uuriti keskkonnatingimuste, nagu pH ja temperatuuri, mõju valkude aktiivsusele, ekspressioonile ja stabiilsusele. Samuti analüüsiti võimalike IBP-sid tootvate bakterite esinemist Läänemere vetikatega seotud bakterikooslustes, tuginedes nii bakterite isoleerimisele kui ka varasemale kirjandusele.

Merevetikatega seotud bakterid on suhteliselt väheuuritud jäädsiduvatele valkude allikas. Seetõttu aitab käesolev töö laiendada teadmisi bakterite IBP-dest ning nende võimalikust kasutamisest looduslike krüoprotektiivsete ühenditena. Töö uudsus seisneb Šoti pruunvetikatega seotud *P. fluorescens*-est pärinevate IBP-de uurimises ning nende biokeemiliste omaduste ja praktiliste toidurakenduste ühendamises üheks terviklikuks käsitluseks.

Pseudomonas fluorescens AQP671 kasvatamiskatsed näitasid, et IBP-de tootmiseks on vajalik orgaaniline lämmastik. Samuti suurendas aminohapete, nagu L-asparagiini, L-valiini ja L-proliini olemasolu kasvukeskkonnas IRI aktiivsust. Lisaks selgus, et valkude aktiivsus oli suurim neutraalses pH vahemikus, samas kui happelised tingimused vähendasid jää rekristallisatsiooni inhibeerivat aktiivsust märgatavalt.

IBP-d puhastati jääafiinsuspuhastuse ja suurusepõhise fraktsioneerimise abil. Puhastatud IRI-aktiivsete fraktsioonide massispektromeetrilise analüüsi põhjal valiti välja kaks kandidaatvalku, millel esines sarnasus teiste teadaolevate bakteriaalsete IBP-dega. Nende aktiivsuse kinnitamiseks viidi kandidaatvalkude rekombinantne ekspressioon läbi *E. coli*-s. Mõlemad valgud, Lap-A adhesiin (PfAdh) ja metallopeptidaas (PfMp), sisaldasid RTX-motiivi, mida on varasemalt seostatud IBP-de jääga seondumis piirkonnaga (*ice-binding site*, IBS), ning mõlemal kinnitati IRI aktiivsus. Metallopeptidaas näitas madalamat inhibeerivat kontsentratsiooni, viidates sellele, et see võib olla peamine *P. fluorescens* AQP671 poolt põhjustatud aktiivsuse allikas. Valkude termilise stabiilsuse analüüs ning võrdlus jääafiinsuspuhastusest saadud aktiivse fraktsiooni ja merikärnkala (*sea raven*) IBP-ga kinnitas samuti, et peamised jääkristallide kasvu inhibeerivad valgud olid PfAdh ja PfMp.

Valkude praktilise rakenduspotentsiaali hindamiseks lisati puhastatud IBP-d külmutatud täistera nisutaigna süsteemidesse. Külmutatud tainas on suure veesisalduse tõttu eriti tundlik külmumiskahjustuste suhtes, kuna jääkristallide kasv võib kahjustada

pärmirakke, lõhkuda gluteenivõrgustikku ja muuta tärklisegraanulite struktuuri. Seetõttu hinnati IBP-de võimet toimida krüoprotektiivsete ühenditena ning parandada taigna stabiilsust külmutatuna säilitamise ajal.

Külmutatud taigna katsed näitasid, et IBP-de lisamine vähendas jää rekristallisatsioonist põhjustatud kahjustusi kaheksa nädala pikkuse säilitamise jooksul. Valkudel oli positiivne mõju pärmi eluvõimele, taigna ja valmis leiva tekstuurile ning sensoorsetele omadustele. Tulemused viitavad sellele, et bakteriaalsed IBP-d võivad olla paljulubavad looduslikud krüoprotektiivsed ühendid külmutatud pagaritoodete ja teiste külmutatud toiduainete jaoks. Lisaks näitas Läänemere vetikatega seotud bakterite võrdlus, et merekeskkonnad võivad olla väärtuslikuks allikaks seni väheuuritud IBP-sid tootvatele mikroorganismidele.

Kokkuvõttes näitab käesolev doktoritöö, et *Pseudomonas fluorescens* AQP671 on funktsionaalsete jääga seonduvate valkude allikas, millel on rakenduspotentsiaal külmutatud toiduainete tehnoloogias. Töö aitab kaasa bakteriaalsete IBP-de paremaks mõistmiseks ning rõhutab nende olulisust looduslike krüoprotektantidena.

Appendix 1

Publication I

Luhila, Õ., Paalme, T., Tanilas, K., & Sarand, I. (2022). Omega-3 fatty acid and B12 vitamin content in Baltic algae. *Algal Research*, *67*.

Algal Research 67 (2022) 102860

Contents lists available at ScienceDirect

Algal Research

journal homepage: www.elsevier.com/locate/algal

Omega-3 fatty acid and B12 vitamin content in Baltic algae

Õnnela Luhila [a], Tiina Paalme [b], Kristel Tanilas [c], Inga Sarand [a,*]

[a] Department of Chemistry and Biotechnology, Tallinn University of Technology, Akadeemia tee 15, 12618 Tallinn, Estonia
[b] Estonian Marine Institute, University of Tartu, Mäealuse 14, 12618 Tallinn, Estonia
[c] Center of Food and Fermentation Technologies, Akadeemia tee 15a, 12618 Tallinn, Estonia

ARTICLE INFO

Keywords:
Seaweed
Baltic Sea
Omega-3
B12 vitamin
GC–MS
HPLC-UV

ABSTRACT

Seaweeds have been gaining popularity in the Western world due to increased interest in alternative food sources and improving the nutritional profile and functionality of food products. This paper analyzed the omega-3 fatty acids such as eicosapentaenoic acid (EPA) and α-linoleic acid (ALA) and B12 vitamin content in the most common Baltic seaweeds. These nutrients have an important part in the human diet. Five seaweeds species (*Fucus vesiculosus*, *Furcellaria lumbricalis, Cladophora glomerata, Pilayella littoralis* and *Ulva intestinalis*) were sampled during April–May, June–July, and August–September. The fatty acids were determined by GC–MS whereas B12 content was analyzed by HPLC-UV. 16S rRNA amplification from community DNA and sequencing was carried out to evaluate B12 synthesizing microorganisms associated with the studied seaweeds. The results showed that *F. vesiculosus* (5.19 ± 0.32 mg/gDW) was the best source of EPA, followed by *F. lumbricalis, C. glomerata, P. littoralis* and *U. intestinalis* irresponsibly of sampling time. The ALA content had little variability between species (1.07–2.45 mg/ g DW). The B12 concentration varied across seasons, being generally lowest during the June–July period. The highest concentration of B12 across all three seasons was in *C. glomerata* samples (53.55 ± 9.69 μg/100gDW). The lowest B12 vitamin concentration was in *F. vesiculosus* (4.14 ± 0.36 μg/100gDW). 16S RNA amplicon analysis revealed a correlation between *Cyanobacteria* and EPA, while no correlation could be found between B12 neither on phyla nor family levels. B12 content in the samples was in correlation with 5 potentially B12 synthesizing bacteria species (*Rhodobacter capsulatus, Rhodobacter sphaeroides, Pseudomonas putida, Xanthomonas oligotrophicus* and *Aeromonas hydrophila)* although the abundance of corresponding OTUs did not exceed 1 %.

1. Introduction

The consistent rise of the global population requires new approaches in food production to overcome the limitations and concerns associated with the traditional agricultural practices [1]. Recently, there has been growing interest in using seaweeds in the food industry as alternative sources of nutrients or to improve the functionality and nutritional profiles of existing foods. Seaweeds have been known to contain a variety of nutrients and bioactive compounds, for example antioxidants, dietary fibers, essential amino acids, polyunsaturated fatty acids (PUFAs), polyphenols, minerals and vitamins [2–5]. Some of them, such as long-chain Omega-3 fatty acids and vitamin B12, are mainly obtained from fish- or animal-based foods. Long-chain Omega-3 fatty acids, particularly eicosapentaenoic acid (EPA) and docosahexaenoic acid (DHA), have been shown to assist in proper fetal development, cardiovascular functions and prevention of neurodegenerative diseases [6–8]. They also have anti-inflammatory, insulin-sensitising and anti-cancer effects. EPA and DHA act as precursors of signalling molecules and are essential components of cell membranes thus modulating cell responses [8]. Their endogenous production in humans from α-linoleic acid (ALA) as a precursor is insufficient and requires additional intake through diets or supplements. Marine fishes and oil from them are the primary sources for these long-chain Omega-3 fatty acids, which accumulate in fish due to consumption of marine algae and phytoplankton. The major Omega-3 fatty acids in terrestrial crops are ALA and its metabolite stearidonic acid (SDA) [9].

Vitamin B12 acts as a cofactor of cytoplasmic methionine synthase and mitochondrial methylmalonyl-CoA mutase thus playing an important role in carbohydrate and normal fat metabolism, formation of red blood cells, the normal functioning of the nervous system and in the translocation of the methyl group in DNA synthesis [10]. Its deficiency has been linked to reduced cognitive function, Alzheimer's disease,

* Corresponding author.
E-mail address: inga.sarand@taltech.ee (I. Sarand).

https://doi.org/10.1016/j.algal.2022.102860
Received 25 March 2022; Received in revised form 14 September 2022; Accepted 16 September 2022
Available online 17 September 2022

ischemic stroke and megaloblastic anemia [11,12]. Vitamin B12 in animal products originates from B12-producing microbiota of ruminant or coprophagic animals or ingestion of B12-fortified animal feed, while fishes thrive essentially on algae, acquiring B12 through bacteria-algae symbiotic association [13]. Worldwide a moderate B12 deficiency is common, especially in developing countries with low intake of animal products but also among elderly population due to age-dependent gastric changes.

The majority of studies determining the amounts of Omega-3 fatty acids and vitamin B12 in algae has been focused on species traditional in Asian countries, as these are the main producers and consumers of seaweeds. It has been concluded that of the total fatty acid amounts detected in different seaweed species, 8–64 % is made up of Omega-3 fatty acids. The results are very species-specific, but generally the main Omega-3 fatty acids found in algae are ALA and EPA [5,14].

Vitamin B12, although only synthesized by bacteria and archaea, can be found in algae as they require it for a variety of reactions and obtain it from the environment [15]. The highest B12 concentrations have generally been detected in green algae species, for example *Chlorella sp* (201.3–285.7 μg/100gDW) and *Ulva prolifera* (63.6 μg/100gDW). Additionally, certain red algae species, for example, *Porphyra sp* (25.1–77.6 μg/100gDW), which is used for the production of nori, also have significant amounts of B12 [15–18].

Very little research has been done regarding nutrients in common Baltic seaweed species. Furthermore, nutrients in seaweed are dependent on growth conditions, and the Baltic Sea has a unique set of these conditions. It is the world's second-largest body of brackish water and has steep gradients in salinity and key nutrient concentrations, a situation which is challenging for many marine organisms [19]. Therefore, the nutrient content may differ from the same species growing elsewhere.

In this paper, we identified and quantified Omega-3 fatty acids found in the most common Baltic seaweed species belonging to green (*Ulva intestinalis* and *Cladophora glomerata*), brown (*Fucus vesiculosus* and *Pileyalla littoralis*) and red (*Furcellaria lumbricalis*) algae. Additionally, bioavailable B12 content was calculated. To further understand the sources of B12 in algae, the microbiome of all studied algae species was analyzed and correlations with known B12 producers were established. The obtained data from different sample periods were compared.

2. Materials and methods

2.1. Materials

Five seaweed species commonly found in the Baltic Sea were collected from the Estonian coast in 2019 during the months of significant biomass growth. The collected species were *Fucus vesiculosus, Furcellaria lumbricalis, Cladophora glomerata, Ulva intestinalis,* and *Pilayella littoralis*. Each of the species was collected a total of three times during their growing season. The collection periods were 1) April to May, 2) June to July and 3) August to September. After collection, all of the samples were frozen at −80 °C.

The chemicals used were hexane (C_6H_{14}), sulfuric acid (H_2SO_4), methanol (CH_3OH), nonadecanoic acid ($C_{18}H_{32}COOH$), eicosapentaenoic acid ($C_{19}H_{26}COOH$), potassium cyanide (KCN), sodium acetate (CH_3COONa), acetic acid (CH_3COOH), NaCl, CTAB lysis buffer (100 mM Tris-HCl pH 8.0, 3 M NaCl, 3 % CTAB, 20 mM EDTA, 1 % (w/v) polyvinylpyrrolidone), chloroform ($CHCl_3$), isoamyl alcohol ($C_5H_{12}O$), ethanol (C_2H_5OH), isopropanol (C_3H_8O), and cyanocobalamine (B12). All of the chemicals were produced by Sigma Aldrich.

2.2. Sample preparation

From the initial frozen biomass, approximately 80 g was weighed out and freeze-dried using a Heto PowerDry PL3000 freeze dryer (Bath, UK). The drying temperature was set at −41 °C and the vacuum at 100 mBar. The dried samples were pulverized using an electric coffee grinder (Bosch). This dried seaweed powder was used for fatty acid and B12 analysis. Additionally, from the frozen mass, 10 g was separated for the analysis of the microbiome.

2.3. Omega-3 fatty acid analysis

Fat was extracted from the freeze-dried seaweed powder using the Soxhlet method. The extractor used was a Velp Scientifica SER 148 (Usmate, Italy), and the solvent for the extraction was hexane. Approximately 2 g of the seaweed powder was weighed out for each replicate and three replicates were made for each sample. The internal standard, nonadecanoic acid, was diluted in hexane and added to the extraction solvent. Following the fat extraction, nitrogen was used to remove the hexane from the sample.

Methyl esters of fatty acids (FAMEs) were prepared in a mixture of methanol/sulfuric acid (ratio, 20:1, v/v) at room temperature for 24 h. FAMEs were then analyzed on a gas chromatograph equipped with a mass spectrometer detector (model 7890A/5957C, Agilent Technologies, USA) and a 30 m long × 0.25 mm internal diameter capillary column Zebron ZB-WAX (Agilent Technologies, USA). The column temperature programming was from 60 °C for 2 min to 150 °C at 13 °C/min to 240 at 2 °C/min and helium was used as the carrier gas at a constant flow rate of 2 mL/min. Detection was initially held in SCAN mode according to which fragments (*m/z* 91.1 and 143.1) were chosen to for the SIM (Select Ion Monitoring) mode. Data were collected and analyzed using the GC MassHunter program (Agilent Technologies, USA). Peaks of FAMEs were identified by their mass spectra, comparing them to those in the integrated database NIST (2005) and in the case of eicosapentaenoic acid with authentic standard. The FAMES were quantified according to the peak area of the internal standard, nonadecanoic acid.

2.4. Vitamin B12 analysis

Approximately 5 g of the dried seaweed powder was weighed into a 100 mL glass bottle, and 50 mL of 50 mM ammonium acetate buffer (pH = 4) and 0.5 mL of 1 % KCN were added. This reaction converted all absorbable B12 forms into a cyanocobalamine form. The mixture was vortexed for 30 s and then placed into a water bath to boil for 30 min, during which it was additionally vortexed for 30 s at 15 min intervals. Then the mixtures were allowed to cool to room temperature, after which they were centrifuged for 15 min at 4000 rpm. The supernatant was removed and filtered through Sartorius Stedim Biotech Minisart 16,534-K filters, which had a pore size of 0.2 μm. This was done to remove polysaccharides that might cause gelling of the solution.

B12 was extracted from the filtered solutions with EASI-EXTRACT B12 affinity columns (R-Biopharm Rhone Ltd., Scotland), which contained a gel with antibodies specific to cyanocobalamine. The columns were used according to the manufacturer's instructions. Depending on the sample, 10–30 mL of the extract was worked through the column and B12 was extracted from the gel with methanol. Methanol was removed from the sample using a vacuum centrifuge (1400 rpm, 60 °C, Eppendorf Concentrator Plus). Samples were diluted in water directly before the HPLC-UV/MS (model: Infinity 1290/6540) analysis. The column used was Agilent Technology C-18, with the dimensions 50 mm × 2.1 mm × 1.8 μm. The gradient (water +0.05 % formic acid (A) and acetonitrile +0.05 % formic acid(B)) used for elution was based on the recommendations given with the affinity column and was as follows: 0–3 min 99 % A + 1 % B, 3–11 min 85 % A and 15 % B, 27 11–12 min 75 % A and 25 % B, 12–12.1 min 90 % A + 10 % B, 12.1–14.5 min 99 % A + 1 % B. The flow rate was set at 0.2 mL/min and the UV detector at 362 nm.

Data were collected and analyzed using the MassHunter program (Agilent Technologies, USA). The cyanocobalamine peak was identified by its UV absorbance and mass spectra, comparing it to the integrated database NIST (2005) and to the standard. B12 was quantified using the

cyanocobalamine standard to create a row of dilutions and a calibration curve.

2.5. Microbiome analysis

The DNA was isolated using a modified CTAB protocol as follows: 40 mL of 0.85 % NaCl was added to approximately 5 g of frozen seaweed sample. The mixture was homogenized with the assistance of 5 mL 425–600 μm (Sigma) glass beads and then centrifuged at 4°C 2400 rpm for 5 min. The supernatant (approximately 30 mL) was removed and centrifuged again under the same conditions. After the second supernatant had been removed, the sample was centrifuged at 5500 rpm for 15 min (at 4°C), the supernatant was carefully discarded and 700 μL of the pelleted bacteria were used for the consequent CTAB treatment. A CTAB lysis buffer was prepared as described by Inglis et al. [20], and 500 μL of pre-warmed (+65 °C) CTAB lysis buffer was added to the pellet, which was re-suspended by pipetting and transferred to a 2 mL tube. Glass beads (two medium spoons (212–300 μm) and two small spoons (100 μm)) were added, and the sample was mixed prior to incubation at 65 °C for 15 min, 600 rpm. Following the initial incubation period, the sample was vortexed at room temperature (RT) for 10 min at maximum speed and then incubated again at 65 °C for 15 min, 600 rpm. The sample was cooled at RT for 5 min and then divided into two 1 mL aliquots.

Chloroform: isoamyl alcohol (24:1 v/v) was used for the DNA extraction, and 1 mL of the mixture was added to the sample, which was vortexed for 10 s and centrifuged at 7600 rpm for 10 min at RT. The upper aqueous phase was transferred to a new tube and the DNA was precipitated using 0.1 times its volume of 5 M sodium acetate (pH 5.2) and 0.66 times its volume of cold isopropanol (stored at −20 °C). The samples were mixed by inversion and stored at −20 °C overnight. The DNA pellet was recovered by centrifugation at 13000 ×*g* (11 755 rpm) for 10 min at RT. Cold 70 % ethanol (1 mL) was added to the pellet prior to centrifuging the sample again at 13000 ×*g* (11 755 rpm) for 10 min at RT. The supernatant was removed by aspiration to avoid loss of the nucleic acid pellet and tubes were left open to dry at room temperature for approximately 1 h. Autoclaved mQ water (30 μL) was added to the sample and the sample was re-suspended by pipetting.

The DNA concentration was measured using a Qubit BR kit (www.illumina.com), and 16S rRNA gene region V4 was sequenced using primers 515F (5′-GTGCCAGCMGCCGCGGTAA) and 806R (5′-GGACTACHVGGGTWTCTAAT) [21]. The sequencing was performed using an Illumina iSeq 100 (San Diego, CA, US) and an iSeq100 i1 reagent kit (2 × 150 bp) according to the manufacturer's protocol.

2.6. Statistical analysis

Excel's Data Analysis ToolPak was used for the statistical analysis calculations, including average values, standard deviation, *p*-values and correlation coefficients, of the data obtained from the Omega-3 fatty acids and B12 analysis.

The BION-meta (https://github.com/nielsl/mcdonald-et-al) program was used for the microbiome data analysis as described earlier [22]. The OTUs (operational taxonomic units) obtained from the sequencing were used for the creation of the NMDS (Non-metric multidimensional scaling) plot.

3. Results

3.1. Dynamics of total fatty acid and Omega-3 fatty acids as EPA and ALA in algae during the active growth period

A GC–MS analysis of the total extracted and methylated fatty acid profiles of five common algal species in the Baltic Sea was performed. Different parts of the coast were sampled three times, from April to September. Table 1 shows the determined total fatty acid. The total FA content ranged from 26.70 mg/gDW to 42.30 mg/gDW. The comparison of both seasonal and individual species average values showed no significant differences. However, species-specific maximum and minimum values correlated differently with sampling periods. Thus, *C. glomerata* had a significantly higher value in spring, whereas *F. vesiculosus* showed the highest concentration in autumn (Table 1). In contrast, the lowest values observed for *F. lumbricalis*, *F. vesiculosus* and *P. littoralis* were in the spring, summer, and autumn periods, respectively.

Table 1
Total fatty acid content (mg/gDW) in five algal species during three periods. Values with the same lower-case character letters within a line do not differ significantly (α = 0.05). Values with the same upper-case character letters within a column do not differ significantly (α = 0.05).

	April–May	June–July	August–September	Average
Pilayella littoralis	37.45 ± 2.38 ^{aA}	37.76 ± 0.28^{aF}	27.70 ± 0.28^{H}	34.30 ± 5.10 ^{K}
Fucus vesiculosus	34.00 ± 0.87^{B}	26.70 ± 1.10	42.22 ± 1.84^{J}	34.31 ± 6.80 ^{K}
Furcellaria lumbricalis	28.03 ± 0.72^{C}	37.45 ± 2.38 ^{bEFG}	38.90 ± 8.91 ^{bJ}	34.59 ± 7.47 ^{K}
Ulva intestinalis	32.47 ± 3.97 ^{cdABC}	33.73 ± 2.73 ^{cE}	28.53 ± 1.45 ^{dH}	31.58 ± 5.72 ^{K}
Cladophora glomerata	42.30 ± 2.34	37.58 ± 2.42 ^{eEF}	36.97 ± 1.11^{eJ}	38.95 ± 3.09 ^{K}

Of all of the fatty acids, eicosapentaenoic acid (EPA) was quantified separately using an internal standard and a standard of the fatty acid, while α-linoleic acid was quantified using only the internal standard (Table 2).

The amount of EPA varied significantly among different algae species. The highest EPA concentration was measured in the samples of *F. vesiculosus* (5.19 ± 0.32 mg/gDW), which was 2–37 times higher than in the other tested species (Table 2). The species-specific values of EPA had no seasonal variation. Unlike EPA values, ALA concentrations did not significantly vary either among species or seasonally and were around 1.07–2.22 mg/ g DW (Table 2).

3.2. Vitamin B12 content in algae during the active growth period

All extracted B12 forms from seaweeds were converted to cyanocobalamin to determine their total content. B12 was detected in all samples at concentrations varying from 4.14 ± 0.36 μg/100gDW to 53.55 ± 9.69 μg/100gDW (Table 3).

The highest average levels of B12 were detected in *C. glomerata* (53.55 ± 9.69 μg/100gDW), while the lowest were in *F. vesiculosus* (4.14 ± 0.36 μg/100gDW) (Table 3). The average levels of B12 in other species were in the range 4.71–33.04 μg/100gDW. In general, B12 levels were lowest during the summer period and could vary by a factor of up to eight compared with other seasons, as in the case of *C. glomerata,* where the autumn value was 53.55 μg/100gDW compared to 6.49 μg/100 g DW detected during the summer.

The acquired B12 concentrations were compared with the B12 contents of three commercial products which contained freeze-dried Atlantic Ocean seaweeds: *Palmaria palmata, Alaria esculenta* and *Saccharina lattissima* (data not shown). The obtained B12 concentrations were within the same range (4.59–15.36 μg/100gDW) as those from the Baltic Sea species.

3.3. 16 S rRNA amplicon analysis of microbiomes of the studied algae

To correlate B12 and Omega-3 levels with potential microbial producers, a 16S rRNA amplicon analysis was performed based on the DNA isolated from the studied algae samples. The NMDS analysis of the sequences obtained showed that the samples were mostly divided into three groups according to the sampling season (Fig. 1). In the upper area of the plot, probes sampled during April–May are found, whereas probes

Table 2
Eicosapentaenoic acid (mg/gDW) and α-linoleic acid (mg/gDW) in five different algal species during three periods, *- the fatty acid was not detected. Values with the same lower-case character letters within a line do not differ significantly (α = 0.05). Values with the same upper-case character letters within a column do not differ significantly (α = 0.05).

	April–May		June–July		August–September		Average	
	EPA	ALA	EPA	ALA	EPA	ALA	EPA	ALA
Pilayella littoralis	0.84 ± 0.07	1.60 ± 0.18^{eA}	0.99 ± 0.10^{b}	1.96 ± 0.15^{C}	1.12 ± 0.11^{b}	1.59 ± 0.21 ^{e}	0.98 ± 0.14	1.71 ± 0.18
Fucus vesiculosus	5.19 ± 0.32^{a}	1.86 ± 0.76 ^{B}	5.09 ± 0.19^{a}	1.48 ± 0.20	4.82 ± 0.11^{a}	2.45 ± 0.19	5.03 ± 0.19	1.93 ± 0.38
Furcellaria lumbricalis	1.96 ± 0.14^{c}	1.60 ± 0.40^{fA}	2.54 ± 0.10	1.92 ± 0.28^{fC}	2.02 ± 0.05^{c}	1.76 ± 0.79 ^{f}	2.17 ± 0.32	1.77 ± 0.33
Ulva intestinalis	0.12 ± 0.01	1.84 ± 0.24^{B}	0.15 ± 0.01	2.15^{g} ± 0.12	-*	2.08^{g} ± 0.13	0.14 ± 0.02	2.02 ± 0.15
Cladophora glomerata	1.25 ± 0.13^{d}	1.89 ± 0.31^{B}	1.23 ± 0.08^{d}	2.24 ± 0.13^{C}	1.47 ± 0.04	1.07 ± 0.56	1.32 ± 0.13	1.82 ± 0.33

Table 3
B12 content (μg/100gDW) in Baltic seaweed. Values with the same upper-case character letters within a column do not differ significantly (α = 0.05). Values with the same lower-case character letters within a line do not differ significantly (α = 0.05).

	April–May	June–July	August–September	Average
Fucus vesiculosus	4.14 ± 0.36^{A}	6.63 ± 0.65^{C}	5.29 ± 0.60	5.35 ± 1.25
Pilayella littoralis	4.71 ± 1.89^{A}	8.08 ± 1.04^{CD}	33.04 ± 9.97	15.28 ± 15.48
Furcellaria lumbricalis	10.72 ± 0.64^{a}	9.10 ± 0.90^{aD}	17.31 ± 3.53^{E}	12.38 ± 4.35
Cladophora glomerata	26.19 ± 3.41^{B}	6.49 ± 0.24^{C}	53.55 ± 9.69	28.75 ± 23.63
Ulva intestinalis	27.64 ± 1.97^{B}	4.86 ± 0.48	16.95 ± 4.41^{E}	16.48 ± 11.40

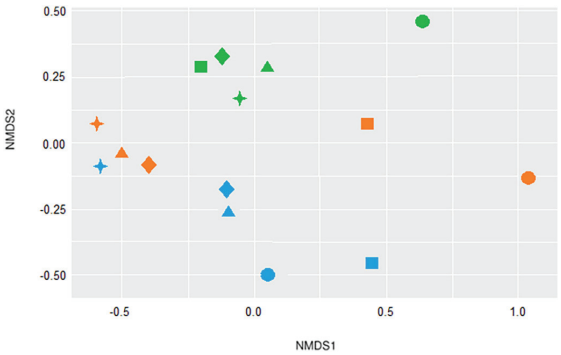

Fig. 1. NMDS plot; colors indicate seasons (green – Spring, orange – Autumn, blue – Summer); shapes indicate algae species (circle – *Ulva intestinalis*, diamond – *Pilayella littoralis*, square – *Cladophora glomerata*, triangle – *Fucus vesiculosus*, star – *Furcellaria lumbricalis*). (For interpretation of the references to colour in this figure legend, the reader is referred to the web version of this article.)

from August–September and June–July are located in the middle and at the bottom of the plot, respectively. Probes were also grouped based on the type of algae. Probes originating from green algae, such as *C. glomerata* and *U. intestinalis,* are mainly located on the right side of the plot, whereas probes from red (*F. lumbricalis*) and brown (*P. littoralis* and *F. vesiculosus*) algae fall on the left side of the plot.

Representatives of 24 different phyla were identified in the samples (see Table S1 in the supplementary materials). Of them, six were dominant in all samples (Fig. 2). These were *Verrucomicrobia, Proteobacteria, Planctomycetes, Cyanobacteria, Bacteroidetes* and *Actinobacteria*. Other phyla made up 1 % or less of the samples.

In total, 17 families formed the core microbiome found in all probes (Fig. 3). Their relative abundance varied among probes but generally representatives of *Verrucomicrobiaceae, Flavobacteriaceae, Rhodospirillaceae, Planctomycetaceae* and *Cyanobacteria* families dominated (on average 3–21 %), totaling up to 74 % in the individual probes.

Our analysis of dominant families in individual probes revealed that the top five families from each probe and their relative abundance in other probes made up 60–95 % of the microbiome in the studied samples. (Fig. 4) The exception was probe FV3 (*F. vesiculosus* autumn), where this level was about 40 %. In comparison, the top 10 families increased the average abundance at most by 12 % (data not shown). In total, 18 families were identified as the top five families from each probe and nine of them, *Comamonadaceae, Cyanobacteria Subsection I Family I, Flavobacteriaceae, Phyllobacteriaceae, Planctomycetaceae, Rhodobiaceae, Rhodospirillaceae, Sphingomonadaceae,* and *Verrucomicrobiaceae,* were part of the core microbiome. Generally, their relative abundance was high.

A correlation analysis between microbiome composition and Omega-3 fatty acids and B12 concentrations showed some correlations among the six dominant phyla. The *Cyanobacteria* phylum was strongly correlated with EPA and somewhat weaker with ALA (Supplementary Material Table S2). The ALA concentration was also weakly correlated with *Verrucomicrobia*. B12 was modestly connected with *Planctomycetes* and *Proteobacteria*. On the family level of the core microbiome, there were only weak correlations for EPA and ALA, whereas among the top five families in the individual probes clear level correlations were seen between EPA and *Psychromonodaceae*, *Sphingomonodaceae* and the new family DEV [23,24] of *Verrucomicrobiales*. ALA correlated moderately with *Sphingobacteriales* KD 3-93, *Sphingomonodaceae* and to some extent with *Verrucomicrobiaceae* (Supplementary Material Table S3-S4). However, no correlations at the genus or species level were found (data not shown).

As for B12, it was strongly correlated with *Commamonodaceae* at the level of the families of the core microbiome and at the level of the top five families in individual probes. B12 was also modestly correlated with *Cytophagaceae*, *Planctomyceae*, *Rhodospirillaceae* and, to some extent, with *Aeromonadaceae* and *Thiotriacaeae*.

To find correlations between B12 and microbiomes at the genera and species levels, the abundance of known B12-synthesizing bacteria was analyzed. Six genera known to include representatives that produce B12 were found in the samples (*Bacillus, Aeromonas, Rhodobacter, Clostridium, Pseudomonas* and *Xanthomonas*). Of the named genera, only *Rhodobacter* and *Pseudomonas* showed weak to moderate correlations with B12 content (see supplementary materials, Table S5). In contrast, the presence of five potentially B12-synthesizing bacteria species (*Rhodobacter capsulatus, Rhodobacter sphaeroides, Pseudomonas putida, Xanthomonas oligotrophicus,* and *Aeromonas hydrophila)* were strongly correlated with the B12 concentrations found in the probes (See supplementary materials, Table S6). Their abundance was higher in the green and red algae species, especially in the spring and autumn period (Fig. 5). *Rhodobacter capsulatus* was dominant in red and green algae

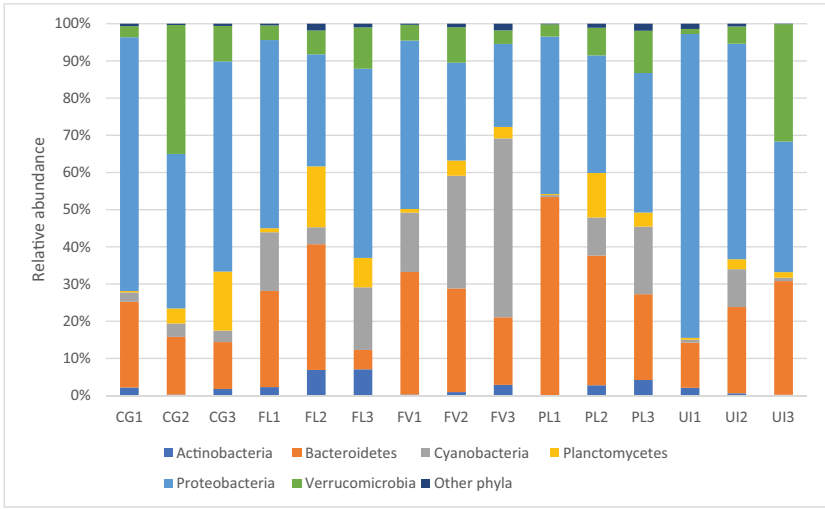

Fig. 2. Relative abundance of dominant phyla detected in seaweed samples (CG – *Cladophora glomerata*, FL – *Furcellaria lumbricalis*, FV – *Fucus vesiculosus*, PL – *Pilayella littoralis*, UI – *Ulva intestinalis*; 1 – April-May, 2 – June-July, 3 – August-September).

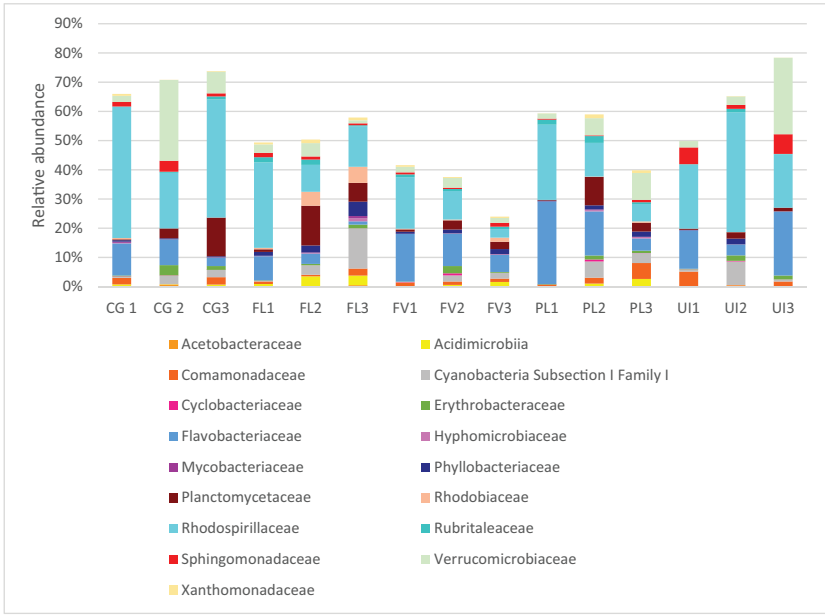

Fig. 3. Relative abundances of families forming the core microbiome (CG – *Cladophora glomerata*, FL – *Furcellaria lumbricalis*, FV – *Fucus vesiculosus*, PL – *Pilayella littoralis*, UI – *Ulva intestinalis*; 1 – April-May, 2 – June-July, 3 – August-September).

species, whereas in the brown algae species *Pseudomonas putida* and *Aeromonas hydrophila* were mainly found. The most commonly found potentially B12-synthesizing bacterial species was *Rhodobacter capsulatus*, which was dominant in the green and red algae species, but could not be found in the brown algae species. In the brown algae species, *Pseudomonas putida* and *Aeromonas hydrophila* were mainly found.

4. Discussion

The Baltic Sea ecosystem is unique due to its geographic isolation, and is characterized by low species and genetic diversity in macrophytes, including macroalgae [19,25]. The content of Omega-3 fatty acid in Baltic seaweeds has been previously analyzed in several studies [26–31]. The EPA concentration has been determined to be 3.89 mg/gDW for *F. vesiculosus*, 0.6–1.0 mg/gDW for *P. littoralis*, 1.35 mg/gDW for *C. glomerata* and 0.16 mg/gDW for *P. littoralis*. The ALA

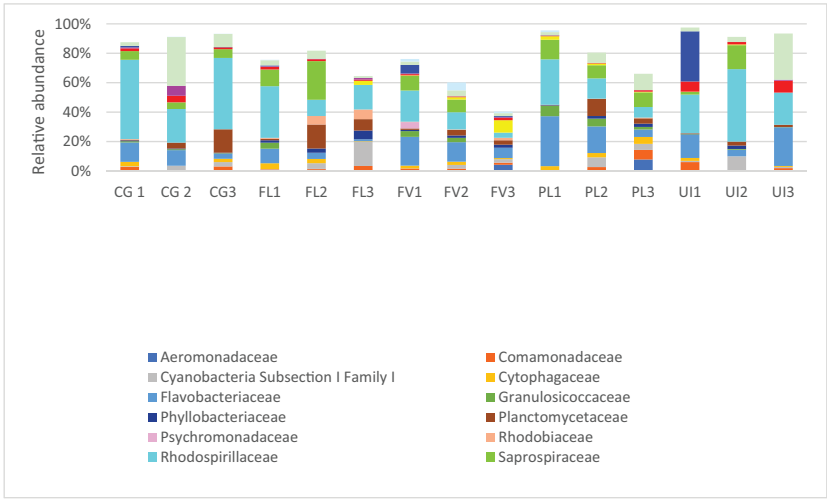

Fig. 4. Relative abundances of the top five families in individual probes (CG – *Cladophora glomerata*, FL – *Furcellaria lumbricalis*, FV – *Fucus vesiculosus*, PL – *Pilayella littoralis*, UI – *Ulva intestinalis*; 1 – April-May, 2 – June-July, 3 – August-September).

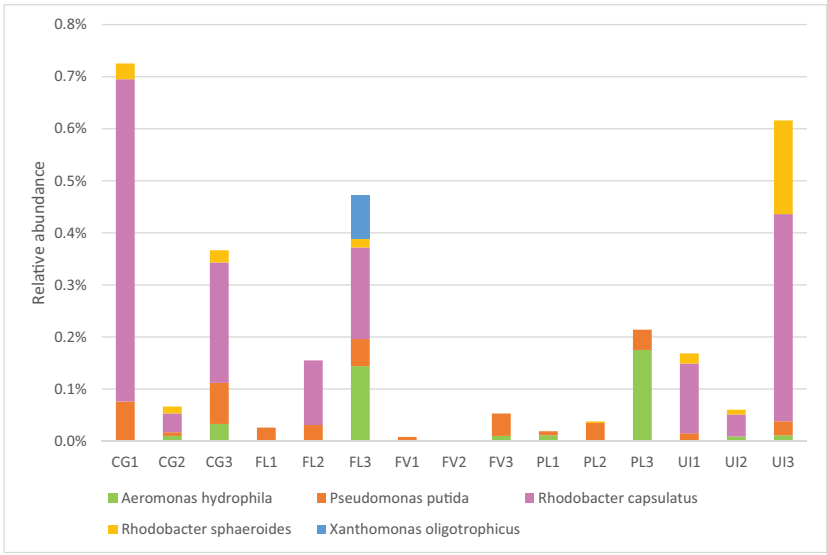

Fig. 5. Relative abundances of theoretical B12 synthesizing bacteria (CG – *Cladophora glomerata*, FL – *Furcellaria lumbricalis*, FV – *Fucus vesiculosus*, PL – *Pilayella littoralis*, UI – *Ulva intestinalis*, 1 – April-May, 2 – June-July, 3 – August-September).

concentrations have been found to be 2.78 mg/gDW for *C. glomerata* and 1.77 mg/gDW for *U. intestinalis*. Although data obtained in this paper generally were in the same range, varying from 0.12 to 5.03 mg/gDW for EPA and 1.07 to 2.22 mg/gDW for ALA, the seasonal variation of these fatty acids was determined for the first time. It was found to be species-specific: for both EPA and ALA, the average concentrations were highest during the June–July period, although the differences were not considered significant. *F. vesiculosus* was the highest EPA producer across all seasons, and was also one of the highest ALA producers, although only in autumn. In general, the ALA results showed little variance and no species could be singled out as the best source of ALA.

General information about B12 in algae shows that brown algae contain less B12 than red or green algae. However, data on specific species are sparse [16–18]. Additionally, although many studies have indicated high B12 levels in algae, not all of them have used reliable methods. None of the species analyzed in this paper has previously been evaluated in the Baltic Sea area. The B12 content in *C. glomerata* has been studied in laboratory conditions at optimal growth speed, reaching B12 levels between 30 and 50 μg/100gDW [32]. In this work, the highest average level of B12 content in sea algae was detected in *C. glomerata* (53.55 ± 9.69 μg/100gDW) in concentrations comparable to *in vitro* data. The average levels of B12 in other species were in the range of 4.14–33.04 μg/100 g DW. In general, B12 levels were lowest during the summer period and could vary by a factor of up to eight

compared with other seasons. Although B12 concentration was not measured in seawater, the content of B12 in algae may reflect changes in microbial communities resulting in either lower B12 synthesis or increased salvage by other auxotrophic-for-B12 microorganisms [33,34]. It has been shown that there is pronounced seasonal variance in both nutrient concentrations and temperature in the Baltic Sea, which have effects on microbial communities [19,25].

The microbiomes of the algal species were analyzed to determine any correlations between the samples and the nutrients analyzed. In total, 24 phyla were detected and six of them were dominant. These were *Verrucomicrobia, Proteobacteria, Planctomycetes, Cyanobacteria, Bacteroidetes* and *Actinobacteria*. Previous work has also showed the clear dominance of *Actinobacteria* in low salinity regions of the Baltic Sea and *Proteobacteria* in higher salinity areas. In this study, representatives of *Proteobacteria* and *Bacteroidetes* were dominant, which correlates with the salinity (6–6.5 ppt) at the collection sites. Most of the detected taxa are related to *Cyanobacteria* blooms in freshwater systems. *Cyanobacteria* blooms are also common during the summer in the Baltic Sea and impact the heterotrophic bacterial communities [19]. Our non-metric multidimensional scaling analysis revealed the seasonal grouping of probes. Probes originating from green algae could be distinguished from probes originating from red or brown algae.

It has been shown that algae themselves are able to produce omega-3 fatty acids, although the content may be affected by microorganisms [5,14]. A strong positive correlation was found between the abundance of *Cyanobacteria* and the EPA concentration. It has been previously proven that polyunsaturated fatty acids (PUFAs) can be produced by *Cyanobacteria* [35]. The relative abundance of *Cyanobacteria* was particularly high in *F. vesiculosus* and certain *F. lumbricalis* and *P. littoralis* samples, which correlates with the higher EPA contents of these samples. The occurrence of PUFA-producing representatives has also been reported in *Gammaproteobacteria* and *Flavobacteria*. Some PUFA-producing representatives of these genera are *Shewanella*, *Moritella*, *Colwellia*, *Alteromonas*, *Photobacterium*, *Flexibacter* and *Psychroserpens*. However, not all species within these genera produce PUFAs [36]. Although across the studied samples *Shewanella, Colwellia* and *Flexibacter* species were detected, their levels did not significantly correlate with the EPA or ALA concentrations measured.

Unlike EPA and ALA, no correlations could be found between the dominant phyla and B12 content. The strongest correlation found was at the family level for *Comamonadaceae*. However, no B12-producing representatives of this family have been described in the literature. The increased number of OTUs found seems to reflect the growth of these bacteria due to the consumption of B12 in the environment, rather than the production. It is known that some members of the microbiome are auxotrophs to B12 and therefore consume the B12 found in the sample [37].

Among the known B12-producing bacteria, the relative abundance of representatives of five species, *Rhodobacter capsulatus, Rhodobacter sphaeroides, Pseudomonas putida, Xanthomonas oligotrophicus* and *Aeromonas hydrophila,* was in correlation with the B12 levels. Comparing the three seasons, the June–July period had much lower levels of the named species. The lower amounts of B12-synthesizing bacteria found during the June–July period could have been the result of other microorganisms dominant during that period competing for the same nutrients and therefore suppressing the growth of B12-synthesizing bacteria.

Of the named five species, *Rhodobacter capsulatus* was the most commonly found, especially in the green and red seaweed samples. It has also been found that bacteria from the *Rhodobacteriales* genus are the most common de novo B12-synthesizing bacteria in the upper layers of the Atlantic Ocean near the American coastline [38]. In the brown seaweed samples, *Pseudomonas putida* and *Aeromonas hydrophila* were the two species most commonly found. The content of the latter was especially high in the August–September sample of *P. littoralis* and *F. lumbricalis*, which both showed higher B12 content compared to other seasons.

The highest B12 content was found in the April–May sample of *C. glomerata*, yet that sample was not found to have the highest content of B12-synthesizing bacteria. Therefore, it can be concluded that other species in the sample may synthesize B12 and that the efficiency of the synthesis is different among the species. *Cyanobacteria*, known to mainly synthesize pseudo-B12, were also found in the samples, but the concentration of *Cyanobacteria* could not be linked to the concentration of B12. Based on other studies of the microbiome of algae samples, it has been found that B12-synthesizing microorganisms mainly belong to the *Proteobacteria, Cyanobacteria* and *Archaebacteria* genera [39]. The low amounts of *Archaebacteria* in the samples analyzed in this study could have been due to the nutrient and salinity differences in the Baltic Sea compared to in the open sea.

This paper provides preliminary results of B12 contents. A metagenomic analysis is needed to link biosynthetic pathways with the properties for commercial productions. Potential uses of seaweed species as sources of EPA and B12 would be algae-based food supplements. Dried algae can be made into powders, which can be used in smoothies, raw food snack bars, seaweed chips and snacks. The powder could also be compressed into pills. However, something to consider before introducing algae as a part of the human diet is product safety, as algae are known to accumulate elements present in their environment, for example, heavy metals.

CRediT authorship contribution statement

Õnnela Luhila performed writing – original draft and editing, investigation and formal analysis of data obtained. Tiina Paalme provided study material, participated in the study conceptualization and performed editing. Kristel Tanilas performed development of B12 extraction and measurement methodology. Inga Sarand performed writing – original draft, review and editing; conceptualization and supervision of the project.

Formatting of funding sources

This study was supported by ERDF and Estonian Research Council via projects RESTA12 and RESTA13.

Declaration of competing interest

The authors declare that they have no known competing financial interests or personal relationships that could have appeared to influence the work reported in this paper.

Data availability

Data will be made available on request.

Acknowledgments

We wish to thank Maria Kuhtinskaja for her assistance in developing the GC–MS methodology and preliminary experiments in the fatty acid analysis and Prof. Toomas Paalme for critical discussions.

Appendix A. Supplementary data

Supplementary data to this article can be found online at https://doi.org/10.1016/j.algal.2022.102860.

References

[1] P. Choudhary, V. Subhash, M. Khade, S. Savant, A. Musale, G.R.K. Kumar, M. Chelliah, S. Dasgupta, Empowering blue economy: from underrated ecosystem to sustainable industry, J. Environ. Manag. 291 (112697) (2021) 1–16.
[2] F.J. Barba, Microalgae and seaweeds for food applications: challenges and perspectives, Food Res. Int. 99 (2017) 969–970.

[3] A. Fehér, M. Gazdecki, M. Véha, M. Szakály, Z. Szakály, A comprehensive review of the benefits of and the barriers to the switch to a plant-based diet, Sustainability 12 (10) (2020) 4136.
[4] S. Roohinejad, M. Koubaa, F.J. Barba, S. Saljoughian, M. Amid, R. Greiner, Application of seaweeds to develop new food products with enhanced shelf-life, quality and health-related beneficial properties, Food Res. Int. 99 (2017) 1066–1083.
[5] G. Silva, R.B. Pereira, P. Valentão, P.B. Andrade, C. Sousa, Distinct fatty acid profile of ten brown macroalgae, Rev. Bras 23 (4) (2013) 608–613.
[6] R. Siddiqui, S. Shaikh, L. Sech, H. Yount, W. Stillwell, G. Zaloga, Omega 3-fatty acids: health benefits and cellular mechanisms of action, Mini-Rev.Med. Chem. 4 (8) (2012) 859–871.
[7] D. Swanson, R. Block, S. Mousa, Omega-3 fatty acids EPA and DHA: health benefits throughout life, Adv. Nutr. 3 (1) (2012) 1–7.
[8] P. Calder, Very long-chain n-3 fatty acids and human health: fact, fiction and the future, Proc. Nutr. Soc. 77 (2018) 52–72.
[9] E. Baker, E. Miles, G. Burdge, P. Yaqoob, P. Calder, in: Metabolism and Functional Effects of Plant-derived Omega-3 Fatty Acids in Humans 64, 2016, pp. 30–56.
[10] C. Gherasim, M. Lofgren, R. Banerjee, Navigating the B12 road: assimilation, delivery, and disorders of cobalamin, J. Biol. Chem. 288 (19) (2013) 13186–13193.
[11] G. Yahn, J. Abato, N. Jadavji, Role of vitamin B12 deficiency in ischemic stroke risk and outcome, Neural Regen. Res. 16 (3) (2021) 470–474.
[12] M. Ryan-Harshman, W. Aldoori, Vitamin B12 and health, Can. Fam. Physician 54 (4) (2008) 536–541.
[13] A. Danchin, S. Braham, Coenzyme B12 synthesis as a baseline to study metabolite contribution of animal microbiota, Microb. Biotechnol. 10 (2017) 688–701.
[14] V.J. Van Ginneken, J.P. Helsper, W. de Visser, H. van Keulen, W.A. Brandenburg, Polyunsaturated fatty acids in various macroalgal species from North Atlantic and tropical seas, Lipids Health Dis. 10 (1) (2011) 104.
[15] V. Joglar, X. Alvarez-Salgado, A. Gago-Martinez, C. Perez-Martinez, B. Pontiller, D. Lundin, J. Pinhassi, E. Fernandez, E. Teira, J. Leao, Cobalamin and microbial plankton dynamics along a coastal to offshore transect in the Eastern North Atlantic Ocean, Environmental Microbiology 23 (3) (2021) 1559–1583.
[16] F. Watanabe, S. Takenaka, H. Katsura, S.A.M.Z.H. Masumder, K. Abe, Y. Tamura, Y. Nakano, Dried green and purple lavers (Nori) contain substantial amounts of biologically active vitamin B12but less of dietary iodine relative to other edible seaweeds, J. Agric. Food Chem. 47 (6) (1999) 2341–2343.
[17] F. Watanabe, S. Takenaka, H. Katsura, E. Miyamoto, K. Abe, Y. Tamura, T. Nakatsuka, Y. Nakano, Characterization of a Vitamin B12 compound in the edible purple laver, Porphyra yezoensis, Bioscience, Biotechnology, and Biochemistry 64 (12) (2000).
[18] F. Watanabe, Y. Yabuta, T. Bito, F. Teng, Vitamin B12-containing plant food sources for vegetarians, Nutrients 6 (5) (2014) 1861–1873.
[19] C. Berner, M. Bertos-Fortis, J. Pinhassi, C. Legrand, Response of microbial communities to changing climate conditions during summer cyanobacterial blooms in the Baltic Sea, Frontiers in Microbiology 9 (2018).
[20] P.W. Inglis, M.D.C.R. Pappas, L.V. Resende, D. Grattapaglia, Fast and inexpensive protocols for consistent extraction of high quality DNA and RNA from challenging plant and fungal samples for high-throughput SNP genotyping and sequencing apapplications, PLOS ONE 13 (10) (2018).
[21] J.G. Caporaso, C.L. Lauber, W.A. Walters, D. Berg-Lyons, C.A. Lozupone, P. J. Turnbaugh, N. Fierer, R. Knight, Global patterns of 16S rRNA diversity at a depth of millions of sequences per sample, PNAS 108 (2010) 4516–4522.
[22] J. Kazantseva, E. Malv, A.E.A. Kaleda, Optimisation of sample storage and DNA extraction for human gut microbiota studies, BMC Microbiol 21 (2021) 158.
[23] Y.O.O. Hu, B. Karlson, S. Charvet, A.F. Andersson, Diversity of pico- to mesoplankton along the 2000 km salinity gradient of the Baltic Sea, Frontiers in Microbiolog 7 (2016) 679, https://doi.org/10.3389/fmicb.2016.00679.
[24] GBIF, Global Biodiversity Information Facility [Online]. Available, 2021. Accessed 24 September, https://www.gbif.org/species/10809088.
[25] K. Ininbergs, B. Bergman, J. Larsson, M. Ekman, Microbial metagenomics in the Baltic Sea: recent advancments and prospects for environmental monitoring, Ambio 44 (2015) 439–450.
[26] K. Ramavat, K. Pazdro, A. Kosakowska, J. Pempkowiak, Fatty acid content in seaweeds from the Baltic Sea and the Indian Ocean, Oceanologia 39 (3) (1997) 279–287.
[27] Y.I. Gubelit, O.N. Makhutova, N.N. Sushchik, A.A. Kolmakova, G.S. Kalachova, M. I. Gladyshev, Fatty acid and elemental composition of littoral “green tide” algae from the Gulf of Finland, the Baltic Sea, Journal of Applied Phycology 27 (1) (2014).
[28] R. Parjikolaei, A. Bruhn, K. Loft Eybye, M. Larsen, M. Rasmussen, K. Christensen, X. Frette, Valuable biomolecules from nine North Atlantic red macroalgae: amino acids, fatty acids, carotenoids, minerals and metals, naturalResources 7 (4) (2016) 157–183.
[29] A. Naseri, S.L. Holdt, C. Jacobsen, Biochemical and nutritional composition of industrial red seaweed used in Carrageenan production, Journal of Aquatic Food Product Technology 28 (9) (2019) 967–973.
[30] J. Lorenzo, R. Agregan, P. Munekata, D. Franco, J. Carballo, S. Sahin, R. Lacomba, F. Barba, Proximate composition and nutritional value of three macroalgae: Ascophyllum nodosum, Fucus vesiculosus and Bifurcaria bifurcata, Mar. Drugs 15 (11) (2017) 360.
[31] T. Řezanka, O. Vyhnálek, M. Podojil, Separation and identification of lipids and fatty acids of the marine algaFucus vesiculosus by TLC and GC—MS, Folia Microbiologica 33 (4) (1988) 309–313.
[32] J.P. Hoflmann, Dependence of photosynthesis and vitamin B12 uptake on cellular vitamin B12 concentration in the multicellular alga Cladophora glomerata (Chlorophyta), Limnol. Oceanogr. 35 (1) (1990) 100–108.
[33] A.C. Doxey, D.A. Kurtz, M.D. Lynch, L.A. Sauder, J.D. Neufeld, Aquatic metagenomes implicate thaumarchaeota in global cobalamin production, ISME J. 9 (2) (2014) 461–471.
[34] M.F. Romine, D.A. Rodionov, Y. Maezato, A.L. Osterman, W.C. Nelson, Underlying mechanisms for syntrophic metabolism of essential enzyme cofactors in microbial communities, The ISME Journal 11 (6) (2017) 1434–1446.
[35] K. Sharathchandra, M. Rajashekhar, Total lipid and fatty acid composition in some freshwater cyanobacteria, J. Algal Biomass Util. 2 (2) (2011) 83–97.
[36] E. Freese, H. Rütters, J. Köster, J. Rullkötter, H. Sass, Gammaproteobacteria as a possible source of eicosapentaenoic acid in anoxic intertidal sediments, Microb. Ecol. 57 (3) (2008) 444–454.
[37] P.H. Degnan, M.E. Taga, A.L. Goodman, Vitamin B 12 as a modulator of gut microbial ecolog, Cell Metab. 20 (5) (2014) 769–778.
[38] L. Gómez-Consarnau, R. Sachdeva, S.M. Gifford, L.S. Cutter, J.A. Fuhrman, S. A. Sañudo-Wilhelmy, M.A. Moran, Mosaic patterns of B-vitamin synthesis and utilization in a natural marine microbial community, Environmental Microbiology 8 (2018) 2809–2823.
[39] K.R. Heal, W. Qin, F. Ribalet, A.D. Bertagnolli, W. Coyote-Maestas, L.R. Hmelo, A. E. Ingalls, Two distinct pools of B12analogs reveal community interdependencies in the ocean, Proceedings of the National Academy of Sciences 114 (2) (2016) 364–369.

Appendix 2

Publication II

Luhila, Õ., Karro, K., Zakrevskaja, K., Nisamedtinov, I., & Paalme, T. (2024). Cryo-protective effect of ice-binding proteins produced by *Pseudomonas fluorescens* AQP671 on wholegrain wheat bread dough during freezing and frozen storage. LWT, 214.

LWT - Food Science and Technology 214 (2024) 117160

Contents lists available at ScienceDirect

LWT

journal homepage: www.elsevier.com/locate/lwt

Cryo-protective effect of ice-binding proteins produced by *Pseudomonas fluorescens* AQP671 on wholegrain wheat bread dough during freezing and frozen storage

Õnnela Luhila [a,*], Karro Kadi [a], Zakrevskaja Karina [a], Nisamedtinov Ildar [a,b,c], Paalme Toomas [a], Laos Katrin [a]

[a] Department of Chemistry and Biotechnology, School of Science, Tallinn University of Technology, Tallinn, Estonia
[b] Competence Center of Food and Fermentation Technologies, Tallinn, Estonia
[c] Lallemand Inc, Montreal, Canada

ARTICLE INFO

Keywords:
Ice-binding proteins
Frozen dough
Bread
Pseudomonas fluorescens

ABSTRACT

Ice-binding proteins (IBPs) of cold-induced *Pseudomonas fluorescens* AQP671 were assessed for their potential as cryoprotective agents in frozen wholegrain wheat dough during freezing and 8 weeks of frozen storage. The protein solution exhibited significant ice-recrystallization inhibition activity at total protein concentrations of 0.1 g/L and above. The addition of IBPs improved the yeast survival rates in the dough post-freezing on average 7.8% compared to the untreated samples. Additionally, yeast survival rates were stable during 8 weeks of frozen storage in samples that had at least 5% (0.09 g/kg) of the total dough weight supplemented with the protein solution. As a result, the rising capacity of the dough was improved by the addition of ice-binding proteins, correlating to their concentration in the dough. Additionally, the freeze tolerance of the starch granules was maintained for at least 6 weeks for all of the IBP-treated samples. Furthermore, the ice-binding proteins had a positive effect on the strength of the dough after thawing, indicating less damage to the gluten structure and improved the overall texture and sensory parameters of the final bread product.

1. Introduction

Freezing as a form of preservation has extended the shelf life and increased the production quantities of dough and related products (Cao et al., 2020a; Zhao et al., 2022). However, the freeze-thaw process can lead to structural and textural changes that negatively impact the quality of the end product. The formation of ice crystals during freezing and the freeze-thaw process can cause starch retrogradation, and disrupt the dough matrix, gluten network and yeast viability resulting in reduced dough strength and compromised baking performance (Ding et al., 2020; Sharadanant & Khan, 2003a; Yang et al., 2019; Zhao et al., 2022). The effect of frozen storage on wholegrain wheat dough has not been thoroughly researched. Previous literature has indicated that whole wheat dough may have better resistance to freezing compared to white wheat dough when it comes to maintaining loaf volume and softness. However, the decrease in quality is still significant, 8.8% and 17.9% decrease in loaf volume and 28.8% and 39.9% decrease in softness, respectively (Bae, Lee, Hou, & Lee, 2014).

Several studies have investigated the potential of improving the quality of frozen food products by integration of a variety of additives, such as hydrophilic gums, cold-active enzymes, natural deep eutectic solvents and polysaccharides with varying degrees of success (Eskandari, Leow, Rahman, & Oslan, 2020, 2024, Mangiagalli, Brocca, Orlando, & Lotti, 2020; Sharadanant & Khan, 2003a; Tian, Zhu, & Sun, 2020; Zhao et al., 2022). In recent years, the application of ice-binding proteins (IBPs) has emerged as a promising strategy to decrease the negative effects of freezing on the quality of frozen food products (Ding et al., 2020; Jia et al., 2012; Nguyen et al., 2018; Saki, Ghaffari, & Nikoo, 2023; Sun, Zhu, & Sun, 2023; Zhao et al., 2022). IBPs are a group of proteins isolated from a diverse range of organisms, including fish, insects, plants, fungi, algae, and microorganisms. Although these proteins share a common function in interacting with ice, they vary significantly in size and structure. The primary shared feature among IBPs is the presence of an ice-binding site (IBS), a planar surface that complements the structure of ice, allowing for effective binding. Their ability to bind to ice crystals may induce ice nucleation or inhibit the growth and

* Corresponding author.
E-mail address: onnela.luhila@taltech.ee (Õ. Luhila).

https://doi.org/10.1016/j.lwt.2024.117160
Received 13 May 2024; Received in revised form 21 November 2024; Accepted 5 December 2024
Available online 9 December 2024

recrystallization of ice. By adsorbing to ice, these proteins can reduce ice crystal size, minimize damage to the structure of food products, and preserve their integrity during freezing and frozen storage (Białkowska, Majewska, Olczak, & Twarda-clapa, 2020).

In this paper, a strain of *Pseudomonas fluorescens* (AQP671) originating from the Ganavan Bay is shown to produce ice-binding proteins exhibiting high ice recrystallization inhibition activity. Analog proteins of Pseudomonas species are present outside of the bacterial cells, are easy to produce and due to their thermal hysteresis and ice recrystallization inhibition activities show potential to be used in frozen foods to improve their quality and shelf-life (Kawahara et al., 2004; Liu, Liang, Wang, et al., 2018; Singh, Hanada, Singh, & Tsuda, 2014). Ice-binding proteins (IBPs) from *Pseudomonas syringae*, which exhibit ice nucleation activity, have been shown to enhance the freezing rate and improve the microstructure of frozen surimi, reducing the oxidation and aggregation of myofibrillar proteins (Saki et al., 2023) Similar effects have been observed for ice-nucleating proteins from *Pseudomonas fluorescens* MACK-4, which enhanced the freezing properties of various food systems, including full-cream milk and 10% starch solutions (Yin, Chen, Tzeng, Chiou, & Jiang, 2005). However, practical applications of IBPs from *Pseudomonas* species with ice recrystallization inhibition activity in frozen dough remain unexplored.

Understanding the cryo-protective effect of IBPs on frozen dough could aid in the development of innovative strategies to improve frozen dough quality and ultimately enhance the sensory attributes of baked products. In this study, we aim to investigate the impact of *Pseudomonas fluorescens* AQP671 IBPs on the cryo-protective properties of wholegrain wheat dough during freezing and frozen storage. By analyzing the effects of IBP supplementation on dough, bread, and baking characteristics, we seek to provide valuable insights into the mechanisms underlying the cryo-protective effect of IBPs. These findings could contribute to the development of novel approaches for the production of high-quality frozen dough and baked goods.

2. Materials and methods

2.1. Materials

Pseudomonas fluorescens strain AQP671 used for the production of ice-binding proteins (IBPs) was provided by Lallemand, Inc. The strain was isolated from a *Laminaria* (brown algae) sample collected at the Ganavan Bay, Oban, Scotland. Wholegrain wheat flour (Tartu Mill, lot 137060), sugar (Extra Line), dry yeast (Kitchen Mood), salt (Santa Maria), canola oil (Olivia) and milk (Alma, 2.5% fat) were purchased from local grocery stores in Tallinn, Estonia. All reagents used were of analytical grade.

2.2. Sample preparation

Pseudomonas fluorescens strain AQP671 was cultivated at 30°C in shaker flasks on media containing 20 g/L glycerol and 10 g/L yeast extract for 48 h. The cells were removed and the supernatant was collected by centrifugation at 1968*g* for 20 min at 10°C. Cells were resuspended in fresh original media for an additional 72 h at 10 °C to promote the IBP production. The culture was centrifuged as above and the supernatant was stored at −20 °C. Negative control and IBP solution were both assessed for ice recrystallization inhibition activity and the total protein concentration was measured using Pierce™ Modified Lowry Protein Assay Kit (Thermo Fisher Scientific) according to the manufacturer's instructions.

2.3. Ice recrystallization inhibition assessment

Ice recrystallization inhibition activity was measured using the modified sucrose sandwich assay as previously described (Kaleda, Tsanev, Klesment, Vilu, & Laos, 2018). A sample was mixed with a 70% sucrose solution (1:1, v/v ratio), 3 μL of the mixture was placed on a microscope slide, covered with a cover glass and the edges sealed with silicone oil. The slide was frozen in liquid nitrogen and placed on a cooling stage (Linkam PE 120, UK) of a microscope (Nikon Eclipse E 200, Japan). The temperature control program (Table 1) for the cold stage was set to the ice crystal melting point of 35% sucrose solution. Motic Images 3.0 program was used to record images at the end of ramps 4 and 6. Images were analyzed using Image J image analysis tool and ice crystal growth rates were calculated using the Ostwald law equation (Budke, Heggemann, Koch, Sewald, & Koop, 2009):

$$k = \frac{r^3 - r_0^3}{t},$$

where.

k – ice crystal growth rate, μm^3/min
r – average ice crystal radius at the end of ramp 6, μm
r_0 – average ice crystal radius at the end of ramp 4, μm
t – time, min.

Table 1
Temperature ramps.

Ramp	Temperature, °C	Time, s	Temperature gradient, °C/min
1	−10,0	30	20
2	−7,0	15	10
3	−9,0	15	10
4	**−6,8**	**60**	**10**
5	−8,0	5	10
6	**−6,8**	**180**	**10**

The 50% dilution points were used to compare samples as well as determine the final dilution used in the dough recipes. A row of dilutions was created using 35% sucrose solution until no inhibition of ice recrystallization could be determined. The dilution at which point the ice crystal growth rate was equal to half of the maximum was the 50% dilution point. All samples were measured in three replications.

To assess the residual IRI activity in the dough, the dough was repeatedly washed with 50 mM phosphate buffer. The final ratio of dough to buffer was 1:2, w/w.

2.4. Dough and bread preparation

The recipe for the dough according to 1 kg of wholegrain wheat flour contained 400 g of milk, 400 g of IBP solution or negative control, 130 g of sugar, 50 g of oil, 17 g of salt and 17 g of dry yeast. The ingredients were incorporated using a Kitchen Aid Heavy Duty 5KPM5 (Whirlpool Corporation, USA) mixer at speed 1 (60 rpm) for 2 min and at speed 2 (90 rpm) for 3 min. The dough was divided into 80 g portions, wrapped in low-density polyethene film and flash frozen at −18 °C for 4 h using a Foster Surf Navigation freezer. The dough was thawed immediately after freezing and further at 2-week intervals at 4 °C overnight (15 h). During storage, the dough was kept at −18 °C.

The negative control contained the uninduced supernatant of *Pseudomonas fluorescens* AQP671, and the samples enhanced with ice-binding proteins contained the cold-induced supernatant of *Pseudomonas fluorescens* AQP671. The final concentrations of the cold-induced *P. fluorescens* supernatant in the dough were 1.25%, 2.5%, 5%, 10% and 20% (indicated as IBP-1.25%, IBP-2.5%, IBP-5%, IBP-10% and IBP-20%). The equivalent total added protein concentration in the doughs were 0.02 mg/mL, 0.04 mg/mL, 0.09 mg/mL, 0.18 mg/mL and 0.36 mg/mL as measured using the Pierce™ Modified Lowry Protein Assay Kit (Thermo Fisher Scientific) according to the manufacturer's instructions.

Once thawed, the dough was held at 32 °C, 80% RH using the Metos System Rational HCPC oven for 45 min to rise and then baked at 200 °C,

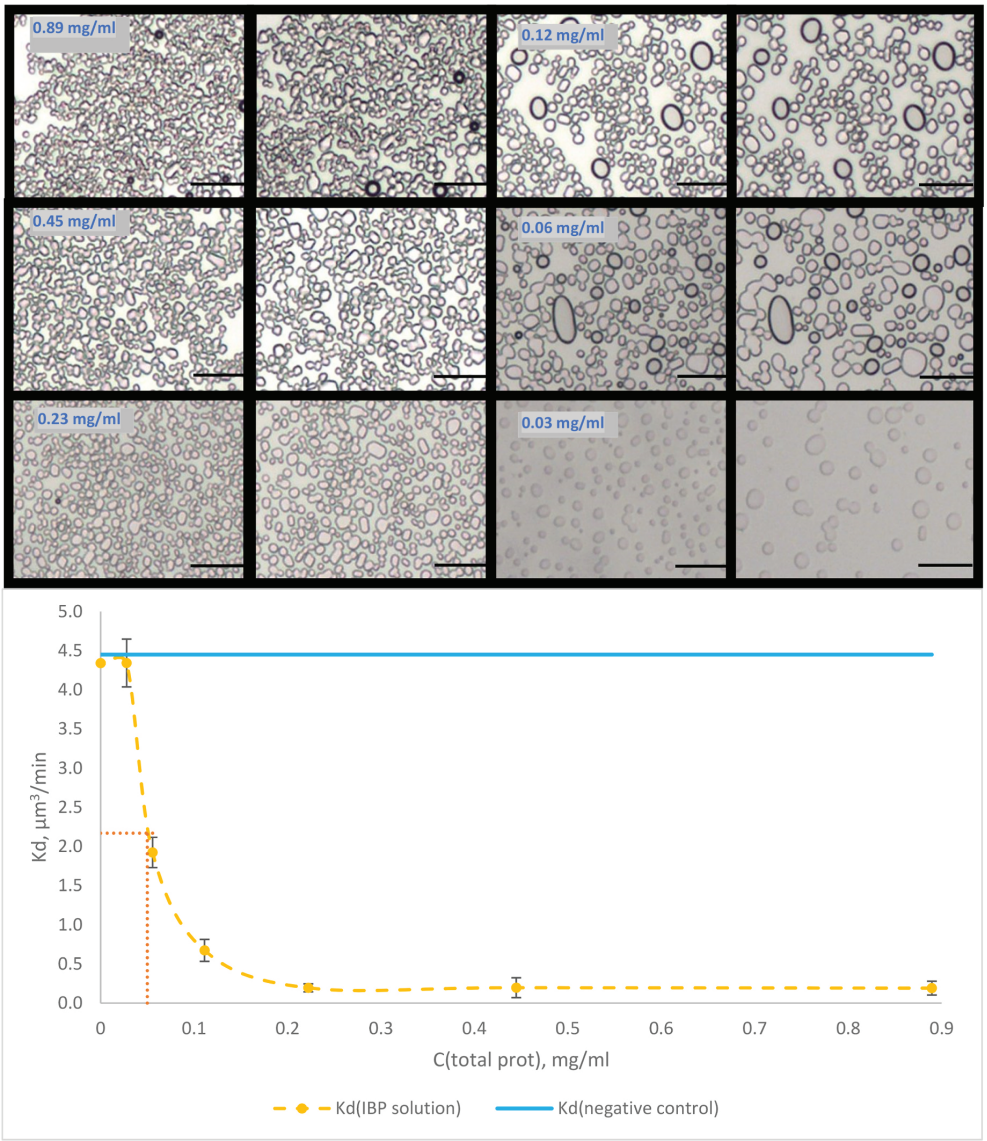

Fig. 1. Above – microscope images of ice crystals in the IBP solution diluted in 70% saccharose solution (2–64x diluted, total protein concentrations 0.03–0.89 mg/mL) during the modified sucrose sandwich assay at ramp 4 (left) and ramp 6 (right). The scale bar is 30 µm. Below – ice crystal growth rates in correlation with the total protein content of the solution. The dotted line indicates the 50% point and the solid blue line is the average ice crystal growth rate of the negative control.

50% RH for 15 min.

2.5. Yeast survival rates

The yeast survival rates were determined as previously reported (Zhao et al., 2022). Thawed dough (20 g) was suspended in distilled water (180 mL) and mixed for 30 min using a magnetic stirrer and then allowed to settle for 15 min. The solution was mixed with methylene blue dye (1:9, v/v) and incubated at room temperature for 10 min. The yeast cells were counted under a microscope (Nikon Eclipse E 200), using the Brüker chamber. All samples were measured in three replications.

2.6. Rising properties of the dough

The dough portions were placed in pre-greased baking molds, flattened and the height of the dough was measured (0.1 cm accuracy). The same measurement was recorded after rising to assess the rising properties of the dough. All measurements were done in 8 replications and results were calculated as a percentage of initial height.

2.7. Specific volume

The specific volume was assessed as described in the literature (Sharadanant & Khan, 2003b). After baking the bread was allowed to

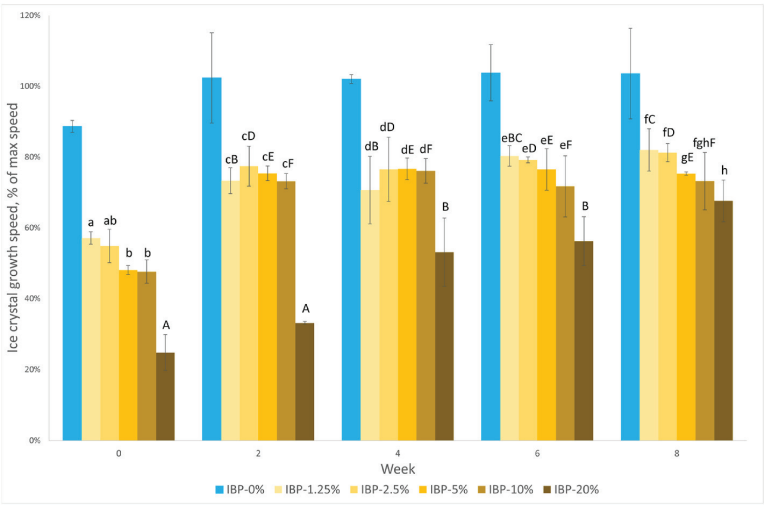

Fig. 2. Ice recrystallization inhibition (IRI) activity of 2x diluted frozen dough extracts in 70% sucrose solution over 8 weeks of frozen storage. Results are expressed as the percentage of average crystal growth speed relative to the negative control. Lowercase letters indicate significant differences between samples at the same storage time, while uppercase letters denote significant differences across all storage times within a given IBP concentration.

cool down (1.5 h) and then weighed. The volume of the loaves was measured using silica gel granules (d = 0.5 cm). A 1 L beaker was filled to the line with the granules, approximately ¾ of the granules were removed, the bread was placed into the beaker and filled again to the line with the granules. The unused granules representing the volume of the bread were measured using a graduated cylinder (2.5 cm^3 accuracy). Specific volume was calculated as cm^3/g and measurements were done in 5 replications.

2.8. Mass decrease in baking and cooling

The weight of the loaves was measured (0.01 g accuracy) before baking, straight after baking as well as 1.5 h after baking, when the loaves had completely cooled down. The mass decrease was calculated as % of the original dough weight for the mass decrease in baking and % of the original baked bread weight for the mass decrease in cooling. All measurements were done in 8 replications.

2.9. Texture profile analysis

The dough and bread texture profile was determined using the TA-XT2i Stable Micro Systems texture profile analyzer and results were analyzed with the Texture Expert Exceed program. The parameters for the analysis were chosen according to the literature (Rodríguez-Sandoval, Fernández-Quintero, Sandoval-Aldana, & Cuvelier, 2008; Zhao et al., 2022).

For the dough analysis, a cylindrical P25 probe (d = 25 mm) was used. The thawed dough was shaped into a 10 × 10 mm cylinder, placed onto the platform, compressed to 30% of its initial height, held for 10 s and compressed again. The speed was set to 1 mm/s.

For the bread analysis, a cylindrical P36R probe (d = 36 mm) was used. A 25 mm slice of bread was cut from the cooled loaf, deformed to 40% of its initial height, held for 5 s and deformed again, the test speed was 1 mm/s.

For both dough and bread, seven textural parameters were determined (hardness, elasticity, springiness, adhesiveness, cohesiveness, chewiness and gumminess) in 5 replications.

2.10. Sensory analysis

The sensory analysis of the bread samples was carried out on the day of baking by 5–7 trained assessors from the Division of Food and Biotechnology at Tallinn University of Technology. All assessors were between the ages of 20–32, one assessor was male and six female. The bread was sliced into 1.5 cm slices and compared to commercially available wholegrain wheat bread (Täisterasepik, Eesti Pagar). The appearance (color, porosity), texture (elasticity, crumbling, moisture, softness, adhesiveness), aroma (intensity, sour, yeast) and taste (intensity, sour, salty, bitter) were graded on a 0–10 scale compared to the set values of the reference.

2.11. Starch microscopy

The size of the starch granules in the dough was analyzed as previously described (Yang et al., 2019) with slight modification. The starch slurry was dried as a thin layer on a microscope slide at 35°C until the weight of the sample was constant. The sample was observed under a microscope (Nikon Eclipse E 200, Japan) at 100x and 400x magnification and the size of the starch granules was measured using the Image J image analysis tool. Approximately 300–500 starch granules were measured for each sample.

2.12. Statistical analysis

The statistical analysis of IRI activity and starch microscopy images was carried out using the Image J image analysis tool as well as Microsoft Excel. The data from the dough and bread experiments were analyzed using analysis of variance (ANOVA) with Tukey's Honest Significant Difference (HSD) test. The analysis was performed using Microsoft Excel's Data Analysis Toolpak, and a significance level of $p < 0.05$ was adopted, with calculations conducted using the ASTATSA program.

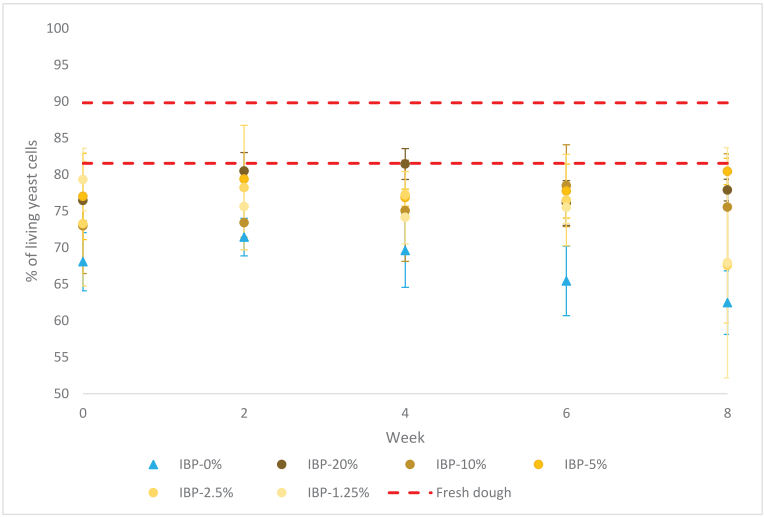

Fig. 3. Living yeast cell counts in thawed dough containing 0–20% ice-binding proteins (IBPs) during 8 weeks of frozen storage. The red dotted lines indicate the value range for the unfrozen fresh dough (85.5 ± 4.3%).

3. Results

3.1. Ice recrystallization inhibition activity

The post-cold-induction supernatant of *Pseudomonas fluorescens* AQP671 showed ice recrystallization inhibition activity. The ice crystal growth rates as well as the determination of the 50% activity point can be seen in Fig. 1.

The average growth rate of ice crystals in the negative control was 4.45 ± 0.23 μm^3/min. Similar rates could be seen in the lowest total protein solution (4.34 ± 0.30 μm^3/min). According to that the approximate 50% dilution for the solution was at the total protein concentration of 0.05 mg/ml or ~35 times diluted. The IRI activity could be considered high (Kd < 1.0 μm^3/min) at a protein concentration of 0.1 mg/ml and above. These results were taken into account when choosing the IBP solution concentrations for the dough recipes.

IBP activity could also be detected in the dough after thawing as seen in Fig. 2.

The ice crystal growth rate was lowest in the dough extract containing the highest concentrations of IBPs correlating to the highest activity. The loss of activity is most prominent at week 4 for the sample containing 20% IBP solution and at week 2 for the other samples, after the initial increase in ice crystal growth speeds, the rates stabilized. The relative rates stayed below the values of the negative control throughout the 8-week experiment, indicating that the frozen storage and freeze-thaw cycles decrease the protein stability, but don't negate it completely.

3.2. Living yeast cell count in dough

Growing ice crystals as well as ice recrystallization have been shown to significantly decrease the living yeast cell count in frozen dough (Nguyen et al., 2018; Phimolsiripol, 2009; Tian et al., 2020). The survival rates of the yeast cells during the 8-week frozen storage of whole

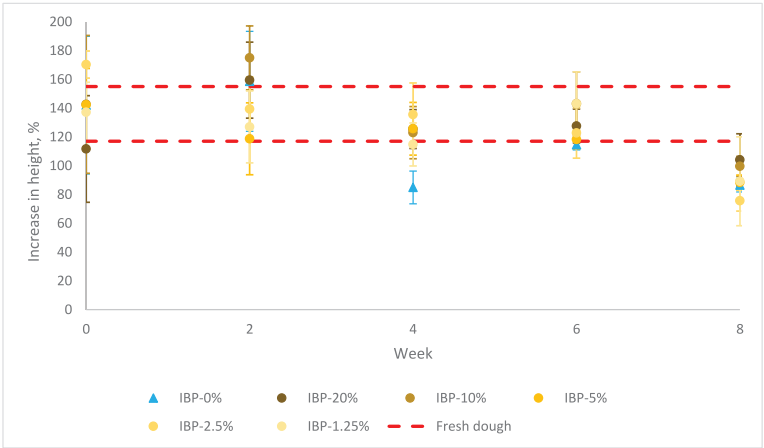

Fig. 4. Rising properties of dough containing 0–20% ice-binding proteins (IBPs) during 8 weeks of frozen storage. Results are expressed as changes in loaf height after rising. The red dotted lines indicate the value range for fresh dough (136.0 ± 19.0%).

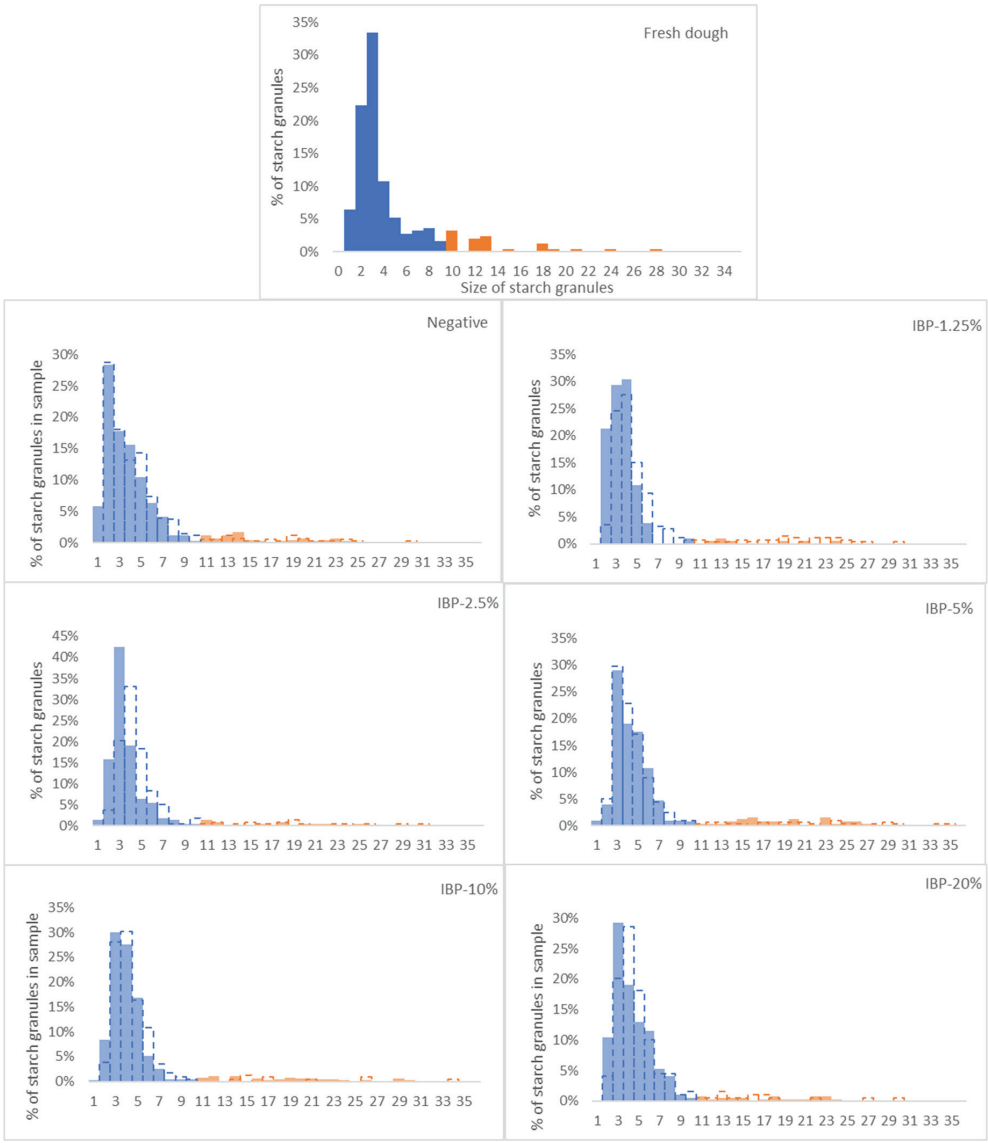

Fig. 5. Size distribution of the starch granules in fresh and frozen dough during 8 weeks of frozen storage. A-type granules are in orange and B-type granules in blue. Dotted bars indicate results at week 0 and colored bars indicate results at week 8.

wheat bread showed a similar tendency as seen in Fig. 3.

The freezing process (time point 0h) decreased the yeast survival rates on average by 9.7 ± 2.7% for the IBP-treated samples and 17.5 ± 4.0% for the negative control compared to the unfrozen dough. The frozen storage also had a negative effect on the survival rates which stayed within a similar range until week 4 for the negative control, and until week 8 for the two lowest IBP concentration samples (IBP-2.5%, and IBP-1.25%) at which point the survival rates started to decrease. The dough samples containing the highest concentrations of ice-binding proteins (IBP-20%, IBP-10%, IBP-5%) showed no significant difference during frozen storage.

These results were not as drastic as previously shown in literature, where the yeast survival rates in frozen dough have been reported to decrease by 53–99% after 45 days of frozen storage (Nguyen et al., 2018; Phimolsiripol, 2009; Tian et al., 2020). The addition of ice-binding collagen peptides had a similar effect of increased yeast viability by 55% reaching maximum yeast survival rates of approximately 70–80% after 4 weeks of frozen storage (Nguyen et al., 2018; Tian et al., 2020).

3.3. Rising properties of the dough

The rising properties of the dough expressed as a change in loaf height, characterize the vitality and CO_2 production of the yeast cells. The changes in rising properties can be seen in Fig. 4.

The dough rising capability of all of the samples decreased during the 8 weeks, most significantly at week 4 correlating to the decreased

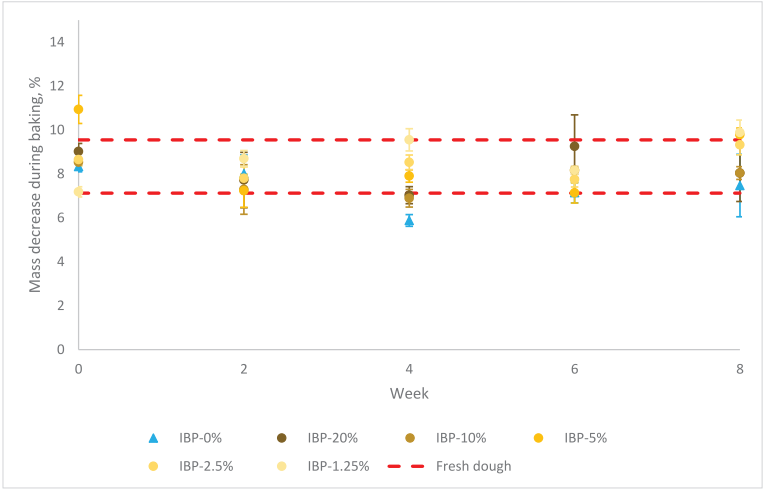

Fig. 6. Mass decrease after baking loaves containing 0–20% ice-binding proteins (IBPs). Results are shown for 8 weeks of frozen storage and expressed as a percentage of initial water. The red lines indicate the value range for fresh dough (8.34 ± 1.71%).

detectable IBP activity and yeast survival rates in the dough. The IBP-20% and IBP-10% samples exhibited the best loaf height retention by the end of the 8 weeks of frozen storage, 88.9% and 85.1% respectively compared to the average result of the freshly prepared, unfrozen dough. The Negative control and samples IBP-5%, IBP-2.5% and IBP-1.25% had a lower loaf height retention capacity ranging from 64.7 to 76.2%.

3.4. Starch microscopy

The retrogradation of starch can cause a variety of undesirable structural transformations in frozen dough. During the freezing process, the pressure of the growing ice crystals causes the starch granules to become rough and incomplete. This process also causes the release of amylose, proteins and lipids (Yang et al., 2019).

Starch granules can be divided into two categories based on size, larger A-type granules with a diameter of 10–35 μm, and smaller B-type granules with a diameter of less than 10 μm. The A-type granules have been shown to have better resistance to freezing (Sandeep, Singh, Isono, & Noda, 2010; Yang et al., 2019). The distribution of these granules in the fresh and frozen doughs can be seen in Fig. 5.

The smaller B-type starch granules were the predominant variety in all of the dough samples, ranging from 87.9 to 97.0% of all starch granules captured in the images.

The larger A-type granules showed no significant changes during freezing, correlating with their reported stability according to the literature (Sandeep et al., 2010). As seen in Fig. 5, the size distribution of the B-type granules shifted towards the smaller sizes during the 8-week storage time for all of the samples.

The mean granule sizes in the unfrozen dough were 12.69 ± 2.69 μm and 3.87 ± 1.76 μm for A- and B-type granules respectively. The decrease in size compared to the fresh dough was most rapid for the negative control sample, which had a mean B-type starch granule size of 3.32 ± 1.12 μm at week 0 and 2.54 ± 1.25 μm at week 8. The IBP-1.25% sample retained a mean starch granule size for the first 6 weeks but had a significant drop at week 8, at which point the mean B-type granule size was 3.04 ± 1.22 μm. This decrease in granule size can be linked to the

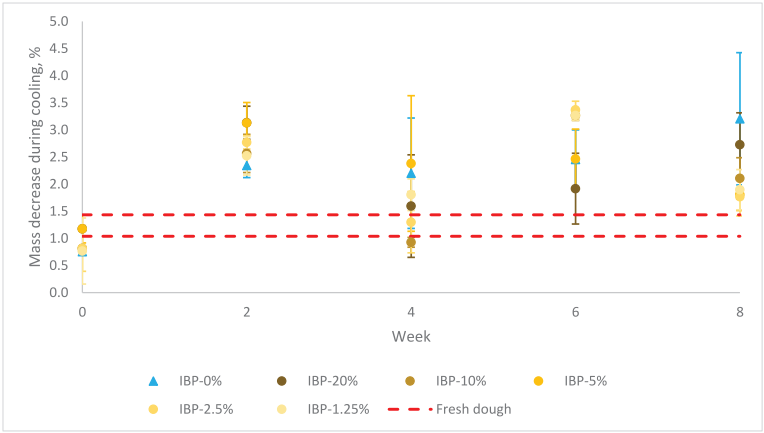

Fig. 7. Mass decrease during cooling loaves containing 0–20% ice-binding proteins (IBPs). Results are shown for 8 weeks of frozen storage and expressed as a percentage of initial water. The red lines indicate the value range for bread prepared from fresh dough (1.24 ± 0.28%).

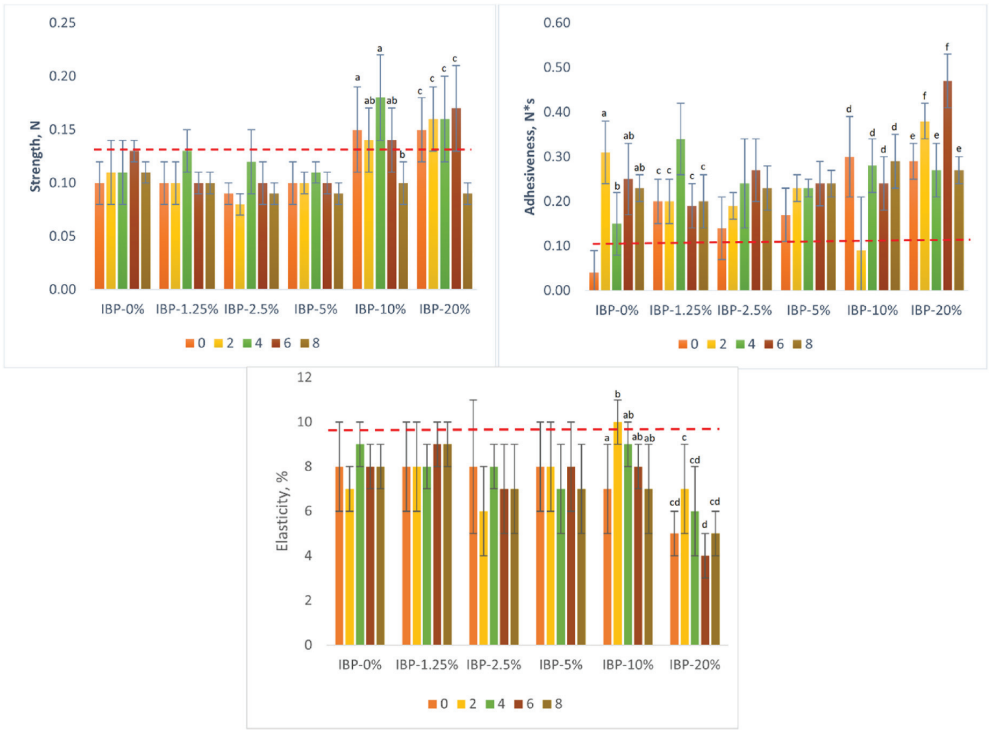

Fig. 8. Dough texture parameters during 8 weeks of frozen storage at two-week intervals. The dotted line indicates the average value for fresh dough. Values with the same lower-case letters within a week do not differ significantly ($\alpha = 0.05$).

growth of ice crystals, which cause the starch granules to become incomplete, leeching amylose, proteins and lipids (Yang et al., 2019). The release of amylose has been linked to the negative effects of baked bread mainly due to the formation of an amylose network which increases the hardness of the bread crumbs (Bárcenas, Haros, Benedito, & Rosell, 2003; Silvas-García et al., 2016). The other IBP-treated samples maintained a mean B-type starch granule size similar to the fresh dough, ranging from 3.42 to 4.12 μm during the 8-week frozen storage period.

3.5. Mass decrease in baking and cooling

The mass change of the bread during baking and cooling characterizes the water-holding capacity of the loaves of bread. The results are expressed as a percentage of initial water mass. The mass decrease during baking is shown in Fig. 6.

The mass decrease during baking varied from 5.88 ± 0.46% to 10.94 ± 0.64% during the 8-week storage period, which was within a similar range of the results for the fresh bread (8.34 ± 1.71%).

The moisture loss for this recipe was lower compared to the estimated 20–25% of initial water during the optimal baking time given in the literature (Nicolas, Vanin, Grenien, & Lucas, 2016). However, the stability of the results and similarity to the unfrozen dough, indicate there is no significant effect of freezing on the water-holding capacity during baking of this wholewheat bread.

Opposing results can be seen during cooling as shown in Fig. 7. The mass decrease during cooling increases in time and is elevated after the initial freezing. The most rapid change can be observed for the negative control, which had a mass decrease almost triple that of the fresh dough by the end of the frozen storage period. However, the differences between the IBP-treated samples and negative control can't be considered significantly different ($p < 0.05$) as there is a large variability between samples of the same recipe which may linked to a decrease in uniformity of the dough balls after freezing and during frozen storage.

3.6. Textural properties of the dough

Dough structure is primarily dependent on the formation of the gluten network during kneading and fermentation (Paraskevopoulou, Provatidou, Tsotsiou, & Kiosseoglou, 2010; Totosaus, López, & Güemes-Vera, 2013). Changes in the gluten network can be caused by the growing ice crystals during freezing and frozen storage (Cao et al., 2020b; Liu, Liang, Wang, et al., 2018; Sharadanant & Khan, 2003b). The addition of non-gluten-forming proteins to the dough can also have a negative effect, as there is a dilution of gluten proteins. This can lead to a weaker dough (Paraskevopoulou et al., 2010; Totosaus et al., 2013).

The texture of the whole wheat dough remained similar to that of fresh dough throughout the frozen storage in terms of cohesiveness and springiness (Full data with statistical analysis in supplementary materials Table S1). As shown in Fig. 8 the two highest IBP concentration doughs showed an improved dough strength during the first 6 weeks of frozen storage, which could be connected to better gluten network preservation. Differences were not significant for lower IBP concentration doughs and the negative control. These results correlate with the gumminess and chewiness of the dough.

The elasticity of the dough decreased after freezing, compared to the freshly prepared dough. The undiluted IBP sample showed a consistently lower elasticity, contrastingly the second-highest IBP concentration appeared to help maintain the elasticity of the dough the longest.

The adhesiveness of the dough had the most deviation over the weeks. In general, the adhesiveness of the dough increased after freezing

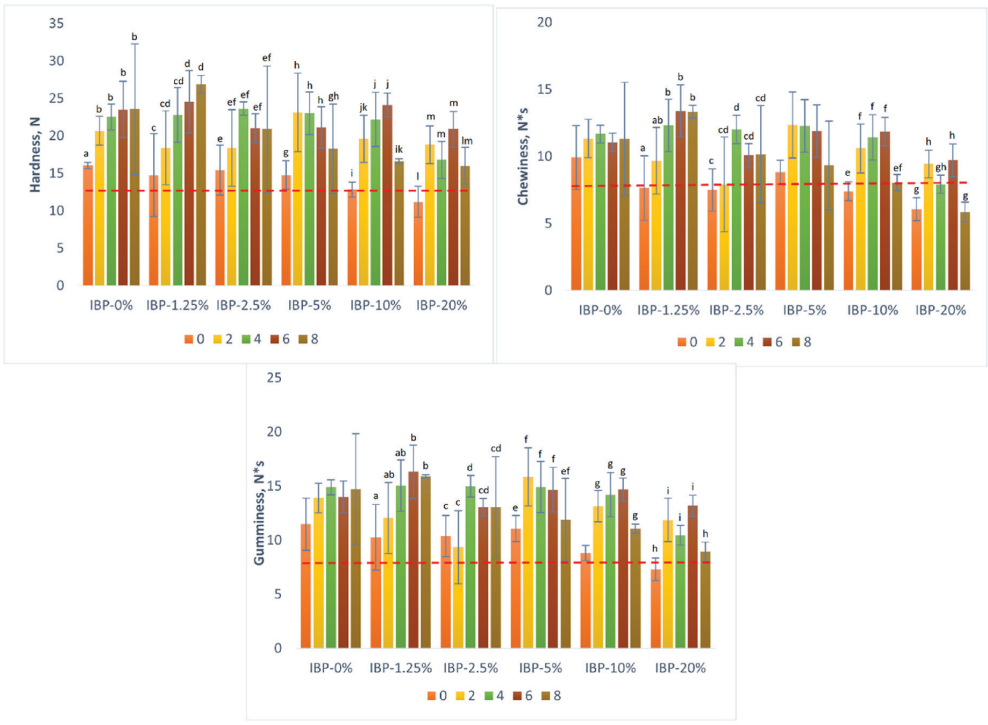

Fig. 9. Bread texture parameters during 8 weeks of frozen storage at two-week intervals. The dotted line indicates the average value for fresh dough. Values with the same lower-case letters within a week do not differ significantly ($\alpha = 0.05$).

when compared to the fresh dough. Both the decrease in elasticity, as well as the increase in adhesiveness, affected the handling of the dough negatively, which additionally affected the accuracy of the measurements as the variance between individual dough sample measurements increased after freezing and during frozen storage.

3.7. Textural properties of the bread

The texture of bread prepared from frozen dough is primarily affected by the quality of the gluten network, the degradation of starch in the dough as well as the survival rates of yeast (Cao et al., 2020a, Cao et al., 2020a; Feng, Ma, & Wang, 2020; Liu, Liang, Wang, et al., 2018;

Fig. 10. Specific volume values during 8 weeks of frozen storage of loaves prepared from dough containing 0–20% ice-binding proteins (IBPs). The dotted lines indicate the values for the fresh dough (1.79 ± 0.15).

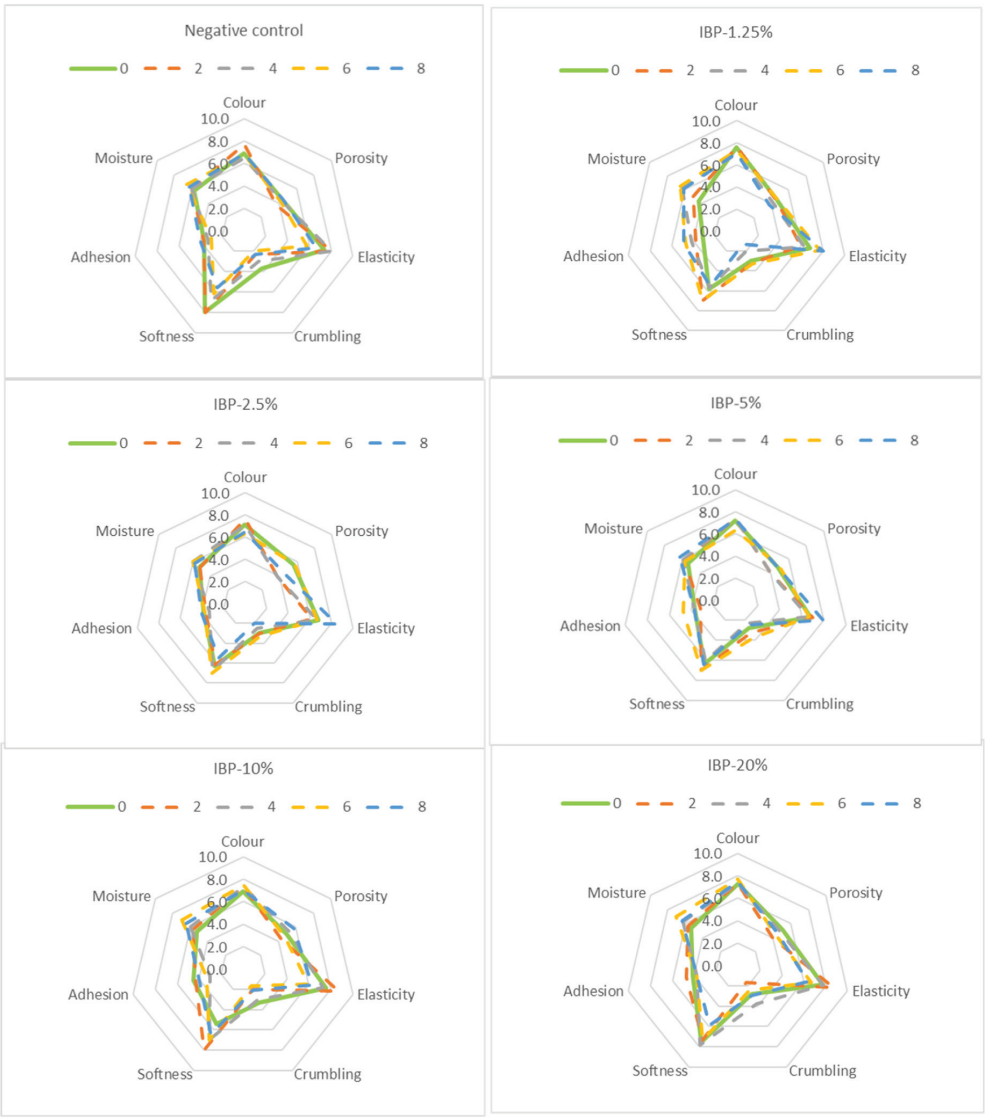

Fig. 11. Appearance and texture of wholewheat breads enhanced with ice-binding proteins compared to the negative control during 8 weeks of frozen storage.

Liu, Liang, Zhang, et al., 2018; Nguyen et al., 2018; Phimolsiripol, 2009). Fig. 9 shows the primary changes in bread texture during 8 weeks.

The hardness, chewiness and gumminess of the bread were negatively affected by the freezing and frozen storage. However, the addition of ice-binding proteins decreased the values of these parameters up to 32.2%, 47.9% and 39.3% compared to the control respectively by the end of the 8-week storage period. The other texture parameters showed little to no difference between samples during the storage period as well as compared to the bread prepared from the unfrozen dough (shown in supplementary materials Table S2).

Similar results have previously been shown with ice-structuring collagen peptides from porcine skin collagen hydrolysates. The hardness and gumminess of steamed bread containing these peptides decreased by approximately 30% compared to the control group after 4 weeks of frozen storage (Nguyen et al., 2018). Additionally, ice-binding proteins from Chinese privet leaves and barley also improved the softness of bread prepared from the frozen dough by approximately 12% and 16% respectively (Ding et al., 2020; Jia et al., 2012).

3.8. Specific volume

The frozen storage of dough can affect both the gluten network as well as the yeast survivability. These parameters have an important role in the specific volume of the loaf (Bae et al., 2014; Chen, Ling, & Shao, 2017; Jia et al., 2012; Liu, Liang, Wang, et al., 2018).

The samples analyzed in this paper showed good resistance to freezing when expressed in specific volumes. The value for freshly prepared wholewheat bread was 1.79 ± 0.15 cm^3/g. The values for the loaves of bread prepared from frozen dough (Fig. 10) stayed within the

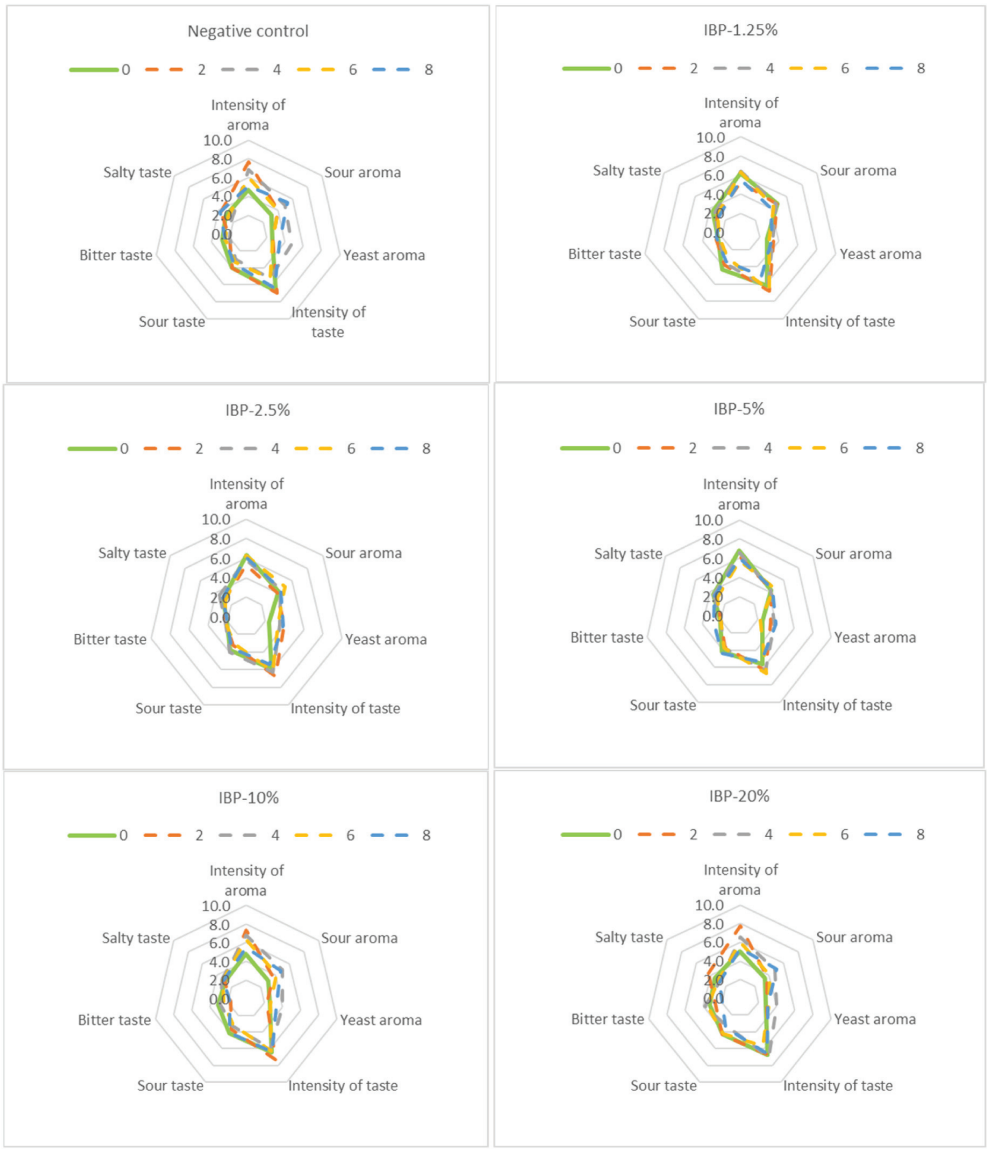

Fig. 12. Sensory evaluation of the taste and aroma of the whole wheat bread enhanced with ice-binding proteins compared to the negative control during 8 weeks of frozen storage.

same range throughout the experiment.

Whole wheat dough has been shown to have better resistance to freezing in terms of loaf volume. The volume of bread prepared with white wheat bread decreased by 17.9% during 4 weeks of frozen storage whereas bread prepared with whole wheat flour decreased by 8.9% during the same period (Bae et al., 2014). Loaf volume has been previously correlated with yeast survival rates. In this study, the correlation between these two parameters is only moderate (with correlation coefficients ranging from 0.3 to 0.7). This suggests that the maintenance of specific loaf volume is more likely influenced by other dough components, such as the gluten network.

However, antifreeze peptides from pig skin collagen increased the specific volume of bread loaves. The decrease in specific volume for the control was 28.06% compared to 10.57% for the enhanced sample (Chen et al., 2017). Similar results were found when ice-structuring proteins from Chinese privet (*Ligustrum vulgare*) leaves were added to the frozen dough. The specific volume of the control bread was significantly lower throughout the 5 weeks of frozen storage (Jia et al., 2012). Recombinant carrot antifreeze protein by *Pichia pastoris* GS115 also improved the specific volume of bread during repeated freeze-thaw cycles (Liu, Liang, Zhang, et al., 2018). Therefore, the addition of ice-binding proteins may have a positive effect on specific volumes subject to the dough recipe.

3.9. Sensory analysis

The sensory evaluation of the six variations of the wholewheat bread is shown in Fig. 11 for appearance and texture and Fig. 12 for taste and aroma.

The appearance and texture were relatively stable in time and across the different samples. The negative control showed a more significant decrease in softness compared to the loaves of bread containing ice-biding proteins. The latter also had a slightly improved retention of porosity and elasticity. The crumbling of the loaves of bread appeared to also increase in time for the negative control and lowest IBP-treated samples. Therefore, the addition of IBPs helps stabilize the appearance and texture of whole wheat bread.

In terms of the taste and aroma parameters, the intensity of taste decreased in the negative control sample, whereas the bread enhanced with ice-binding proteins showed little to no difference. Contrarily, the intensity of the aroma as well as the yeast and sour aroma, appeared to increase during the 8-week experiment, most significantly for the negative control sample.

4. Conclusions

The incorporation of ice-binding proteins into frozen food products stands out as a promising and innovative approach to enhance both the quality and shelf life, addressing the drawbacks associated with conventional freezing methods. This study specifically delved into the cryoprotective impact of ice-binding proteins originating from *Pseudomonas fluorescens* AQP671 on wholegrain wheat dough throughout freezing and an 8-week frozen storage period. The results demonstrated an improvement in yeast survival rates and vitality, improved dough strength and enhanced starch stability. Ultimately, the addition of these proteins led to a bread product with improved textural and sensory attributes. This research highlights the potential of ice-binding proteins as a valuable tool in advancing frozen food technology, however further research into the safety and applicability of these proteins in more complex dough matrices is necessary to fully understand their potential.

CRediT authorship contribution statement

Õnnela Luhila: Writing – original draft, Visualization, Supervision, Project administration, Methodology, Formal analysis, Data curation, Conceptualization. **Karro Kadi:** Writing – review & editing, Investigation, Formal analysis, Data curation. **Zakrevskaja Karina:** Writing – review & editing, Formal analysis, Data curation. **Nisamedtinov Ildar:** Writing – review & editing, Resources, Project administration. **Paalme Toomas:** Writing – review & editing, Supervision, Project administration, Funding acquisition. **Laos Katrin:** Writing – review & editing, Supervision, Project administration, Methodology, Conceptualization.

Compliance with ethics requirements

This article does not contain any studies with human or animal subjects.

Declaration of competing interest

The authors declare that they have no known competing financial interests or personal relationships that could have appeared to influence the work reported in this paper.

Acknowledgments

This work was supported by Eesti Teadusagentuur and the European Regional Development Fund [RESTA12 & RESTA13].

Appendix A. Supplementary data

Supplementary data to this article can be found online at https://doi.org/10.1016/j.lwt.2024.117160.

Data availability

Data will be made available on request.

References

Bae, W., Lee, B., Hou, G. G., & Lee, S. (2014). Physicochemical characterization of whole-grain wheat flour in a frozen dough system for bake off technology. *Journal of Cereal Science, 60*(3), 520–525. https://doi.org/10.1016/j.jcs.2014.08.006

Bárcenas, M. E., Haros, M., Benedito, C., & Rosell, C. M. (2003). Effect of freezing and frozen storage on the staling of part-baked bread. *Food Research International, 36*(8), 863–869. https://doi.org/10.1016/S0963-9969(03)00093-0

Białkowska, A., Majewska, E., Olczak, A., & Twarda-clapa, A. (2020). Ice binding proteins: Diverse biological roles and applications in different types of industry. *Biomolecules, 10*(2). https://doi.org/10.3390/biom10020274

Budke, C., Heggemann, C., Koch, M., Sewald, N., & Koop, T. (2009). Ice recrystallization kinetics in the presence of synthetic antifreeze glycoprotein analogues using the framework of LSW theory. *Journal of Physical Chemistry B, 113*(9), 2865–2873. https://doi.org/10.1021/jp805726e

Cao, H., Zheng, X., Liu, H., Yuan, M., Ye, T., Wu, X., et al. (2020a). Cryo-protective effect of ice-binding peptides derived from collagen hydrolysates on the frozen dough and its ice-binding mechanisms. *LWT (Lebensmittel-Wissenschaft & Technologie), 131* (May), Article 109678. https://doi.org/10.1016/j.lwt.2020.109678

Cao, H., Zheng, X., Liu, H., Yuan, M., Ye, T., Wu, X., et al. (2020b). Cryo-protective effect of ice-binding peptides derived from collagen hydrolysates on the frozen dough and its ice-binding mechanisms. *LWT (Lebensmittel-Wissenschaft & Technologie), 131* (June), Article 109678. https://doi.org/10.1016/j.lwt.2020.109678

Chen, X., Ling, W., & Shao, L. (2017). The cryoprotective effects of antifreeze peptides from pigskin collagen on texture properties and water mobility of frozen dough subjected to freeze – thaw cycles Texture profile analysis. *European Food Research and Technology, 243*(7), 1149–1156. https://doi.org/10.1007/s00217-016-2830-x

Ding, X., Li, T., Zhang, H., Guan, C., Qian, J., & Zhou, X. (2020). Effect of barley antifreeze protein on dough and bread during freezing and freeze-thaw cycles. *Foods, 9*(11), 1–14. https://doi.org/10.3390/foods9111698

Eskandari, A., Leow, T. C., Rahman, M. B. A., & Oslan, S. N. (2020). Antifreeze proteins and their practical utilization in industry, medicine, and agriculture. *Biomolecules, 10* (12), 1–18. https://doi.org/10.3390/biom10121649

Eskandari, A., Leow, T. C., Rahman, M. B. A., & Oslan, S. N. (2024). Advanced freezing point insights into regulatory role of antifreeze proteins, their fundamentals, and obstacles in food preservation. *European Food Research and Technology, 250*(4), 1103–1121. https://doi.org/10.1007/s00217-023-04449-w

Feng, W., Ma, S., & Wang, X. (2020). Quality deterioration and improvement of wheat gluten protein in frozen dough. *Grain & Oil Science and Technology, 3*(1), 29–37. https://doi.org/10.1016/j.gaost.2020.02.001

Jia, C., Huang, W., Wu, C., Zhong, J., Rayas-Duarte, P., & Guo, C. (2012). Frozen bread dough properties modified by thermostable ice structuring proteins extract from Chinese privet (Ligustrum vulgare) leaves. *Cereal Chemistry, 89*(3), 162–167. https://doi.org/10.1094/CCHEM-11-11-0136

Kaleda, A., Tsanev, R., Klesment, T., Vilu, R., & Laos, K. (2018). Ice cream structure modification by ice-binding proteins. *Food Chemistry, 246*(April 2017), 164–171. https://doi.org/10.1016/j.foodchem.2017.10.152

Kawahara, H., Nakano, Y., Omiya, K., Muryoi, N., Nishikawa, J., & Obata, H. (2004). Production of two types of ice crystal-controlling proteins in antarctic bacterium. *Journal of Bioscience and Bioengineering, 98*(3), 220–223. https://doi.org/10.1016/S1389-1723(04)00271-3

Liu, M., Liang, Y., Wang, Y., Zhang, H., Wu, G., Wang, L., et al. (2018). Effects of recombinant carrot antifreeze protein from Pichia pastoris GS115 on the physicochemical properties of hydrated gluten during freeze-thawed cycles. *Journal of Cereal Science, 83*(August), 245–251. https://doi.org/10.1016/j.jcs.2018.08.016

Liu, M., Liang, Y., Zhang, H., Wu, G., Wang, L., Qian, H., et al. (2018). Production of a recombinant carrot antifreeze protein by Pichia pastoris GS115 and its cryoprotective effects on frozen dough properties and bread quality. *LWT (Lebensmittel-Wissenschaft & Technologie), 96*(February), 543–550. https://doi.org/10.1016/j.lwt.2018.05.074

Mangiagalli, M., Brocca, S., Orlando, M., & Lotti, M. (2020). The "cold revolution". Present and future applications of cold-active enzymes and ice-binding proteins. *New Biotech, 55*(September 2019), 5–11. https://doi.org/10.1016/j.nbt.2019.09.003

Nguyen, C. T., Yuan, M., Yu, J. S., Ye, T., Cao, H., & Xu, F. (2018). Isolation of ice structuring collagen peptide by ice affinity adsorption, its ice-binding mechanism and breadmaking performance in frozen dough. *Journal of Food Biochemistry, 42*(3). https://doi.org/10.1111/jfbc.12506

Nicolas, V., Vanin, F., Grenien, D., & Lucas, T. (2016). Modeling bread baking with focus on overall deformationand local porosity evolution. *AIChE Journal, 62*(11), 3825–4172. https://doi.org/10.1002/aic

Paraskevopoulou, A., Provatidou, E., Tsotsiou, D., & Kiosseoglou, V. (2010). Dough rheology and baking performance of wheat flour-lupin protein isolate blends. *Food Research International, 43*(4), 1009–1016. https://doi.org/10.1016/j.foodres.2010.01.010

Phimolsiripol, Y. (2009). Shelf life determination of frozen bread dough stored under fluctuating temperature conditions. *Kasetsart Journal - Natural Science, 43*(1), 187–197.

Rodríguez-Sandoval, E., Fernández-Quintero, A., Sandoval-Aldana, A., & Cuvelier, G. (2008). Effect of processing conditions on the texture of reconstituted cassava dough. *Brazilian Journal of Chemical Engineering, 25*(4), 713–722. https://doi.org/10.1590/S0104-66322008000400008

Saki, N., Ghaffari, M., & Nikoo, M. (2023). Effect of active ice nucleation bacteria on freezing and the properties of surimi during frozen storage. *LWT (Lebensmittel-Wissenschaft & Technologie), 176*(January), Article 114548. https://doi.org/10.1016/j.lwt.2023.114548

Sandeep, S., Singh, N., Isono, N., & Noda, T. (2010). Relationship of granule size distribution and amylopectin structure with pasting, thermal, and retrogradation properties in wheat starch. *Journal of Agricultural and Food Chemistry, 58*(2), 1180–1188. https://doi.org/10.1021/jf902753f

Sharadanant, R., & Khan, K. (2003a). *Effect of Hydrophilic Gums on Frozen Dough . I . Dough Quality, C*, 764–772. https://doi.org/10.1094/CCHEM.2003.80.6.764

Sharadanant, R., & Khan, K. (2003b). Effect of hydrophilic gums on the quality of frozen dough : II . Bread characteristics. C. https://doi.org/10.1094/CCHEM.2003.80.6.773 .

Silvas-García, M. I., Ramírez-Wong, B., Torres-Chávez, P. I., Bello-Pérez, L. A., Carvajal-Millán, E., Barrón-Hoyos, J. M., et al. (2016). Effect of freezing rate and storage on the rheological, thermal and structural properties of frozen wheat dough starch. *Starch/Staerke, 68*(11–12), 1103–1110. https://doi.org/10.1002/star.201500123

Singh, P., Hanada, Y., Singh, S. M., & Tsuda, S. (2014). Antifreeze protein activity in Arctic cryoconite bacteria. *FEMS Microbiology Letters, 351*(1), 14–22. https://doi.org/10.1111/1574-6968.12345

Sun, L., Zhu, Z., & Sun, D. W. (2023). Regulating ice formation for enhancing frozen food quality: Materials, mechanisms and challenges. *Trends in Food Science and Technology, 139*(July), Article 104116. https://doi.org/10.1016/j.tifs.2023.07.013

Tian, Y., Zhu, Z., & Sun, D. W. (2020). Naturally sourced biosubstances for regulating freezing points in food researches: Fundamentals, current applications and future trends. *Trends in Food Science and Technology, 95*(May 2019), 131–140. https://doi.org/10.1016/j.tifs.2019.11.009

Totosaus, A., López, H., & Güemes-Vera, N. (2013). Effect of lupinus (lupinus albus) and jatropha (jatropha curcas) protein concentrates on wheat dough texture and bread quality: Optimization by a D-optimal mixture design. *Journal of Texture Studies, 44*(6), 424–435. https://doi.org/10.1111/jtxs.12031

Yang, Z., Yu, W., Xu, D., Guo, L., Wu, F., & Xu, X. (2019). Impact of frozen storage on whole wheat starch and its A-Type and B-Type granules isolated from frozen dough. *Carbohydrate Polymers, 223*(April), Article 115142. https://doi.org/10.1016/j.carbpol.2019.115142

Yin, L. J., Chen, M. L., Tzeng, S. S., Chiou, T. K., & Jiang, S. T. (2005). Properties of extracellular ice-nucleating substances from Pseudomonas fluorescens MACK-4 and its effect on the freezing of some food materials. *Fisheries Science, 71*(4), 941–947. https://doi.org/10.1111/j.1444-2906.2005.01048.x

Zhao, A., Shi, P., Yang, R., Gu, Z., Jiang, D., & Wang, P. (2022). Isolation of novel wheat bran antifreeze polysaccharides and the cryoprotective effect on frozen dough quality. *Food Hydrocolloids, 125*(August 2021), Article 107446. https://doi.org/10.1016/j.foodhyd.2021.107446

Appendix 3

Publication III

Luhila, Õ**.,** Nisamedtinov, I., Paalme, T., Laos, K., & Olspert, A. (2025). The effect of temperature and nitrogen source modulation on Pseudomonas fluorescens AQP671 ice recrystallization inhibition activity. *Plos*, *20*(9), 1–12.

RESEARCH ARTICLE

The effect of temperature and nitrogen source modulation on *Pseudomonas fluorescens* AQP671 ice recrystallization inhibition activity

Õnnela Luhila[1]*, Ildar Nisamedtinov[1,2,3], Toomas Paalme[1], Katrin Laos[1], Allan Olspert[1]

1 Department of Chemistry and Biotechnology, School of Science, Tallinn University of Technology, Tallinn, Estonia, **2** Competence Center of Food and Fermentation Technologies, Tallinn Estonia, **3** R&D, Lallemand Incorporated, Montreal, Canada

* onnela.luhila@taltech.ee

OPEN ACCESS

Citation: Luhila Õ, Nisamedtinov I, Paalme T, Laos K, Olspert A (2025) The effect of temperature and nitrogen source modulation on *Pseudomonas fluorescens* AQP671 ice recrystallization inhibition activity. PLoS One 20(9): e0333261. https://doi.org/10.1371/journal.pone.0333261

Editor: Zhongzheng Yan, East China Normal University, CHINA

Received: May 6, 2025

Accepted: September 10, 2025

Published: September 25, 2025

Data availability statement: All relevant data are within the manuscript and its Supporting Information files.

Funding: This work was supported the European Regional Development Fund (https://ec.europa.eu/regional_policy/funding/erdf_en)

Abstract

Cold-adapted organisms have developed many different mechanisms to protect themselves from freezing temperatures. One of these mechanisms is ice recrystallization inhibition (IRI) activity. IRI refers to the ability of certain proteins and compounds to prevent the growth of ice crystals during freeze–thaw processes. The IRI activity of *Pseudomonas fluorescens* AQP 671 culture media was evaluated in relation to various nitrogen sources, incubation temperatures and pH conditions. The highest IRI activities were achieved with amino acids L-asparagine, L-proline, or L-valine, particularly under prolonged low-temperature cultivation. A rapid increase in IRI activity was observed during the first 24 hours, in response to cold shock, correlating with cell density. The activity was detected at temperatures below 15 °C, with the highest IRI activities achieved at 5–10 °C. The optimal pH range for high IRI activity was pH 6–8, and it was negatively affected by low (2–4) and high (10–12) pH values. These findings highlight the importance of both environmental conditions and nutrient composition in the expression of IRI activity in *Pseudomonas fluorescens* AQP671 culture media.

1. Introduction

In cold-adapted organisms, ice-binding proteins (IBPs) have emerged as pivotal biomolecules safeguarding cellular structural integrity and viability [1]. These proteins exhibit unique interactions with ice surfaces, manifesting in two distinct properties: thermal hysteresis (TH) signifying the variance between melting and freezing points, and ice-recrystallization inhibition (IRI), i.e., the inhibition of growth of larger ice crystals at the expense of smaller ones [2]. Despite their shared role in enhancing freeze-thaw tolerance of cellular membranes and structures, TH and IRI are non-correlated phenomena [2,3].

via projects RESTA12 (TP) and RESTA 13 (TP). The funders did not play any role in the study design, data collection and analysis, decision to publish, or preparation of the manuscript.

Competing interests: The authors have declared that no competing interests exist.

IBPs, which vary in terms of size, structure, and activity levels, have been identified across various organisms, including fish, insects, plants, algae, fungi, and microorganisms [1,4,5]. Despite these variations, all these proteins share a common trait of exhibiting cryoprotective properties [1,2,6–9].

Microbial IBPs show a particular potential for biotechnological applications due to their relatively low cost and ease of production compared to plant or animal IBPs [10]. Most research on the practical applications of bacterial IBPs focuses on ice nucleating proteins (INPs), which have been used to enhance frozen food quality (e.g., surimi, milk, and starch solutions) and for artificial snow production [11–14]. Antifreeze-active IBPs have shown promise in crop preservation via biofertilizer enrichment and in preserving frozen foods [15,16]. For example, psychrophilic yeast, *Glaciozyma martini*, was recently found to produce an extracellular, glycosylated 27 kDa ice-binding protein with IRI activity that showed cryoprotective effects in frozen fruit and vegetable preservation as well as in the cell survival of *Saccharomyces cerevisiae* after freezing [10].

Studies suggest that nutrient composition can significantly modulate ice nucleation and thermal hysteresis activities of bacterial IBPs [17–19]. Previously isolated at the coast of Ross Island, Antarctica, a strain of *Pseudomonas fluorescens* (KUAF-68) has been noted for producing two distinct IBPs, one of them (MW 80kDa) displaying low thermal hysteresis values that could be increased in the media by the addition of L-asparagine and the other one (MW 600kDa) exhibiting ice nucleation activity that could be increased in the media by the addition of glycine [17]. In *Pseudomonas fluorescens* strain MACK-4, INP activity was reduced in the presence of inorganic nitrogen sources, suggesting that these compounds suppress IBP production. Independent experiments further indicate that the source of nitrogen exerts a stronger influence than the source of carbon on both cellular growth and IBP synthesis. Among organic nitrogen sources such as yeast extract, peptone, and tryptone, no significant differences were observed in their ability to promote IBP production [19]. In addition, supplementation of the growth medium with L-serine and L-alanine has been reported to enhance INP activity in *Pantoea ananatis* [17,18]. Despite these studies, comprehensive research on the ice recrystallization inhibition (IRI) activity of bacterial IBPs and the impact of environmental parameters on the functionality and expression of these proteins is still rather limited to date.

This study focuses on another strain of *Pseudomonas fluorescens* (AQP671) sourced from Ganavan Bay, North Scotland, which appears to produce at least two distinct IBPs based on experimental observations. The IBPs are characterized by ice recrystallization inhibition activity. Our study aims to describe the interplay of temperature, pH, and nitrogen source composition in the growth medium on the expression of IRI activity, with potential biotechnological significance.

2. Materials and methods

Preparation and cultivation of *P. fluorescens* under variable environmental conditions

Pseudomonas fluorescens strain AQP671, isolated from Ganavan Bay, Scotland (UK), was provided by Lallemand Inc. The bacteria were maintained at 30 °C on

Lysogeny Broth Agar (LB, Lab M) for 24 h and cultivated at 30 °C in mineral medium (pH 7) containing $MgSO_4$ (1.5 g/L) and KH_2PO_4 (1.5 g/L), adding glycerol (20 g/L) as the carbon source, and NH_4Cl (3 g/L) as the nitrogen source. Cultivation was carried out on a shaker (Innova 43 Incubator Shaker Series) at 180 rpm, followed by growth in a 7 L bioreactor (Biobench, Applikon, The Netherlands). In the bioreactor, the pH was controlled at 7.0 using titration with 5M NaOH and dissolved oxygen concentration pO2 > 10% of air saturation by adjusting the aeration rate and stirrer speed. The bioreactor was inoculated (1:9, v/v) with the 48-h shake flask-grown pre-culture and grown until glycerol was almost depleted (~40 h). Then, for initiation of IBP production, the temperature was decreased to 5 °C, and glycerol (20 g/L) and NH4Cl (3 g/L) or yeast extract (Lab M, 10 g/L) were added. The incubation length at 5 °C was 32 h for the NH_4Cl experiment and 100 h for the experiment using yeast extract as a nitrogen source.

To study the impact of individual amino acids, a portion of the culture was also withdrawn prior to the temperature shift-down and used to inoculate shake flasks (1:9, v/v) containing 20 mL of mineral medium with glycerol (20 g/L) and a single amino acid added as the sole nitrogen source. Each flask contained only one of the following amino acids: L-alanine, L-arginine, L-asparagine, L-glutamine, L-isoleucine, L-methionine, L-proline, L-serine, L-threonine, or L-valine, added in a concentration that corresponded to 1 g N/L. These results were compared to those obtained using mineral medium supplemented with either yeast extract or ammonium chloride as the nitrogen source. The nitrogen content of the yeast extract was estimated based on the total amino acid content provided by the manufacturer. The total incubation time at 5 °C was 168 h.

Similar experiments were carried out to study the effect of temperature in the presence of L-asparagine as the nitrogen source. The temperature values of 5, 10, 15, and 20 °C were selected to represent a biologically relevant range spanning from cold stress conditions, which are known to induce ice-binding protein production, up to moderate temperatures favorable for bacterial growth. Samples were collected at 24-hour intervals for a total of 96 h.

To evaluate the effect of pH on ice recrystallization inhibition activity, the pH of the culture supernatant obtained after 24 h of incubation at 5 °C was adjusted to 2, 4, 6, 8, 10, and 12 covering the physiological pH range relevant to *Pseudomonas fluorescens'* natural environment, as well as extreme pH values to assess protein stability and activity under stress conditions.

Analytical methods

Optical density (OD) was used to estimate the biomass concentration, expressed as grams of dry weight per liter *(X = 0.375 gDw/L * OD)*. The concentration of glycerol (using a SunChrom HPLC system equipped with a Rezex™ ROA-Organic Acid H^+ (8%) column (Phenomenex) and both UV-Vis and refractive index (RI) detectors), extracellular protein (using Pierce™ modified Lowry assay kit, Thermo Fischer Scientific) and ice recrystallization inhibition (IRI) activity were measured in the culture supernatant after removing the biomass by centrifugation at 13 000 rpm for 1 min (Biofuge Pico, Heraeus, Hanau, Germany).

IRI activity was measured using the modified "sucrose sandwich" assay with some modifications, as previously described [20]. 25 µl of supernatant of *P. fluorescens* AQP671 culture media was mixed with a 70% sucrose solution (1:1, v/v ratio), and 3 µl of the solution was placed on a glass microscope slide, covered with a cover slip, and the edges were sealed with silicone oil. The microscope slide was then flash-frozen in liquid nitrogen and placed on a cooling stage (Linkam PE 120, UK) of a microscope (Nikon Eclipse E 200, Japan). The temperature for the cooling stage was set to be close to the ice crystal melting point of 35% sucrose solution (T = −6.8 °C) and set to change according to the preset profile (Fig 1). The images of ice crystals were obtained using the Motic Images 3.0 program at the end of temperature ramps 4 and 6 (highlighted in green and red, respectively). Images were analyzed using the Image J image analysis tool, and the ice crystal growth rates were calculated using the Ostwald law equation [21] (Eq. 1).

$$k = \left(r^3 - r_0^3\right)/t \tag{1}$$

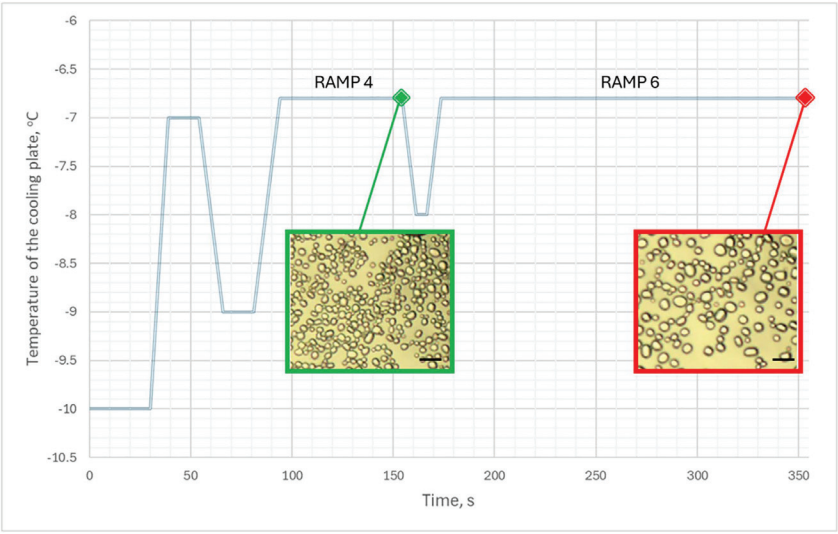

Fig 1. Temperature profile set points of the cooling plate for ice recrystallization inhibition (IRI) activity assessment. Images are taken at time points 154 and 354 s, highlighted in green and red accordingly. The microscope images shown are for the 35% sucrose solution at −6.8 °C.

https://doi.org/10.1371/journal.pone.0333261.g001

where,

k – ice crystal growth rate, μm³/min

r – average ice crystal radius at the end of temperature ramp 6, μm

r_0 – average ice crystal radius at the end of temperature ramp 4, μm

t – time, min.

The dilution $D_{k50\%}$ of the sample, resulting in a 2-fold decrease of the maximum crystal growth speed k, was utilized to express the ice recrystallization inhibition activity (IRI). The dilution $D_{k50\%}$ was determined by preparing a series of 2-fold dilutions of the sample. The first dilution, 1:1 (v/v) of the sample, was made with a 70% sucrose solution, and the following 1:1 (v/v) with a 35% sucrose solution to maintain the 35% (m/v) sucrose concentration. Dilutions were made until the original sample was diluted up to 128 times (Fig 2).

The dilution D at which the ice crystal growth rate k reached half of the maximum speed ($D_{k50\%}$) was calculated by solving the quadratic equation (Eq. 2) corresponding to the second-order polynomial trendline of the dilution graph as follows:

$$y = aD_{k50\%}^2 + bD_{k50\%} + c$$

$$y = 50$$

$$D_{k50\%} = \frac{-b \pm \sqrt{b^2 - 4a(c-50)}}{2a} \quad (2)$$

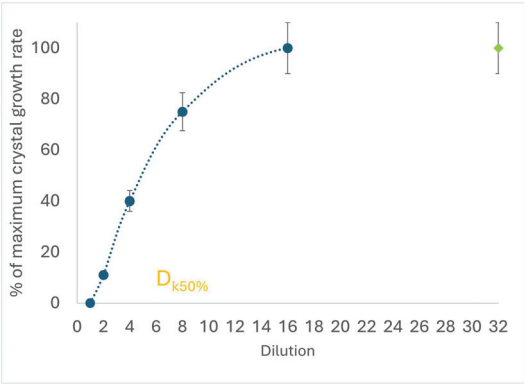

Fig 2. Graphical assessment of ice recrystallization inhibition (IRI) activity. Data represents mean values with standard deviation error bars (n = 3). The IRI activity is expressed as $D_{k50\%}$, calculated from the quadratic polynomial trend line (blue dotted line). The green marker at 32 × dilution indicates a plateau in ice crystal growth rates across the dilution series.

https://doi.org/10.1371/journal.pone.0333261.g002

where,

a, b, c – quadric, linear and constant term

y – ice crystal growth rate relative to the maximum growth rate, %

$Dk_{50\%}$ - dilution at the growth rate corresponding to 50% of the maximum growth rate

This point was defined as the $D_{k50\%}$ inhibition point, corresponding to IRI activity. All samples were measured in triplicate.

Statistical analysis

Statistical analysis (ANOVA, two-tailed paired t-test and Pearson's Correlation Coefficient) for the results was done with Excel Data Analysis tools. Results are presented with 95% confidence intervals. A p-value < 0.05 was considered statistically significant.

Compliance with ethics requirements

This article does not contain any studies with human or animal subjects.

3. Results and discussion

Expression of IRI activity in *Pseudomonas fluorescens* AQP671 culture

IRI activity during cultivation of *P. fluorescens* AQP671 on mineral media at 25 °C and after switching to 5 °C using yeast extract or NH_4Cl as the nitrogen sources is shown in Fig 3. IRI activity of the culture media could not be detected during growth at 25 °C and after cultivation at the shift-down temperature (5 °C) when glycerol and NH_4Cl were added. However, a rapid increase in IRI activity was observed if yeast extract was added to culture media instead of NH_4Cl. Notably, IRI activity continued to rise throughout the 140 h incubation phase, reaching a dilution ($D_{Kd50\%}$) of 40, even after the culture had reached the stationary phase. Although this phenomenon has not previously been described for IBPs, other cold-inducible proteins, such as cold-shock proteins in *Bacillus subtilis* and *Caulobacter crescentus*, are known to be upregulated during the stationary phase [22,23].

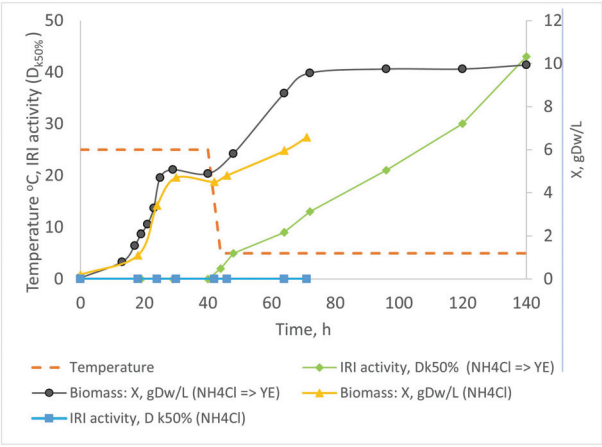

Fig 3. Comparison of two experiments assessing the growth and ice recrystallization inhibition (IRI) activity of Pseudomonas fluorescens AQP671 cultivated with different nitrogen sources following a temperature shift-down to 5 °C. In Experiment 1, ammonium chloride (NH_4Cl) was used as the nitrogen source throughout cultivation (biomass (X): yellow line; IRI activity: blue line). In Experiment 2, yeast extract was added as the nitrogen source after the temperature shift-down (biomass (X): black line; IRI activity: green line). The bioreactor temperature set point is shown by the orange line.

https://doi.org/10.1371/journal.pone.0333261.g003

The effect of individual amino acids on ice recrystallization inhibition activity

After reaching a biomass concentration of 10 gDw/L in the bioreactor, part of the culture was transferred into the flasks containing pre-cooled (5 °C) base media supplemented with individual organic nitrogen sources: L-alanine (A), L-arginine (R), L-asparagine (N), L-glutamine (Q), L-isoleucine (I), L-methionine (M), L-proline (P), L-serine (S), L-threonine (T), and L-valine (V), or yeast extract (YE) as a control, and incubated on shaker at 5 °C for 168 h. The biomass growth of individual nitrogen sources during the induction of IBP production by temperature shift-down is shown in Fig 4.

Despite the equal nitrogen concentration (1 g N/L) supplied with different amino acids, the growth of *P. fluorescens* AQP671 (5 gDW/L) was most pronounced in the media containing yeast extract. This can be explained by a good balance of nutrients in yeast extract [24]. In addition to various nitrogen sources, yeast extract provides sugars, vitamins, and trace elements, which can support cellular metabolism and may contribute to the increased biomass yield. Thus, the growth-promoting effect of yeast extract cannot be attributed solely to its nitrogen content [24,25]. The culture media containing a single amino acid reached much lower biomass concentrations, ranging from 0.7 gDW/L (L-threonine) to 1.5 gDW/L (L-alanine).

The impact of different nitrogen sources on the expression of IRI activity and total extracellular protein synthesis at 5 °C after 168 h of incubation is shown in Fig 5.

The highest IRI activity, $D_{k50\%,}$ of the culture media was achieved with L-asparagine, followed by yeast extract, L-proline, and L-valine. The other amino acids resulted in lower IRI activity. When comparing IRI activity relative to total protein content in the cultivation media, L-asparagine resulted in significantly higher specific activity than the other nitrogen sources tested.

The change in IRI activity over time can be seen in Fig 6. All the nitrogen sources showed a rapid increase in IRI activity for the first 24 h in response to the decrease in temperature.

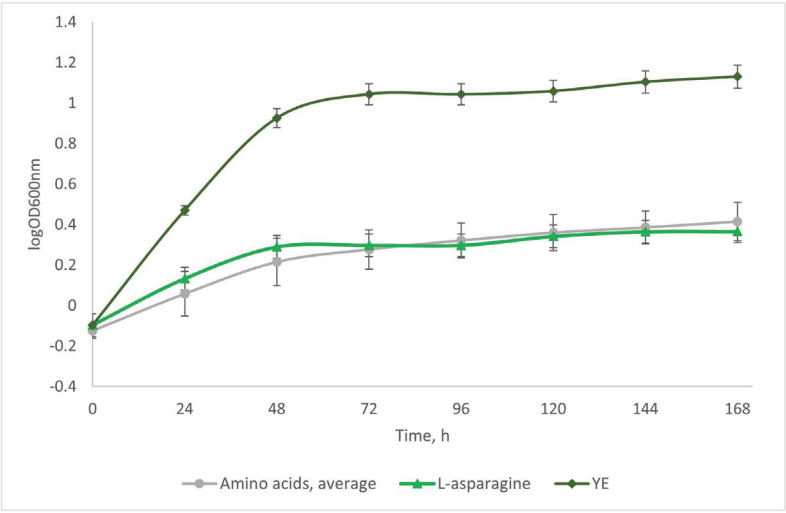

Fig 4. Change in the optical density during the growth of P. fluorescens AQP671 in the base medium containing a variety of amino acids or yeast extract as a nitrogen source. L-asparagine (green) is highlighted as the nitrogen source giving the highest IRI activity by the end of the experiment. Data represent mean values with standard deviation error bars (n = 3).

https://doi.org/10.1371/journal.pone.0333261.g004

According to the observed changes in IRI activity, the nitrogen sources were grouped into two categories. The first was the high-activity group, comprising L-asparagine, yeast extract, L-proline, and L-valine (Fig 6a), where IRI activity increased linearly ($R^2 > 0.9$) throughout the entire experiment. An increase in ice recrystallization inhibition could be observed in this group during prolonged incubation at 5 °C, despite the cessation of biomass production (Fig 4).

The second group was the moderate to low-activity group, which included L-isoleucine, L-alanine, L-arginine, L-methionine, L-threonine, L-glutamine, and L-serine, with activity increasing at a much slower rate and reaching a plateau with the stop of growth (Fig 4) around $D_{k50\%}$ values of 2–3 (Fig 6b).

The measured IRI activities were very strongly in positive correlation with the cell densities measured in the culture media at different sampling points for most nitrogen sources (Pearson correlation coefficient (PCC) > 0.9), excluding L-asparagine (PCC = 0.87), L-glutamine (PCC = 0.83), and L-threonine (PCC = 0.64) which showed weaker association between cell density and IRI activity.

It can be assumed that organic nitrogen sources are required for IRI activity, as IRI activity could not be seen in the cold-induced culture when NH_4Cl was used as the sole nitrogen source. This correlates with previous literature, where it was shown that the INP activity of *Pseudomonas fluorescens* MACK-4 IBPs was lowered in the presence of inorganic nitrogen [19]. Unfortunately, the IRI activities could not be directly related to IBP concentrations on a protein basis, as specific activity is unknown. It is worthwhile to note that similar results have been found when assessing the thermal hysteresis activity of *P. fluorescens* strain KUAF-68, which showed an almost two-fold increase in activity when L-asparagine was supplemented into the growth media at a concentration of 0.025% (w/v N) [17].

The mechanisms behind the increased IRI activity observed in the presence of particular amino acids have not been researched. However, it has been shown that asparagine/aspartate, glutamine/glutamate, arginine and serine were the amino acids most abundantly consumed throughout the growth phases for *Pseudomonas putida* [26]. Additionally, *Pseudomonas* species are known to produce enzymes facilitating the nitrogen assimilation from L-asparagine, making it

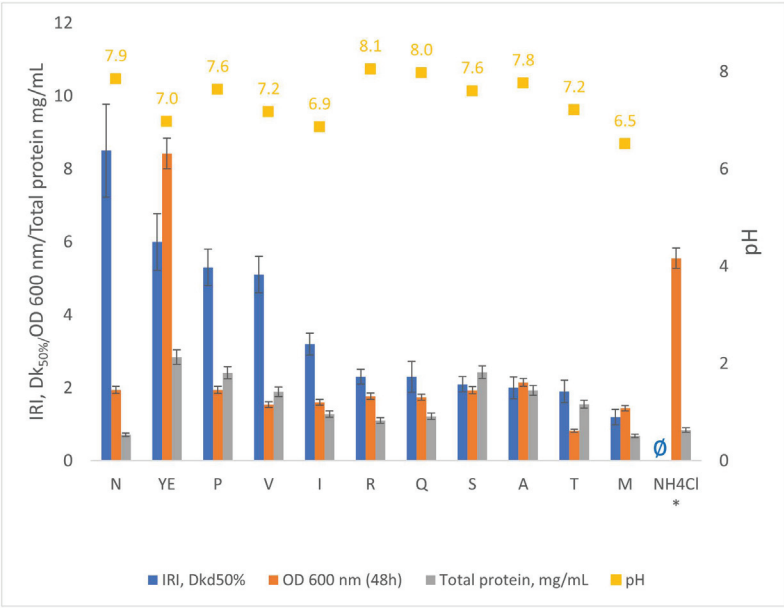

Fig 5. The effect of nitrogen source (L-asparagine (N), yeast extract (YE), L-proline (P), L-valine (V), L-isoleucine (I), L-arginine (R), L-glutamine (Q), L-serine (S), L-alanine (A), L-threonine (T), L-methionine (M) on P. fluorescens AQP671 IRI activity (blue bars) after 48 h incubation at 5 °C. Orange bars – the biomass concentration (OD 600 nm) at 48 h, grey bars – total protein concentration in the culture media at 168 h of incubation, yellow boxes - pH of the culture media after 168 h of incubation. Data represent mean values with standard deviation error bars (n = 3). The full data for each time point can be found in the supporting materials, S1 Table. * As a comparison, NH4Cl results correspond to the results from the experiment in the bioreactor at 71 h, shown in Fig 3, ∅ – no activity detected.

https://doi.org/10.1371/journal.pone.0333261.g005

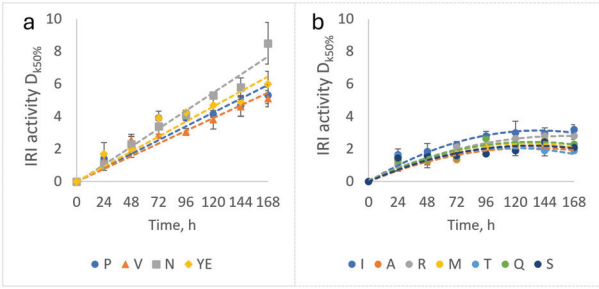

Fig 6. The change in ice recrystallization inhibition activity in Pseudomonas fluorescens AQP671 culture supplemented with different nitrogen sources during incubation at 5 °C on shaker, 180 rpm. a – high activity group: L-proline (P), L-valine (V), L-asparagine (N) and yeast extract (YE), b – low activity group: L-isoleucine (I), L-alanine (A), L-arginine (R) and L-methionine (M), L-threonine (T), L-glutamine (Q), L-serine (S). Data represent mean values with standard deviation error bars (n = 3).

https://doi.org/10.1371/journal.pone.0333261.g006

an easily available nitrogen source [27]. In particular, L-asparaginase from *Pseudomonas fluorescens* has been shown to have high affinity to L-asparagine while having low affinity to glutamine [28]. Additionally, amino acids, compared to inorganic nitrogen sources, use different metabolic pathways for their assimilation, which may lead to amino-acid-specific gene regulation needed for IBP production [29,30].

The effect of pH on ice recrystallization inhibition activity of supernatant

The effect of pH on IRI activity was assessed by growing bioreactor-derived precultures in 5 °C flasks containing 1 g N/L L-asparagine as nitrogen source until biomass concentration reached 1 g DW/L. The pH of the culture supernatant was then adjusted to 2, 4, 6, 8, 10, and 12 and analyzed almost immediately for ice-binding protein activity. The IRI activity of the cold-induced *P. fluorescens* AQP671 culture supernatant at different pH values is shown in Fig 7. The activity was most prominent at pH values 6 and 8 and decreased rapidly at acidic (pH 2 and pH 4) and moderately at alkaline (pH 10 and pH 12) conditions.

These results differ to some extent from previous literature data, which reported that fish and insect antifreeze proteins with both thermal hysteresis and ice recrystallization inhibition activities exhibit little to no pH dependence [31–34]. By contrast, type III antifreeze proteins and spruce budworm ice-binding proteins showed a slight decrease in absolute activity under low pH conditions, similarly to the IBPs investigated in this study [35]. This decrease was attributed to alterations in the secondary structure propensities of some protonated residues of IBPs, leading to a reduction in the total number of proximal water molecules and disrupting the water solvation structure at the basal and ice-binding interfaces of IBPs [35,36].

Marinomonas primoryensis IBPs (MpIBPs) exhibited the highest similarity in pH stability to *P. fluorescens* AQP671 IBPs. Thus, MpIBPs did not interact with ice at pH ≤ 4 or pH ≥ 13, at 6 ≤ pH ≤ 12 demonstrated a reduction in ice crystal grain size and at 6 ≤ pH ≤ 10 exhibited dynamic ice shaping [37]. These results indicate that the impact of pH on IBP stability is not universal but may be dependent on the species producing these IBPs and their molecular structures.

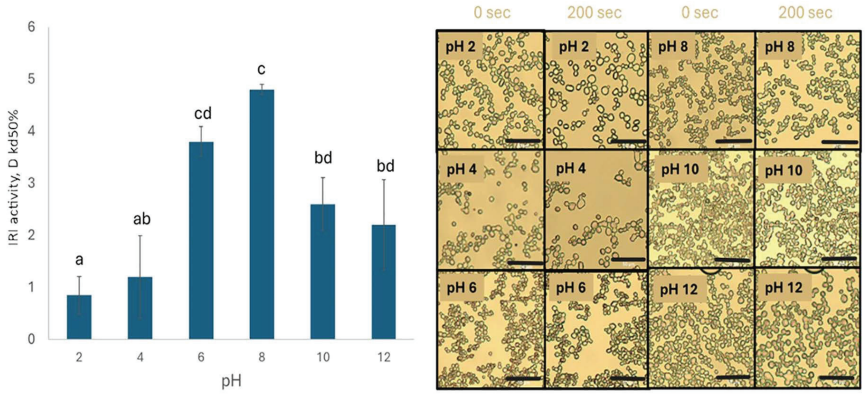

Fig 7. Ice recrystallization inhibition activity in P. fluorescens AQP671 culture supernatant. Data represents mean values with standard deviation error bars (n = 3). Lowercase letters indicate significant differences between samples according to the t-test values ($p < 0.05$) (left). Microscopic images of the ice crystals in the culture supernatant (2x diluted) at different pH values. The scale vars are 50 μm (right).

https://doi.org/10.1371/journal.pone.0333261.g007

The effect of temperature on expression of ice recrystallization inhibition activity

To assess temperature effects on IRI activity, the bioreactor-grown preculture was incubated for 96 h at 5, 10, 15, or 20 °C in the medium containing L-asparagine as a nitrogen source. IRI activity in the culture supernatant was observed at temperatures of 15 °C and lower (Fig 8).

The results also show that the total protein content and IRI activity, when normalized to cell density, increased with lowering cultivation temperatures. However, similarly to the previous experiment with different amino acids, the total protein concentration in the culture media did not correlate with IRI activity, suggesting that the proteins responsible for IRI activity may constitute only a small fraction of the total proteins present. This corroborates previous findings that IRI activity can occur at as low as nano- to micromolar concentrations of IBPs [2,38].

The total protein as well as IRI activity per unit of biomass increased with the decrease of expression temperature, while the concentration of biomass decreased. IRI activity per protein content changed little, if at all (Fig 8).

The increase in IRI activity remained linear throughout the experiment at 5–10 °C. The IRI activities at 5, 10 and 15 °C were the same during the 72 h incubation ($p < 0.05$) and statistical differences could be seen only at the 96-hour sampling point, with the highest activity measured at 10 °C and the lowest at 15 °C (data shown in Supporting materials S2 Table).

Overall, the IBP induction temperatures determined in this work were similar to those determined for other bacterial IBPs, including *P. fluorescens* strain KUAF-68 (5 °C), *Pseudomonas putida* GR12−2 (10 °C) and *Moraxella sp* (10 °C) [17].

4. Conclusions

Our study demonstrates that the ice recrystallization inhibition (IRI) activity expressed by *P. fluorescens* AQP671 is significantly influenced by the nitrogen source, pH and incubation temperature. The highest IRI activity was observed with L-asparagine, L-proline, and L-valine, particularly under conditions of prolonged cold stress. The IRI activity was equally expressed at temperatures of 15 °C and below, while no activity was detected at temperatures above 20 °C. The activity per unit was most prominent at neutral pH values and decreased rapidly at acidic and moderately at alkaline pH values. These findings suggest that both environmental factors and nutrient composition play crucial roles in the expression of

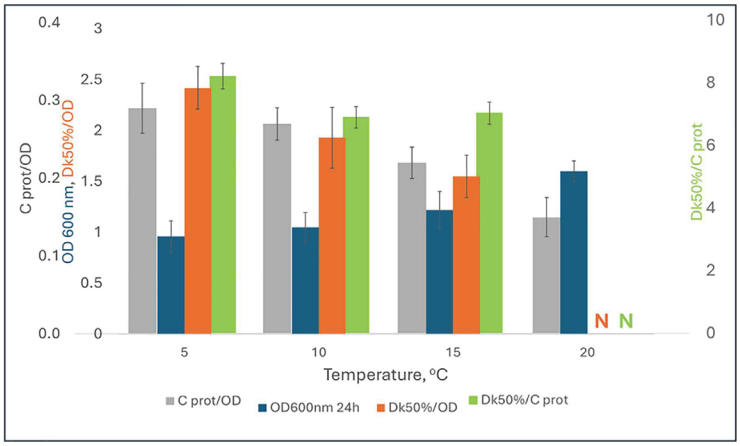

Fig 8. Total protein concentration normalized to cell density (gray), biomass concentration at 24 h (blue), IRI activity normalized to biomass concentration (orange) and IRI activity normalized to total protein concentration in the culture media of P. fluorescens AQP671 after incubation for 24 h at 5, 10, 15 and 20 °C. Data represent mean values with standard deviation error bars (n = 3). N – not detected.

https://doi.org/10.1371/journal.pone.0333261.g008

IRI activity in *Pseudomonas fluorescens* AQP671. A limitation of this study was that the IRI protein was not isolated nor sequenced, and could not be quantified in terms of mass per volume.

Supporting information

S1 Table. Ice recrystallization inhibition activity expressed as 50% dilution point, normalized to cell density and total protein content.
(DOCX)

S2 Table. Ice recrystallization inhibition activity (Dkd50%) in the culture medium of *P. fluorescens* AQP671 at 5, 10 and 15 °C.
(DOCX)

Author contributions

Conceptualization: Õnnela Luhila, Ildar Nisamedtinov, Toomas Paalme.

Data curation: Õnnela Luhila.

Formal analysis: Õnnela Luhila.

Investigation: Õnnela Luhila.

Methodology: Õnnela Luhila, Ildar Nisamedtinov.

Supervision: Ildar Nisamedtinov, Toomas Paalme, Katrin Laos, Allan Olspert.

Visualization: Õnnela Luhila.

Writing – original draft: Õnnela Luhila.

Writing – review & editing: Ildar Nisamedtinov, Toomas Paalme, Katrin Laos, Allan Olspert.

References

1. Bar Dolev M, Braslavsky I, Davies PL. Ice-binding proteins and their function. Annu Rev Biochem. 2016;85:515–42. https://doi.org/10.1146/annurev-biochem-060815-014546 PMID: 27145844
2. Ramløv H, Friis DS. Contents of volume 2-antifreeze proteins: Biochemistry, molecular biology, and application. Vol. 2. 2020.
3. Lee JH, Lee SG, Do H, Park JC, Kim E, Choe Y-H, et al. Optimization of the pilot-scale production of an ice-binding protein by fed-batch culture of Pichia pastoris. Appl Microbiol Biotechnol. 2013;97(8):3383–93. https://doi.org/10.1007/s00253-012-4594-y PMID: 23203635
4. Białkowska A, Majewska E, Olczak A, Twarda-Clapa A. Ice binding proteins: diverse biological roles and applications in different types of industry. Biomolecules. 2020;10(2):274. https://doi.org/10.3390/biom10020274 PMID: 32053888
5. Mangiagalli M, Brocca S, Orlando M, Lotti M. The "cold revolution". Present and future applications of cold-active enzymes and ice-binding proteins. N Biotechnol. 2020;55:5–11. https://doi.org/10.1016/j.nbt.2019.09.003 PMID: 31546027
6. Singh P, Hanada Y, Singh SM, Tsuda S. Antifreeze protein activity in Arctic cryoconite bacteria. FEMS Microbiol Lett. 2014;351(1):14–22. https://doi.org/10.1111/1574-6968.12345 PMID: 24283367
7. Tomalty HE, Graham LA, Eves R, Gruneberg AK, Davies PL. Laboratory-scale isolation of insect antifreeze protein for cryobiology. Biomolecules. 2019;9(5):180. https://doi.org/10.3390/biom9050180 PMID: 31075842
8. Venketesh S, Dayananda C. Properties, potentials, and prospects of antifreeze proteins. Crit Rev Biotechnol. 2008;28(1):57–82. https://doi.org/10.1080/07388550801891152 PMID: 18322856
9. Zhao A, Shi P, Yang R, Gu Z, Jiang D, Wang P. Isolation of novel wheat bran antifreeze polysaccharides and the cryoprotective effect on frozen dough quality. Food Hydrocolloids. 2022;125:107446. https://doi.org/10.1016/j.foodhyd.2021.107446
10. Majewska E, Twarda-Clapa A, Jędrzejczak-Krzepkowska M, Kamińska-Dwórznicka A, Zakłos-Szyda M, Białkowska AM. Antifreeze proteins produced by Antarctic yeast from the genus Glaciozyma as cryoprotectants in food storage. PLoS One. 2025;20(3):e0318459. https://doi.org/10.1371/journal.pone.0318459 PMID: 40048460
11. Saki N, Ghaffari M, Nikoo M. Effect of active ice nucleation bacteria on freezing and the properties of surimi during frozen storage. LWT. 2023;176:114548. https://doi.org/10.1016/j.lwt.2023.114548

12. Yin L-J, Chen M-L, Tzeng S-S, Chiou T-K, Jiang S-T. Properties of extracellular ice-nucleating substances from Pseudomonas fluorescens MACK-4 and its effect on the freezing of some food materials. Fish Sci. 2005;71(4):941–7. https://doi.org/10.1111/j.1444-2906.2005.01048.x
13. Baloh P, Els N, David RO, Larose C, Whitmore K, Sattler B, et al. Assessment of artificial and natural transport mechanisms of ice nucleating particles in an Alpine Ski Resort in Obergurgl, Austria. Front Microbiol. 2019;10:2278. https://doi.org/10.3389/fmicb.2019.02278 PMID: 31636618
14. Gurian-Sherman D, Lindow SE. Bacterial ice nucleation: significance and molecular basis. FASEB J. 1993;7(14):1338–43. https://doi.org/10.1096/fasebj.7.14.8224607 PMID: 8224607
15. Cid FP, Rilling JI, Graether SP, Bravo LA, Mora M de LL, Jorquera MA. Properties and biotechnological applications of ice-binding proteins in bacteria. FEMS Microbiol Lett. 2016;363(11):fnw099. https://doi.org/10.1093/femsle/fnw099 PMID: 27190285
16. Muñoz PA, Márquez SL, González-Nilo FD, Márquez-Miranda V, Blamey JM. Structure and application of antifreeze proteins from Antarctic bacteria. Microb Cell Fact. 2017;16(1):138. https://doi.org/10.1186/s12934-017-0737-2 PMID: 28784139
17. Kawahara H, Nakano Y, Omiya K, Muryoi N, Nishikawa J, Obata H. Production of two types of ice crystal-controlling proteins in Antarctic bacterium. J Biosci Bioeng. 2004;98(3):220–3. https://doi.org/10.1016/S1389-1723(04)00271-3 PMID: 16233695
18. Muryoi N, Matsukawa K, Yamade K, Kawahara H, Obata H. Purification and properties of an ice-nucleating protein from an ice-nucleating bacterium, Pantoea ananatis KUIN-3. J Biosci Bioeng. 2003;95(2):157–63. https://doi.org/10.1016/s1389-1723(03)80122-6 PMID: 16233385
19. Chen M-L, Chiou T-K, Tsao C-Y, Jiang S-T. Enhancement of the expression of ice-nucleation activity of Pseudomonas fluorescens MACK-4 isolated from mackerel. Fish Sci. 2003;69(1):195–203. https://doi.org/10.1046/j.1444-2906.2003.00606.x
20. Kaleda A, Tsanev R, Klesment T, Vilu R, Laos K. Ice cream structure modification by ice-binding proteins. Food Chem. 2018;246:164–71. https://doi.org/10.1016/j.foodchem.2017.10.152 PMID: 29291835
21. Budke C, Heggemann C, Koch M, Sewald N, Koop T. Ice recrystallization kinetics in the presence of synthetic antifreeze glycoprotein analogues using the framework of LSW theory. J Phys Chem B. 2009;113(9):2865–73. https://doi.org/10.1021/jp805726e PMID: 19708116
22. Santos JS, da Silva CAPT, Balhesteros H, Lourenço RF, Marques MV. CspC regulates the expression of the glyoxylate cycle genes at stationary phase in Caulobacter. BMC Genomics. 2015;16(1):638. https://doi.org/10.1186/s12864-015-1845-1 PMID: 26311251
23. Graumann PL, Marahiel MA. Cold shock proteins CspB and CspC are major stationary-phase-induced proteins in Bacillus subtilis. Arch Microbiol. 1999;171(2):135–8. https://doi.org/10.1007/s002030050690 PMID: 9914312
24. Tao Z, Yuan H, Liu M, Liu Q, Zhang S, Liu H, et al. Yeast extract: characteristics, production, applications and future perspectives. J Microbiol Biotechnol. 2023;33(2):151–66. https://doi.org/10.4014/jmb.2207.07057 PMID: 36474327
25. Filtenborg JEF, Thrane U. The significance of yeast extract composition on. Vol 185. 1990. pp. 433–4.
26. Molina L, Rosa RL, Nogales J, Rojo F. Pseudomonas putida KT2440 metabolism undergoes sequential modifications during exponential growth in a complete medium as compounds are gradually consumed. Environ Microbiol. 2019;21(7):2375–90. https://doi.org/10.1111/1462-2920.14622 PMID: 30951237
27. de Groot N, Lichtenstein N. The action of Pseudomonas fluorescens extracts on asparagine and asparagine derivatives. Biochim Biophys Acta. 1960;40:99–110. https://doi.org/10.1016/0006-3002(60)91319-6 PMID: 13829573
28. Sindhu R, Manonmani HK. Expression and characterization of recombinant l-asparaginase from Pseudomonas fluorescens. Protein Expr Purif. 2018;143:83–91. https://doi.org/10.1016/j.pep.2017.09.009 PMID: 29079538
29. Brown CM, Macdonald-Brown DS, Stanley SO. The mechanisms of nitrogen assimilation in pseudomonads. Antonie Van Leeuwenhoek. 1973;39(1):89–98. https://doi.org/10.1007/BF02578844 PMID: 4144177
30. Hervás AB, Canosa I, Little R, Dixon R, Santero E. NtrC-dependent regulatory network for nitrogen assimilation in Pseudomonas putida. J Bacteriol. 2009;191(19):6123–35. https://doi.org/10.1128/JB.00744-09 PMID: 19648236
31. Chao H, Sönnichsen FD, DeLuca CI, Sykes BD, Davies PL. Structure-function relationship in the globular type III antifreeze protein: identification of a cluster of surface residues required for binding to ice. Protein Sci. 1994;3(10):1760–9. https://doi.org/10.1002/pro.5560031016 PMID: 7849594
32. Kristiansen E, Ramløv H, Hagen L, Pedersen SA, Andersen RA, Zachariassen KE. Isolation and characterization of hemolymph antifreeze proteins from larvae of the longhorn beetle Rhagium inquisitor (L.). Comp Biochem Physiol B Biochem Mol Biol. 2005;142(1):90–7. https://doi.org/10.1016/j.cbpc.2005.06.004 PMID: 15993638
33. Leiter A, Rau S, Winger S, Muhle-Goll C, Luy B, Gaukel V. Influence of heating temperature, pressure and pH on recrystallization inhibition activity of antifreeze protein type III. J Food Eng. 2016;187:53–61. https://doi.org/10.1016/j.jfoodeng.2016.04.019
34. Li N, Andorfer CA, Duman JG. Enhancement of insect antifreeze protein activity by solutes of low molecular mass. J Exp Biol. 1998;201(Pt 15):2243–51. https://doi.org/10.1242/jeb.201.15.2243 PMID: 9662495
35. Gauthier SY, Kay CM, Sykes BD, Walker VK, Davies PL. Disulfide bond mapping and structural characterization of spruce budworm antifreeze protein. Eur J Biochem. 1998;258(2):445–53. https://doi.org/10.1046/j.1432-1327.1998.2580445.x
36. Peramo A. Molecular dynamics studies show solvation structure of type III antifreeze protein is disrupted at low pH. Comput Biol Chem. 2018;73:13–24. https://doi.org/10.1016/j.compbiolchem.2018.01.006
37. Delesky EA, Thomas PE, Charrier M, Cameron JC, Srubar WV III. Effect of pH on the activity of ice-binding protein from Marinomonas primoryensis. Extremophiles. 2020;25(1):1–13. https://doi.org/10.1007/s00792-020-01206-9
38. Vance TDR, Bayer-Giraldi M, Davies PL, Mangiagalli M. Ice-binding proteins and the "domain of unknown function" 3494 family. FEBS J. 2019;286(5):855–73. https://doi.org/10.1111/febs.14764 PMID: 30680879

Curriculum vitae

Personal data

Name: Õnnela Luhila
Date of birth: 18.01.1996
Place of birth: Estonia, Kuressaare
Citizenship: Estonian

Contact data

E-mail: onnela.luhila@taltech.ee

Education

2020–2026	Tallinn University of Technology, PhD
2018–2020	Tallinn University of Technology, MSC
2015–2018	Tallinn University of Technology, BSC
2012–2015	Saaremaa Ühisgümnaasium, High school

Language competence

Estonian	Fluent
English	Fluent
German	B1 level
Russian	A2 level
Swedish	A2 level

Professional employment

2022–…	Tallinn University of Technology, School of Science, Department of Chemistry and Biotechnology, Early-stage researcher
2019-2020	West-Tallinn Central Hospital, clinical chemistry laboratory technician
2017 June-August	Good Mood Food, product development intern
2017 June-August	Karmeli, intern

Supervisions

2021 March–July	Cindie Maitre, Institut National Supérieur des Sciences Agronomiques, de l'Alimentation et de l'Environnement (AgroSup Dijon), intern
2022	Kairit Kruusimägi "The effect of ice-binding proteins on the properties of frozen wheat dough and bread prepared from it" (Master's degree)
2022 March–July	Quentin Aufranc, Institut National Supérieur des Sciences Agronomiques, de l'Alimentation et de l'Environnement (AgroSup Dijon), intern
2023 June–August	Giedre Baltusnikaite, Kaunas University of Technology, intern
2024 March–July	Antoine Candaele, Institut National Supérieur des Sciences Agronomiques, de l'Alimentation et de l'Environnement (AgroSup Dijon), intern
2024	Kadi Karro "The effect of ice-binding proteins on the properties of frozen whole wheat dough and bread" (Master's degree)
2025	Karina Zakrevskaja "Effects of ice-binding proteins on the microstructure and ice recrystallization of frozen whole wheat dough" (Bachelor's degree)

Elulookirjeldus

Isikuandmed

Nimi: Õnnela Luhila
Sünniaeg: 18.01.1996
Sünnikoht: Eesti, Kuressaare
Kodakondsus: Eesti

Kontaktandmed

E-post: onnela.luhila@taltech.ee

Hariduskäik

2020–2026	Tallinna Tehnikaülikool, PhD
2018–2020	Tallinna Tehnikaülikool, MSC
2015–2018	Tallinna Tehnikaülikool, BSC
2012–2015	Saaremaa Ühisgümnaasium, keskharidus

Keelteoskus

Eesti keel	kõrgtase
Inglise keel	kõrgtase
Saksa keel	B1 tase
Vene keel	A2 tase
Rootsi keel	A2 tase

Teenistuskäik

2022–…	Tallinna Tehnikaülikool, Loodusteaduskond, Keemia ja biotehnoloogia instituut, doktorant-nooremteadur
2019-2020	Lääne-Tallinna Keskhaigla, kliinilise keemia laborant
2017 juuni-august	Good Mood Food, tootearenduse praktikant
2017 juuni-august	Karmeli, praktikant

Juhendamised

2021 märts–juuli	Cindie Maitre, *Institut National Supérieur des Sciences Agronomiques, de l'Alimentation et de l'Environnement* (AgroSup Dijon), praktikant
2022	Kairit Kruusimägi „Jääga seonduvate valkude mõju külmutatud nisujahutaigna ja sellest valmistatud saia omadustele" (magistritöö)
2022 märts–juuli	Quentin Aufranc, *Institut National Supérieur des Sciences Agronomiques, de l'Alimentation et de l'Environnement* (AgroSup Dijon), praktikant
2023 juuni–august	Giedre Baltusnikaite, Kaunase Tehnoloogiaülikool, praktikant
2024 märts–juuli	Antoine Candaele, *Institut National Supérieur des Sciences Agronomiques, de l'Alimentation et de l'Environnement* (AgroSup Dijon), praktikant
2024	Kadi Karro „Jääga seonduvate valkude mõju külmutatud täistera nisujahust taigna ja saia omadustele" (magistritöö)
2025	Karina Zakrevskaja „Jääga seonduvate valkude mõju külmutatud täistera nisujahust taina mikrostruktuurile ja jää rekristallisatsioonile" (bakalaureusetöö)

ISSN 2585-6901 (PDF)
ISBN 978-9916-80-544-2 (PDF)